# NEURAL MECHANISMS FOR SENSORY PREDICTIONS IN A CEREBELLUM-LIKE STRUCTURE

Timothy William Requarth

Submitted in partial fulfillment of the requirements for the degree of Doctor of Philosophy under the Executive Committee of the Graduate School of Arts and Sciences

Columbia University

2014

## ABSTRACT

## NEURAL MECHANISMS FOR SENSORY PREDICTIONS IN A CEREBELLUM-LIKE STRUCTURE

Timothy William Requarth

Any animal must be able to predict and cancel the sensory consequences of its own movements to avoid ambiguity in the origin of sensory input. Theoretical and human behavioral studies suggest that nervous systems contain internal models that use copies of outgoing motor signals along with incoming sensory feedback to predict the consequences of movements. Many studies propose the cerebellum as one possible site of such internal models. Yet whether such an internal model exists and how such an internal model might be implemented in neural circuits is largely speculative. Early work in cerebellum-like structures of mormyrid fish identified neural mechanisms of sensory predictions at the levels of synapses, cells, and circuits, and successfully linked those mechanisms to the systems-level function—the cancellation of electrosensory input due to the fish's own behavior. However, those early studies were restricted to predicting and cancelling the electrosensory consequences of relatively simple and rather specialized electromotor behavior. The research described here takes an *in vivo* electrophysiological approach to generalize the previous work in mormyrid fish to the more ubiquitous problem of predicting and cancelling the sensory consequences of movements. First, I demonstrate that neurons in the electrosensory lobe of weakly electric mormyrid fish generate predictions at the cellular level, termed negative images, about the sensory consequences of the fish's own movements based on ascending spinal corollary discharge signals. Second, I examine the interactions between corollary discharge and proprioceptive feedback under conditions that

simulate real movements. Using experiments and modeling, I show that plasticity acting on random, nonlinear mixtures of corollary discharge and proprioceptive signals can account for key properties of negative images observed in vivo. Mossy fibers originating in the spinal cord carry randomly mixed, though linear, corollary discharge and proprioceptive signals, while properties of granule cells observed in vivo are consistent with a nonlinear re-coding of these signals. The conclusion of these studies is that both corollary discharge and proprioception, in combination with an associative neural network endowed with synaptic plasticity, provide a powerful and flexible basis for solving the ubiquitous problems of predicting the sensory consequences of movements.

## Table of Contents

## List of Figures

### Chapter 1



### Chapter 2



### Chapter 3

**Chapter 4**

**Acknowledgements**

This work would not have been possible without the support of many people over many years.

First, I'd like to thank my scientific mentors. I first walked into a laboratory at age 25. Dr. Sandra Weintraub and Dr. Marsel Mesulam were kind enough to take in a totally inexperienced late bloomer. Their research on dementi, aphasia, and language processing remains near and dear to my heart. I'd also like to thank Ravi Allada, my advisor in Northwestern University's Master's Program and Neurobiology. He was patient and intelligent in his guidance. I'd also like to thank the members of my thesis committee: Larry Abbott, Mickey Goldberg, and Randy Bruno, and my outside reader, Curt Bell, whose seminal work in electric fish made this thesis possible. The directors of the graduate program: Ken Miller, Carol Mason, and Darcy Kelley, who provided kindness and guidance throughout graduate school. Finally, I'd like to thank my advisor, Nate Sawtell. Nate is an outstanding mentor and scientist. I thank him as well for treating me as much as a colleague as a student.

Second, I'd like to thank the other members of the lab and the administration. I was Nate's first graduate student, helping him to set up the lab. I'd like to thank my partner in crime during this period, the intrepid post-doc Karina Alvina. I'd also like to thank my compatriots with whom I weathered many years: Karina Scalise, Shobhit Singla, and the relative but welcome newcomer, Armen Enikopolov. They have all offered excellent intellectual feedback, technical support, and companionship. I'd like to thank our lab managers, who made work and life flow a little bit easier: Allison Villacis, Anna Safarty and Alyson Lowell. I'd also like to thank the department administrators, Cecil Oberbeck and Alla Kerzhner, for making everything behind the scenes easy and smooth.

Finally, I want to thank my friends and family. I am indebted to my friends and roommates, Carl Schoonover and Andrew Fink, for their company, intellectual fervor, and sage advice. I'd like to thank Greg Wayne for teaching me to code and introducing me to the basics of theoretical neuroscience. I'd like to specially thank Patrick Kaifosh for helping to develop the computational model in Chapter 3 and for adding analytical results that greatly strengthen the conclusions of the results. I'd like to thank the members of Neuwrite, who added to graduate school a complementary intellectual environment that is truly unique. I'd like to thank my friends not in graduate school, Alex Harvey, Sam Richman, Dana Abrassart, and John Stewart, for showing me what this city has to offer south of 168$^{th}$ street. I'd like to thank my girlfriend, Meehan Crist, who provided love, support and a kind ear during many late nights and frustrating times at the lab, and who also helped me celebrate the good times. I'd like to thank my family: my mother, Connie, my stepfather, Fred, and my sister, Suzy, for their unwavering support. Lastly, I'd like to thank my late father, William, for providing the inspiration to pursue science as a career.

# CHAPTER 1

# INTRODUCTION

## CHAPTER 1: INTRODUCTION

*Historical context and motivation*

Removing predictable sensory input is a very general function of sensory processing. Animals must register what is new in the environment; predictable sensory input provides no new information, and may even interfere with the acquisition of new information. One form of potentially disruptive sensory input arises whenever an animal moves. Sensory receptors are indifferent to the source of input, so the animal must be able to predict and remove the sensory consequences of its own movements in order to process behaviorally relevant stimuli more effectively. For example, rapid eye movements result in retinal stimulation similar to those produced by motion in the external world. Yet, visual perception is stable. As early as the 17$^{th}$ century, Descartes analyzed the perceptions that occurred when he pressed on his eye with his finger. If the eye is pressed in the darkness with an afterimage on the retina, no motion of the afterimage is perceived. An active eye movement, however, will result in apparent movement of the afterimage. Experience with a real image is the reverse: the image appears to move when the eye is pressed, but does not move with voluntary eye movement. Later scientists, including Purkinje, Helmholtz and Mach, suggested that an active eye movement elicited an extraretinal signal to compensate for eye movement, while pressing the eye passively did not.

In 1950, von Holst and Mittelstaedt (von Holst 1950) and Roger Sperry (Sperry 1950) independently provided the first experimental evidence for such a signal and formalized the notion that self-generated sensory input, termed reafference, could be predicted and removed by using central signals related to imminent movements. Von Holst and Mittelstaedt inverted the head of a blowfly by 180 degrees, observing that the fly, in the light but not the dark, would then

circle continually. They concluded that under normal conditions the fly would compare transformed copies of motor outflow to visual inflow, stabilizing movement by negative feedback. They termed the copy of motor outflow "efference copy." Inverting the head turned this negative feedback cycle into positive feedback, causing the fly to circle. Sperry inverted the eye of a fish and made the similar observation that the fish would circle indefinitely, concluding that there may be some compensatory signal related to movements routed to visual centers. He termed these feedforward copies of motor signals corollary discharge (CD). CD pathways have since been characterized in a number of invertebrate and vertebrate systems, from crickets to primates (Poulet and Hedwig 2007; Crapse and Sommer 2008).

Leading theoretical accounts of human motor control posit a role for CD signals in predicting and canceling the sensory consequences of movements. Online predictions of the sensory consequences of motor commands, termed forward models, may be critical for generating fast and accurate movements despite noise and delays in sensory feedback (Wolpert and Miall 1996; Shadmehr, Smith et al.). Clinical, electrophysiological, and theoretical results indicate that the mammalian cerebellum may be involved in predicting the sensory consequences of motor commands (Wolpert, Miall et al. 1998; Bastian 2006; Ebner and Pasalar 2008; Anderson, Porrill et al. 2012; Brooks and Cullen 2013). Indeed, some suggest that failures of the CD system may give rise to positive symptoms in schizophrenia (Ford and Mathalon 2012). However, in all cases, the underlying neural mechanisms remain largely unknown.

In addition, self-generated movements engage not only CD signals but also other sensory input streams, including proprioception. Though both sensory and motor signals could, in principle, be used to distinguish between self-generated and external stimulation, there are few cases in which their respective roles have been extensively explored (Guthrie, Porter et al. 1983;

Wang, Zhang et al. 2007; Wurtz 2008). Work in other systems, such as the visual system, suggests that proprioceptive signals may be too inaccurate or delayed to effectively cancel self-generated movements (Wang, Zhang et al. 2007; Wurtz 2008). Can proprioception be used to generate sensory predictions about movements? What is the nature of sensory predictions based on two streams of information? What are the respective roles of CD and proprioception in sensory predictions?

Studies of cerebellum-like circuits in the electrosensory system of mormyrid fish have uniquely elucidated neural mechanisms of how copies of motor outflow are used to predict and cancel the electrosensory consequences of behavior. In addition, work in electric fish has demonstrated that the effects of proprioceptive input related to body movements is plastic. Understanding the full complexity of how electric fish use such information to generate predictions should provide general insights into how any nervous system generates predictions based on past experience.

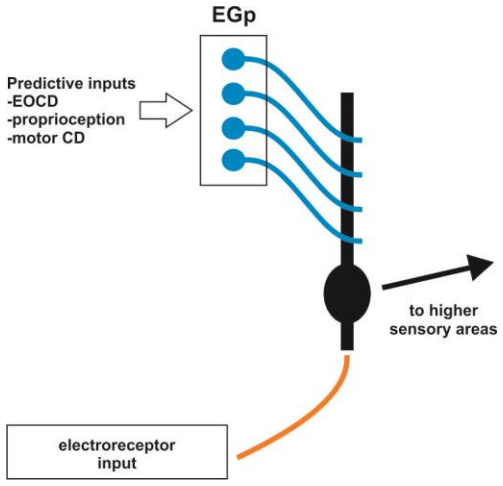


**Figure 1.1**. **Cerebellum-like circuitry of the mormyrid ELL.** EGp granule cells (blue) carrying predictive information conveyed by mossy fibers send parallel fibers to ELL principal neurons (black), which also receive electroreceptor input from the periphery (orange). ELL efferent cells project to higher levels of electrosensory processing.

*The electrosensory system and cerebellum-like structures*

A surprising number of animals possess sensory systems capable of detecting weak electric fields (Bullock and Heiligenberg 1986). Weak, low-frequency electric fields are ubiquitous in aquatic environments, generated by the muscle activity of living creatures, or by the flow of ions in water currents. Animals that can detect these low-frequency external voltage sources, typically with a set of electroreceptors distributed over their skin, are said to have a passive electrosensory system (Kalmijn 1971). Two orders of freshwater fish have developed an additional "active" electrosensory system in that they generate a weak, high-frequency electric field in pulses or waves, known as the electric organ discharge (EOD). Such fish detect nearby objects by distortions in self-generated transdermal current flow, mediated by a separate set of electroreceptors tuned to the high frequency of the EOD (Lissmann and Machin 1958). Thus, those fish endowed with a passive electrosensory system and the more exotic active electrosensory system can detect both external voltage sources (passively) and the impedances of nearby objects (actively). *Gnathonemus petersii*, the model system of this research, is an African freshwater fish of the family Mormyridae with both passive and active electrosensory systems.

In mormyrids, the primary afferents of electroreceptors terminate in the deep layers of a cerebellum-like structure forming a somatotopic map of the sensory surface. This structure is known as the electrosensory lateral line lobe (ELL) (**Figure 1.1**). and is the first stage of central processing of electrosensory input (Bullock and Heiligenberg 1986). Principal cells in ELL have basilar dendrites that are strongly affected by primary afferent input from electroreceptors. These cells also have apical dendrites in a molecular layer that receive parallel fiber (PF) input from granule cells (GCs) in an external granule cell mass known as the eminentia granularis posterior (EGp). GCs giving rise to PFs receive signals that include CD related to motor commands,

proprioceptive input, and descending input from higher electrosensory processing structures. These PF signals are termed predictive as they are often associated with changes in electrosensory input and can thus be used as raw material to form adaptive predictions.

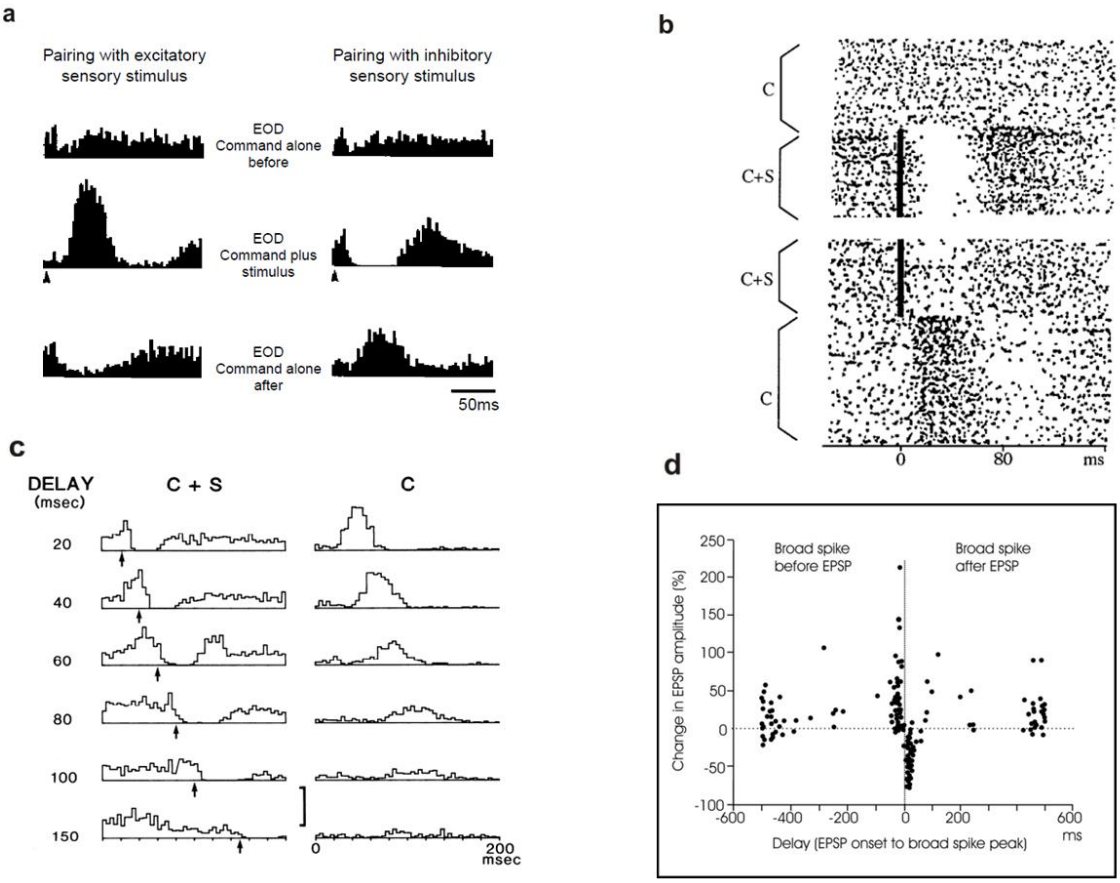


**Figure 1.2. Negative images of predicted sensory responses in the passive electrosensory region of the mormyrid ELL and anti-Hebbian learning rule. (a)** Histograms on the left show the response to EOD motor command alone before pairing (top), responses to command paired with a brief (1 ms) excitatory electrosensory stimulus (arrowhead), and responses to the command alone after pairing (bottom). Histograms on the right show the same cell in response to a brief inhibitory stimulus. In both cases, the responses to the command alone are opposite to the effects of the previously paired stimuli**. (b)** Raster display of another cell showing the effect of pairing the EOD command (C, time 0) with a sensory stimulus (S, indicated by black bar). **(c)** Effects of varying stimulus delay on response to EOD command alone after 3-4 min of pairing. Arrowhead indicates time of stimulus. Note temporal specificity of negative image. **(d)** Anti-Hebbian learning rule. The dots show results from *in vitro* slice experiments in which parallel fiber-evoked EPSPs were paired with postsynaptic dendritic spikes evoked by intracellular current pulses. Changes in EPSP size were measured as a function of the relative timing of the EPSP and the spike during pairing. EPSP depression was present only if the postsynaptic spike was evoked ~50 ms following EPSP onset. Other delays produced potentiation. (**(a)** reproduced from Bell, 2001; **(b)** reproduced from (Bell 1981); **(c)** reproduced from (Bell 1982); **(d)** modified from (Bell, Han et al. 1997)).

Early studies in the mormyrid passive electrosensory system provided a clear example of how CD could be used to predict and cancel the sensory consequences of a motor command. The passive electrosensory system in mormyrids is subserved by a class of electroreceptors that responds to minute low-frequency bioelectric fields generated by aquatic animals. These receptors also have a vigorous and sustained response to the large-amplitude, high-frequency pulses of the EOD (**Figure 1.2a-c**), but these responses interfere with the function of the passive system to detect small, low-frequency fields (Bell and Russell 1978). Furthermore, the exact response of the electroreceptors to the EOD varies with water conductivity and the surrounding environment. Thus, an adaptive mechanism is needed to effectively cancel the interference of the EOD.

In addition to peripheral electrosensory input, the principal cells of ELL receive, via PFs, EOCD information coupled to the motor command to discharge the electric organ (electric organ corollary discharge, or EOCD). The electric organ is a modified muscle located on the tail, so EOCD can be studied in the fish by blocking the neuromuscular junction with curare, which eliminates the EOD. However, the motor command that would normally produce an EOD is still issued. Importantly, the electromotor neuron volley (EMN) that would produce an EOD can be easily measured with an electrode near the tail, which allows precise experimental control over the relationship between motor commands and their sensory consequences (in this case the amplitude and timing relative to the EOD motor command). *In vivo* recordings from ELL neurons show that by pairing an artificial stimulus at fixed delays from the EMN leads to changes in the effects of EOCD signals alone that resemble a "negative image" of the neuron's response to the paired stimulus (Bell 1981) (**Figure 1.2a-c**). This negative image forms over the course of minutes and is specific to the polarity, amplitude, and time course of the neuron's

response to the paired stimulus (Bell 1982) **(Figure 1.2c**). During the pairing period, the addition of a negative image minimizes the central effect of predictable input.

Subsequent *in vivo* and *in vitro* studies showed that the predicted negative images are due in part to plastic changes within ELL. Pairing an intracellular current injection at a fixed delay to the EMN instead of an electrosensory stimulus and observing the formation of a negative image led to the conclusion that the changes must have taken place at the cell's synapses (Bell, Caputi et al. 1993). Further investigation revealed that these cells exhibit anti-Hebbian spike-timing dependent plasticity (Bell, Han et al. 1997) (**Figure 1.2d**). PF inputs that precede (predict) the occurrence of a postsynaptic spike are depressed while inputs occurring at other delays are potentiated. This type of anti-correlative or anti-Hebbian plasticity provides a cellular mechanism consistent with the characteristics of the formation of a negative image. Modeling studies demonstrated that negative images resulting from the experimentally measured anti-Hebbian learning rule are more stable and accurate than those produced by other learning rules (Roberts and Bell 2000; Williams, Roberts et al. 2003). In conclusion, the cellular mechanism of anti-Hebbian plasticity in the context of cerebellar connectivity leads to the functional consequence of removing the interfering effects of the EOD from the passive electrosensory processing.

Combined with evidence from other cerebellum-like structures in gymnotiform (Bastian 1996) and elasmobranch (Bodznick, Montgomery et al. 1999) fishes, a general hypothesis emerged that cerebellum-like circuitry can act as an adaptive filter for generating predictions based on PF associations with sensory inputs and removing those predictions from the neural response. Anti-Hebbian spike-timing dependent plasticity has also been found in the cerebellum-like mammalian auditory processing structure, the dorsal cochlear nucleus, provoking a similar

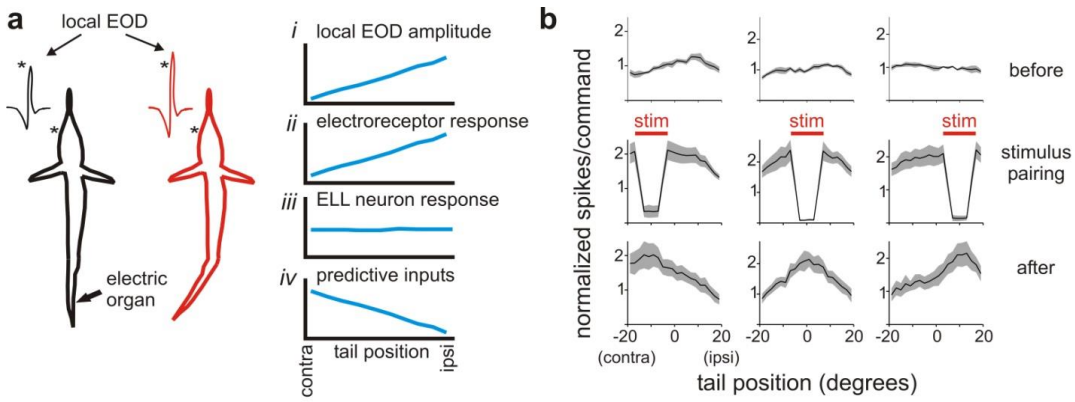


**Figure 1.3**. **ELL neurons predict the electrosensory consequences of tail movements. (a)** Left, cartoon depicting the effect of tail position on the fish's EOD amplitude. Bending the tail increases the amplitude of the EOD pulse measured near the skin (*) on the side of the fish now closer to the electric organ. Right, the strength of the local EOD amplitude and the electroreceptor response are increased by ipsilateral tail bends (*i-ii)*, but ELL neurons are unresponsive to tail bends *(iii)* because of predictive inputs *(iv)* that cancel the effects of electroreceptor input. **(b)** Effects of pairing an electrosensory stimulus at different tail positions (columns) in ELL efferent cells. The effect of the stimulus (red bar) was inhibitory. Note that spiking did not depend on tail position before pairing (top row), but there was a clear dependence after pairing (bottom row). The change was due to a negative image of the effects of the stimulus during pairing. Gray outlines indicate SEM. (Adapted from (Sawtell and Williams 2008)).

functional interpretation (Tzounopoulos, Kim et al. 2004). The cerebellum itself has also been proposed to function as an adaptive filter (Fujita 1982; Dean and Porrill 2008; Dean, Porrill et al.).

Just as EODs interfere with the processing of passive electrosensory information, tail movements interfere with the processing of active electrosensory information. The electric organ that emits the discharge is located on the fish's constantly moving tail. Thus, for the electroreceptors distributed over one side of the fish's body, when the tail (and thus the electric organ) moves ipsilaterally to that side, those receptors register a relative increase in the amplitude of the EOD than when the tail was at the midline. Similarly, when the tail is in position contralateral to that same side, those same receptors will register an EOD of smaller amplitude.

When a conducting object is in the environment, it too will cause a local increase in the amplitude of the EOD (and conversely, an insulating object will cause a local decrease). The fish

must separate the EOD amplitude change that is due to the external object and the amplitude change due to its own tail movement. Measurements show that those due to even a few degrees of tail movement can be greater than the local EOD amplitude change of many behaviorally relevant stimuli (Chen, House et al. 2005). Yet, ELL neurons that robustly respond to subtle changes in local conductivity due to external objects are invariant to changes in tail position (**Figure 1.3a**). Thus, there must exist a mechanism for extracting information from small EOD amplitude changes embedded in much larger, but predictable, changes.

The early work on the passive electrosensory system suggests that ELL contains the circuitry and plasticity mechanism to solve just such a problem. To cancel EOD amplitude changes due to tail position, ELL must receive information about the timing of the EOD (known to be conveyed by EOCD inputs) and some source of information about tail position (such as proprioceptive input). Indeed, recent work showed that plastic proprioceptive PF input to ELL neurons can be used to form negative images of the electrosensory consequences of tail position (Sawtell and Williams 2008) (**Figure 1.3b**). This study paralyzed the fish and moved the tail passively from side to side while pairing EOD mimics only with those EMNs that fell within a particular range of the tail position. The EOD mimic was delivered at a fixed delay following the EMN, and negative images were formed, but restricted to those EMNs that occurred within the paired range of tail positions. Thus, proprioceptive input and EOCD can be combined to form negative images temporally locked to the EMN and spatially specific to tail position.

Are these mechanisms described above for generating negative images powerful and flexible enough to solve the more difficult problem of generating negative images in the context of rapid, normal patterns of movements? The EOD motor command is a stereotyped event generated by a small number of neurons in a dedicated command nucleus (Bennett, Pappas et al.

1967; Grant, Bell et al. 1986). Movement motor commands are generated by a far more complex motor system, and also engage proprioceptive feedback. It is not known whether movement CD exists or whether proprioceptive feedback is accurate enough to cancel rapid movements. Neither is it known how these two streams of information interact under conditions that approximate real movements. Finally, how movement-related CD signals may be coded at the level of individual neurons remains an open question.

*Predictive inputs to ELL and transformations in GC circuitry*

To decipher how ELL forms predictions of the electrosensory consequences of movements, it is critical to understand the nature of the predictive input signals related to movement. GCs in EGp give rise to PFs that synapse on the principal cells of ELL (**Figure 1.1**). As in the mammalian cerebellum, GCs receive inputs, referred to as mossy fibers (MFs), from many brain regions and convey a variety of sensory and motor information, some related to the fish's tail movements.

There are two distinct MF pathways by which proprioceptive information related to the tail reaches ELL (Szabo, Libouban et al. 1979; Bell, Finger et al. 1981; Szabo, Libouban et al. 1990). The first is a dorsal column pathway consisting of the axons of primary sensory neurons that project to the lateral funicular nucleus (FL2), which in turn provides mossy fiber input to the ipsilateral EGp (Srivastava 1979). The second originates from a lateral cell column extending over all spinal segments and sends mossy fibers directly to the contralateral EGp (Szabo, Libouban et al. 1990). In addition, MFs may convey CD from higher motor centers such as the optic tectum or the mesencephalic locomotor region (MLR). One possibility, as my results will suggest, is that CD inputs originate in the spinal cord. Spinocerebellar pathways conveying

motor signals have been extensively studied in mammals (Oscarsson 1965; Arshavsky, Gelfand et al. 1978; Hantman and Jessell 2010; Jankowska, Nilsson et al. 2011; Fedirchuk, Stecina et al. 2013; Spanne and Jorntell 2013). Yet roles for such pathways in predicting the sensory consequences of movements have not been clearly defined.

MFs are recoded in GCs prior to being conveyed to ELL. Therefore, understanding the how GCs transform MF input is of critical importance as it is GC responses, not MF responses, that constitute the raw material out of which negative images are sculpted. However, even though GC circuitry is similar in both cerebellum-like structures and the cerebellum itself, little is known about GC activity patterns or function in either.

Influential theories (Marr 1969; Albus 1971) posit that the large number of GCs serve to sparsely recode MF inputs, such that only a small fraction of the GC population is active for a given pattern of MF input. Sparse coding may increase the capacity of Purkinje cells to discriminate different MF input patterns through associative plasticity at PF synapses by decreasing pattern interference. Such a capacity is thought to be important for motor learning, but the question of sparse coding in mammalian GCs remains open (Arenz, Bracey et al. 2009).

A recent study in mormyrid ELL found evidence for multimodal integration in GCs, suggestive of sparse coding. This study also linked multimodal responses in GCs to the ability of principal cells to generate negative images via anti-Hebbian plasticity (Sawtell 2010). From in vivo whole-cell recordings in awake, paralyzed fish, the author showed that some GCs integrate excitatory input from two distinct classes of MFs. One class conveyed proprioceptive information about body position while the other conveyed EOCD signals. Most cells did not fire unless both signals were active simultaneously, thereby encoding information about the conjunction of a motor command and a particular body configuration. The author went on to

show that principal neurons were capable of generating negative images specific to particular tail positions and particular times relative to the electric organ motor command—the same combinations of signals encoded by individual GCs. Such predictions of motor commands that take proprioceptive context into account are likely to be of general use. For example, predicting the consequences of a reaching movement requires both the motor command issued and the hand's starting position.

GC circuitry may also have a role in generating temporal representations, as has been proposed in the context of eye-blink conditioning (Medina, Garcia et al. 2000; Medina and Mauk 2000) and adaptive filter models (Fujita 1982). However, such representations have not been investigated in mammalian GCs in vivo. Previous work in mormyrid fish shows that ELL principal cells generate temporally-specific predictions as long as 200 ms after the EOD motor command. It is known that CD responses in MFs appear to be extremely brief and restricted to a short delay after the EOD motor command. Thus, GC circuitry must temporally expand CD signals into a format appropriate for sensory cancellation.

A recent study in mormyrid ELL provided the most complete description to date of GC recoding (Kennedy, Wayne et al. 2014). Using in vivo intracellular recordings from hundreds of GCs, they found that temporal expansion indeed occurs in GCs. They also directly demonstrated that GC responses, along with anti-Hebbian plasticity, can sufficiently account for negative images in vivo. Interestingly, they found that GC responses were not delay lines, as suggested by previous theoretical work (Roberts and Bell 2000), but highly non-uniform. Modeling suggested that such a non-uniform temporal basis is well-matched to the temporal structure of self-generated inputs, which may allow for rapid and accurate sensory cancellation. This study shed light on how copies of motor commands are translated into an appropriate format to cancel

sensory inputs. Such a capacity may be critical in the context of real movements as negative images in ELL neurons must match the temporal profiles of movements even if responses in MFs are brief.

*Cerebellum-like structures and the cerebellum*

The work described here may have broad applicability in part because cerebellum-like structures and the cerebellum have highly similar cell types and local circuitry. The similar cells include GCs and PFs, Golgi cells, unipolar brush cells, inhibitory molecular layer interneurons such as stellate cells, and principal cells that have spine-covered dendrites extending into the molecular layer. In terms of the local circuitry, one of the most important similarities is that both cerebellum-like and cerebellum receive two types of inputs. Principal cells in cerebellum-like structures receive PF input and peripheral input while Purkinje cells in the cerebellum receive PF input and climbing fiber input from the inferior olive. PF input is similar in both cases in that it conveys a variety of information from all over the brain to many principal cells or Purkinje cells. In both cases the second input (peripheral in the case of cerebellum-like structures and climbing fiber input in the case of the cerebellum) conveys very specific information.

However, the nature of this second input is also what distinguishes cerebellum-like structures from the cerebellum. In the cerebellum, each Purkinje cell receives a single climbing fiber input whereas principal cells in cerebellum-like structures do not have such single-fiber inputs. Yet, climbing fibers and peripheral sensory input are also similar. Climbing fibers often signal sensory events, including retinal slip (Maekawa and Simpson 1972), somatosensory stimulation (Ekerot and Jorntell 2001), and vestibular stimulation (Barmack and Shojaku 1992). Although the inferior olive is not a sensory relay, sensory stimuli clearly influence its activity.

PF input of both cerebellum-like structures and the cerebellum convey a rich variety of information. In cerebellum-like structures, this information can be associated with peripheral sensory input and thus be used to predict changes in sensory input. Similarly, in the cerebellum, the PFs convey information that can predict the occurrence of a climbing fiber. For example, climbing fibers can signal retinal slip (Maekawa and Simpson 1972) while PF convey vestibular information related to head movements (Lisberger and Fuchs 1974), CD information about eye movements (Noda and Warabi 1982), and proprioceptive information from the neck (Matsushita and Tanami 1987). All of these signals could, in principle, be used to predict movement of images across the retina.

These similarities suggest that the cerebellum too may be involved in sensory predictions. A variety of experimental, clinical, and theoretical studies support this idea (Wolpert, Miall et al. 1998; Nixon and Passingham 2001; Paulin 2005; Diedrichsen, Criscimagna-Hemminger et al. 2007). In the clinical domain, it has long been known that cerebellar damage causes movement abnormalities. Interestingly, there is no loss of movement, but rather more subtle deficits such as such as lack of coordination, increased variability, tremor, and poor accuracy. A number of researchers have suggested that these deficits can be explained by a role for the cerebellum in predictive control. The term predictive means the feedforward part of a movement that is planned and unaffected by peripheral sensory input. Several studies indicate that predictive control is deficient in patients with cerebellar damage (Smith and Shadmehr 2005; Morton and Bastian 2006). Such patients do not adapt to predictable perturbations of movement, although they can respond reactively to unpredictable perturbations, suggesting that peripheral feedback is intact.

Theoreticians have provided one conceptual framework, termed a forward model, to explain how the cerebellum acts in a predictive manner. A forward model is an internal model that mimics the causal flow of a process by predicting the expected state (sensory consequences) given the current state (sensory inflow) and the motor command (motor outflow) (Wolpert, Ghahramani et al. 1995; Wolpert and Miall 1996). Forward models may be important in generating rapid movements in which peripheral sensory feedback, such as proprioception, is noisy or delayed. Since motor commands for one phase of a movement often must be issued before peripheral sensory feedback returns from the previous phase, a forward model that predicts the sensory consequences of movements based on motor commands and estimates of current state would allow the next motor command to be issued appropriately. Many cerebellar deficits can be understood as the absence of a predictive forward model (Bastian 2006).

Besides local circuitry, cell types, and possibly similar roles in sensory predictions, there are also many similarities between plasticity in the cerebellum and in cerebellum-like structures. For example, in the mormyrid ELL, at the synapses between PFs and Purkinje-like MG cells, synaptic depression requires a pairing a postsynaptic dendritic spike with PF input. In the cerebellum, Purkinje cell response depression to PF stimulation requires pairing with climbing fiber input or postsynaptic depolarization (Ito 2001; Jorntell and Hansel 2006). Interestingly, simple spike activity often resembles the opposite of climbing fiber responses in many systems in which this has been examined (Graf, Simpson et al. 1988; Stone and Lisberger 1990; Barmack and Shojaku 1992; Kobayashi, Kawano et al. 1998; Ebner, Johnson et al. 2002). This relationship is reminiscent of negative images in cerebellum-like structures.

Although synaptic plasticity between the two structures may share qualitative features, the mechanisms are probably not the same. For example, plasticity in the mormyrid ELL (Han,

Grant et al. 2000) and the mammalian DCN (Tzounopoulos, Kim et al. 2004) depends upon NMDA receptor activation. Synaptic plasticity at PF synapses onto Purkinje cells does not (Ito 2001).

*Conclusion*

Predictions based on past experience are critical for perceptual stability, motor adaptation, and cognitive function. Predicting and removing uninformative sensory input due to movements ensures that behaviorally relevant stimuli are processed more effectively. Predictions are also important for rapid movements in which sensory feedback is too delayed to be useful for motor control. Forward models that estimate the change in the state of the body that result from outgoing motor commands may be a mechanism for such predictions. Cerebellum-like circuits in the weakly electric mormyrid fish provide unique opportunities for understanding such mechanisms. Previous *in vivo, in vitro,* and modeling studies have identified neural correlates for predictions based on past experience. In addition, the link between the plasticity mechanisms and the formation of these predictions is securely established. Anti-Hebbian spike-timing dependent plasticity at PF synapses onto Purkinje-like principal cells in a cerebellum-like structure cancel the neural response to predictable electrosensory input, such as input due to the animal's own movements.

The work described here generalizes these results to organisms without an electrosensory system. I find that ELL neurons can form predictions based not on electromotor CD but on feedforward movement-related CD signals in the context of the animal's own movements. Second, I investigate the interactions between these CD and proprioception under conditions that approximate real movements, and how these two signals are coded in MFs and re-coded in GCs.

# CHAPTER 2

# PLASTIC COROLLARY DISCHARGE PREDICTS SENSORY CONSEQUENCES OF MOVEMENTS IN A CEREBELLUM-LIKE STRUCTURE

# CHAPTER 2: PLASTIC COROLLARY DISCHARGE PREDICTS SENSORY CONSEQUENCES OF MOVEMENTS IN A CEREBELLUM-LIKE STRUCTURE

## Introduction

Predicting the sensory consequences of an animal's own behavior is a critical function of the nervous system. In the sensory domain, predicting and cancelling sensory input caused by an animal's own movements allows for more effective processing of behaviorally relevant stimuli (Sperry 1950; von Holst 1950; Cullen 2004). Though many sensory regions, including sensory areas of the mammalian cerebral cortex, receive input from motor systems, the functions of such inputs remain largely unknown (Poulet and Hedwig 2007; Crapse and Sommer 2008). According to theoretical accounts of motor control, online predictions of the sensory consequences of motor commands, known as forward models, are critical for generating fast and accurate movements despite noise and delays in sensory feedback (Wolpert and Miall 1996; Shadmehr and Krakauer 2008). Though converging lines of evidence suggest that the mammalian cerebellum is involved in predicting sensory consequences of motor commands (Wolpert, Miall et al. 1998; Bastian 2006; Ebner and Pasalar 2008; Anderson, Porrill et al. 2012; Brooks and Cullen 2013), detailed knowledge of the underlying circuit mechanisms is lacking. Finally, numerous lines of evidence suggest that failures of corollary discharge-based predictions contribute to psychotic symptoms in schizophrenia (Ford and Mathalon 2012), though here as well the underlying mechanisms are unknown.

Studies of weakly electric mormyrid fish have provided unique insights into the cellular and circuit mechanisms for predicting the sensory consequences of a simple electromotor behavior—the EOD. Mormyrid fish emit brief, highly stereotyped EOD pulses for communication and active electrolocation. However, the fish's own EOD also affects passive

electroreceptors tuned to detect external electrical fields (Bell and Russell 1978). This problem is solved at the level of ELL principal cells, where input from electroreceptors is integrated with input from a mossy fiber-granule cell-parallel fiber system conveying timing signals related to the EOD, known as electric organ corollary discharge (EOCD). Anti-Hebbian plasticity at parallel fiber synapses onto principal cells sculpts patterns of activity that are temporally-specific negative images of principal cell response to the EOD (Bell 1981; Bell, Caputi et al. 1993; Bell, Han et al. 1997; Roberts and Bell 2000). Negative images serve to cancel out responses to the fish's own EOD, allowing responses to external fields to be processed more effectively.

The circuitry of the mormyrid ELL is similar in numerous respects to that of the mammalian cerebellum, including the presence of a mossy-fiber granule cell system that provides plastic input to Purkinje-like cells via a system of parallel fibers, as well as Golgi cells, unipolar brush cells, and inhibitory molecular layer interneurons (Bell, Han et al. 2008). ELL neurons also receive electrosensory input, which, although clearly different from climbing fiber input to Purkinje cells, may function analogously to the climbing fiber insofar as both serve to instruct plasticity at parallel fiber synapses. Indeed, roles for granule cells and parallel fiber plasticity established in previous experimental and theoretical studies of ELL (Bell 1981; Bell, Han et al. 1997; Roberts and Bell 2000; Kennedy, Wayne et al. 2014) closely resemble longstanding Marr-Albus (Marr 1969; Albus 1971) and adaptive filter models (Fujita 1982; Dean, Porrill et al. 2010) of mammalian cerebellar cortex. Given these similarities, studies of ELL may shed light on the more complex problem of understanding adaptive functions of the mammalian cerebellum (Boyden, Katoh et al. 2004; Ke, Guo et al. 2009; Schonewille, Gao et al. 2011; Gao, van Beugen et al. 2012).

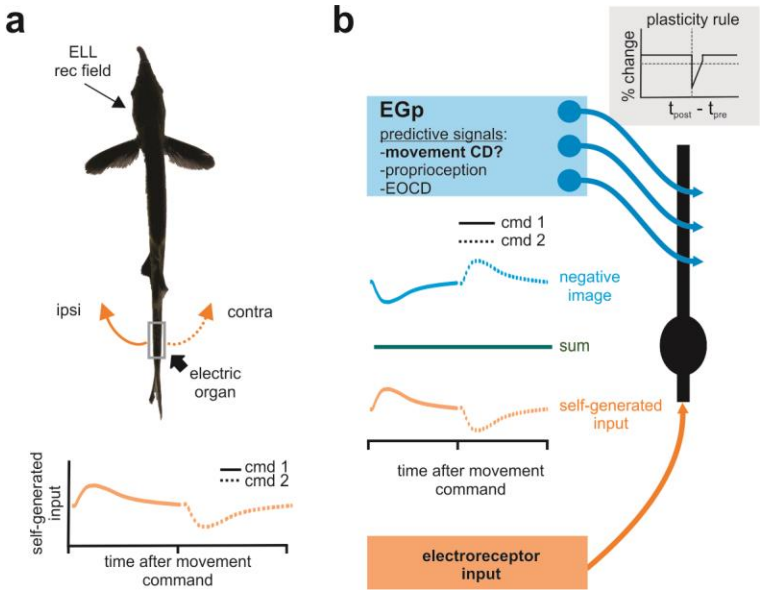


**Figure 2.1. A simple scheme for predicting movement consequences in ELL. (a)** For some ELL neurons (depending on the location of their receptive field on the body), self-generated changes in the electric field due to movements of the electric organ in the tail (filled arrow) are proportional to tail displacement from the midline, with tail movements towards the side of the receptive field resulting in an increase in the local electric field amplitude and an increase in electroreceptor activation. The electrosensory consequences of two different tail movements as a function of time are schematized in the bottom panel. **(b)** ELL principal cells integrate electrosensory input with a variety of sensory and motor signals conveyed via a mossy fiber-granule cell pathway. Granule cells are located in an external cell mass, known as the eminentia granularis posterior (EGp) and receive excitatory mossy fiber input from a variety of sources. Previous studies have described mossy fibers conveying EOD motor command timing information and proprioceptive input, but whether mossy fibers convey corollary discharge (CD) signals related to movements is unknown. Anti-Hebbian plasticity at synapses between granule cells and ELL principal cells underlies the cancellation of predictable patterns of electrosensory input. In order to effectively predict the sensory consequences of movements, principal cells must be able to store multiple negative images related to different movement commands.

Are mechanisms described previously for generating negative images of the effects of the EOD powerful and flexible enough to solve the more difficult problem of generating negative images of the sensory consequences of movements (**Figure 2.1**)? Whereas the EOD motor command is a completely stereotyped event generated by a small number of neurons in a dedicated command nucleus (Bennett, Pappas et al. 1967; Grant, Bell et al. 1986), movement motor commands are numerous, diverse and generated by a far more complex and distributed motor system. Here we show that in addition to EOCD signals, ELL neurons also receive movement-related corollary discharge signals from the spinal cord. Despite the major differences

between the EOD and movements, ELL neurons form flexible and accurate negative images based on this movement-related corollary discharge. These results provide direct neurophysiological evidence for predictions of the sensory consequences of movements based on plastic corollary discharge. These results also suggest that the fairly complete and well-tested model of corollary discharge function established for the mormyrid ELL in the context of specialized electromotor behavior may be broadly relevant for understanding how corollary discharge signals operate in other systems in the context of movements.

## Results

### Corollary discharge responses during fictive swimming

Previous anatomical and physiological studies have thoroughly characterized EOCD inputs to ELL conveying information about the timing of the EOD motor command (Bell, Finger et al. 1981; Bell, Libouban et al. 1983; Bell and Grant 1992; Bell, Dunn et al. 1995; Kennedy, Wayne et al. 2014). However, it is not known whether ELL also receives corollary discharge signals related to motor commands that initiate swimming movements. Identifying such movement-related corollary discharge signals requires isolating them from somatosensory and electrosensory signals. To this end we developed a fictive swimming preparation. First, we evoked rhythmic swimming movements by continuous microstimulation (40 or 100 Hz) of the mesencepahlic locomotor region (MLR) (McClellan and Grillner 1984; Fetcho and Svoboda 1993; Uematsu and Todo 1997; Le Ray, Juvin et al. 2011). Movements ranged from 1-6 Hz and ceased upon termination of microstimulation. The frequency of the movements was always far below the frequency of continuous microstimulation, and, clearly graded with stimulus intensity at relatively low current strengths, although the absolute values of

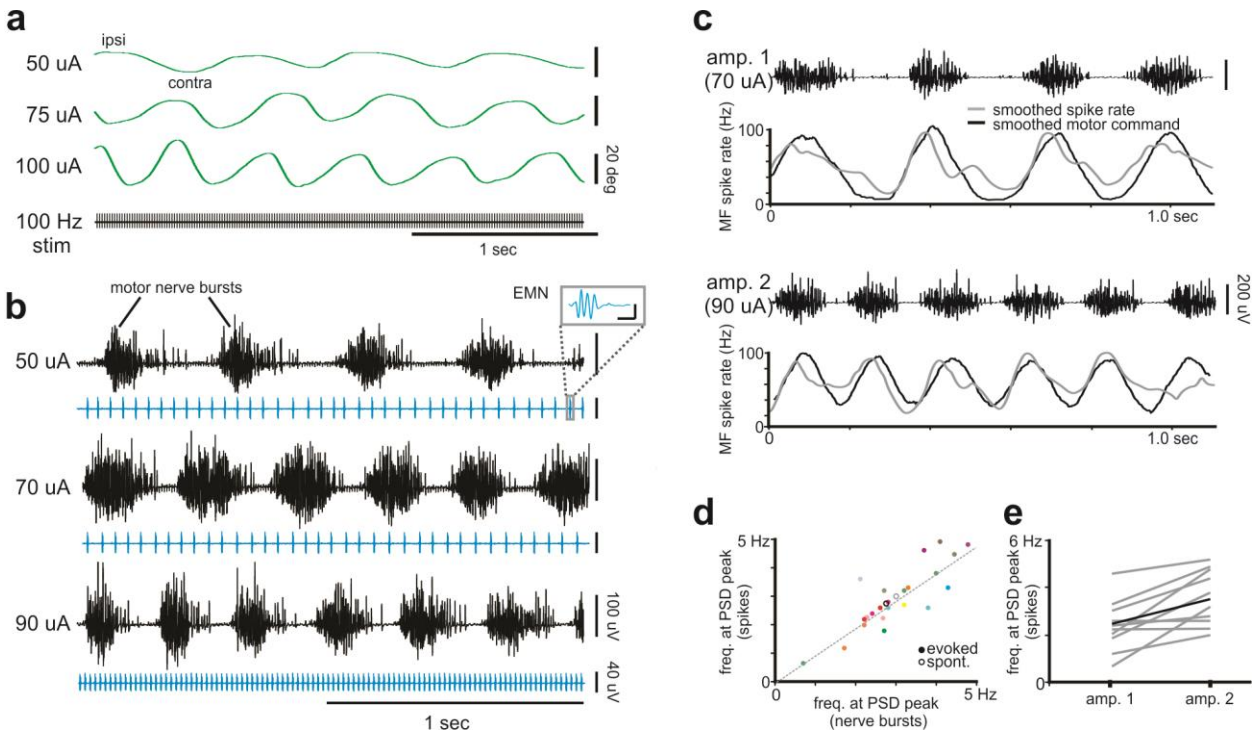


**Figure 2.2. Motor patterns and mossy fiber responses evoked by fictive swimming. (a)** Tail position measured by laser displacement sensor in response to three intensities of 100 Hz microstimulation in the mesencephalic locomotor region (MLR). **(b)** Recordings of dorsal ramus of the ventral root show motor patterns evoked by three intensities of 100 Hz MLR microstimulation. Bottom rows (blue) depict the spinal electromotoneuron volley (EMN) that in an unparalyzed fish would cause an EOD. EMN was measured simultaneously via an electrode near the electric organ. Scale bars, inset: 10uV, 3 ms. **(c)** Smoothed spike rate (20 ms Gaussian window) from an extracellular recording of an EGp mossy fiber in response to microstimulation-evoked fictive swimming at two frequencies. Black trace is the rectified and smoothed motor command signal recorded in the dorsal ramus of the ventral root, scaled for ease of comparison to mossy fiber firing rate. **(d)** Frequency at power spectral density (PSD) peak from smoothed spike rate trace vs. frequency at PSD peak from rectified, smoothed motor nerve burst trace for all recorded mossy fibers at all tested microstimulation-evoked frequencies. Each color corresponds to the same mossy fiber. Open circles indicate spontaneous fictive swimming. Gray dotted line is the regression line. **(e)** Frequency of firing rate at PSD peak for all mossy fibers in which microstimulation evoked two frequencies of fictive swimming movements. Black line indicates the mean. Mossy fibers were analyzed regardless of whether motor nerve signals were obtained.

the current strength varied across fish (**Figure 2.2a**). After characterizing the movements evoked by microstimulation we paralyzed the fish (eliminating movement-related somatosensory and

electrosensory signals) and monitored motor commands directly by recording from motor nerves exiting the spinal cord in the dorsal ramus of the ventral root. Nerve recordings revealed rhythmic bursts of activity, the frequency of which graded with microstimulation current intensity, comparable to swimming frequencies prior to paralysis (**Figure 2.2b, top traces**). As

expected, simultaneously recorded motor commands to discharge the electric organ were entirely distinct from activity recorded from spinal motor nerves (**Figure 2.2b, bottom traces**) in that the timing of their occurrences was unrelated to motor nerve activity. Hence, motor nerve activity reflects commands related to swimming movements.

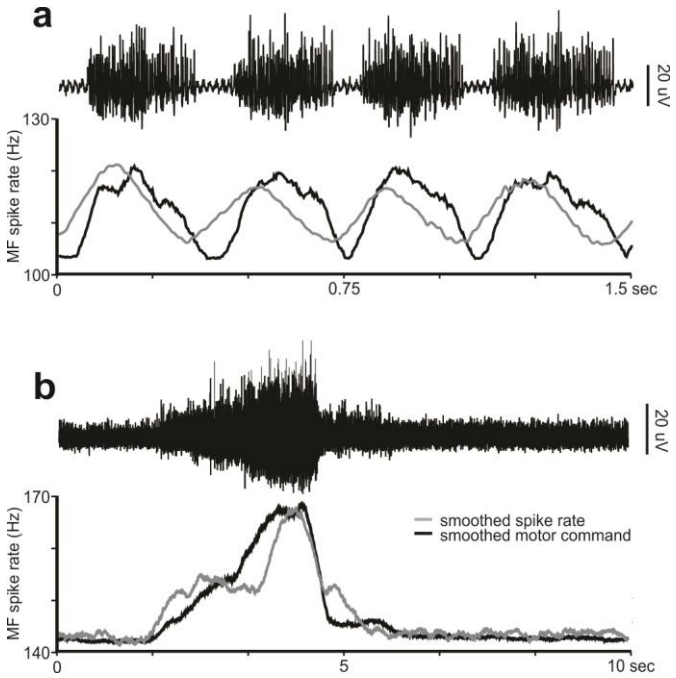


**Figure 2.3. Mossy fibers respond to spontaneous motor nerve activity. (a)** Smoothed spike rate (20 ms Gaussian window) from an extracellular recording of an EGp mossy fiber in response to rhythmic spontaneous fictive swimming. Black trace is the rectified and smoothed motor command signal recorded in the dorsal ramus of the ventral root, scaled for ease of comparison. **(b)** Smoothed spike rate (20 ms Gaussian window) from an extracellular recording of an EGp mossy fiber in response to non-rhythmic spontaneous fictive swimming. Black trace is the rectified and smoothed motor command signal recorded in the dorsal ramus of the ventral root, scaled for ease of comparison.

Previous studies have shown that mossy fiber inputs to the eminentia granularis posterior (EGp)—a cell mass that contains the granule cells that project to ELL (**Figure 2.1b**)—originate from several sources in the brain and spinal cord (Szabo, Libouban et al. 1979; Bell, Finger et al. 1981; Szabo, Libouban et al. 1990) and convey a variety of information including EOCD, proprioceptive, and electrosensory signals (Bell, Grant et al. 1992; Sawtell 2010; Kennedy, Wayne et al. 2014). To test whether some mossy fibers convey movement-related corollary

discharge, we combined the fictive preparation described above with extracellular recordings from putative mossy fiber axons in EGp (Bell, Grant et al. 1992; Sawtell 2010; Kennedy, Wayne et al. 2014). A subset of tonically-active mossy fibers exhibited firing rate modulation (greater than three S.D. from baseline) during spontaneous (**Figure 2.3**) or microstimulation-evoked motor nerve activity (n=23 of 48 fibers; **Figure 2.2c**). Further analysis was performed on those fibers that included periods of rhythmic motor nerve activity (19 of 23 fibers had such periods). For these fibers, rhythmic firing rate modulations were correlated with motor nerve activity (cross-correlation between firing rate and smoothed motor nerve bursts, $r=0.40\pm0.18$; n=19 fibers).We also observed a strong correlation between the frequency of mossy fiber firing rate modulation (as measured by the frequency at which the peak occurred in the power spectral density (PSD); see **Experimental Procedures**) and frequency (at PSD peak) of smoothed motor nerve bursts (r=0.79, n=19 fibers, 1-3 frequencies per fiber for n=29 total observations; **Figure 2.2d**), including for spontaneous bursts (n=2 fibers; open circles on **Figure 2.2d**). For a subset of mossy fibers we microstimulated at two different amplitudes. For these fibers, the frequency of firing rate modulation (at PSD peak) increased with microstimulation intensity (amp1: $2.37\pm1.17$ Hz; amp2: $3.71\pm1.19$ Hz, n=9 fibers, p=0.0039, sign test; **Figure 2.2e**). Hence, a subset of mossy fibers conveys graded motor information related to the frequency of rhythmic swimming movements.

Since any movement that alters the position of the electric organ relative to electroreceptors has electrosensory consequences, corollary discharge signals should be engaged for different types of movements. To test this, we used microstimulation of the optic tectum, homologue of the mammalian superior colliculus, to evoke rapid, isolated tail and trunk movements characteristic of orienting or escape behavior (Herrero, Rodriguez et al. 1998;

Saitoh, Menard et al. 2007). A brief microstimulation train (500 Hz, 10-15 pulses) applied to the tectum evoked a single, rapid unilateral tail movement, the speed and amplitude of which graded smoothly with

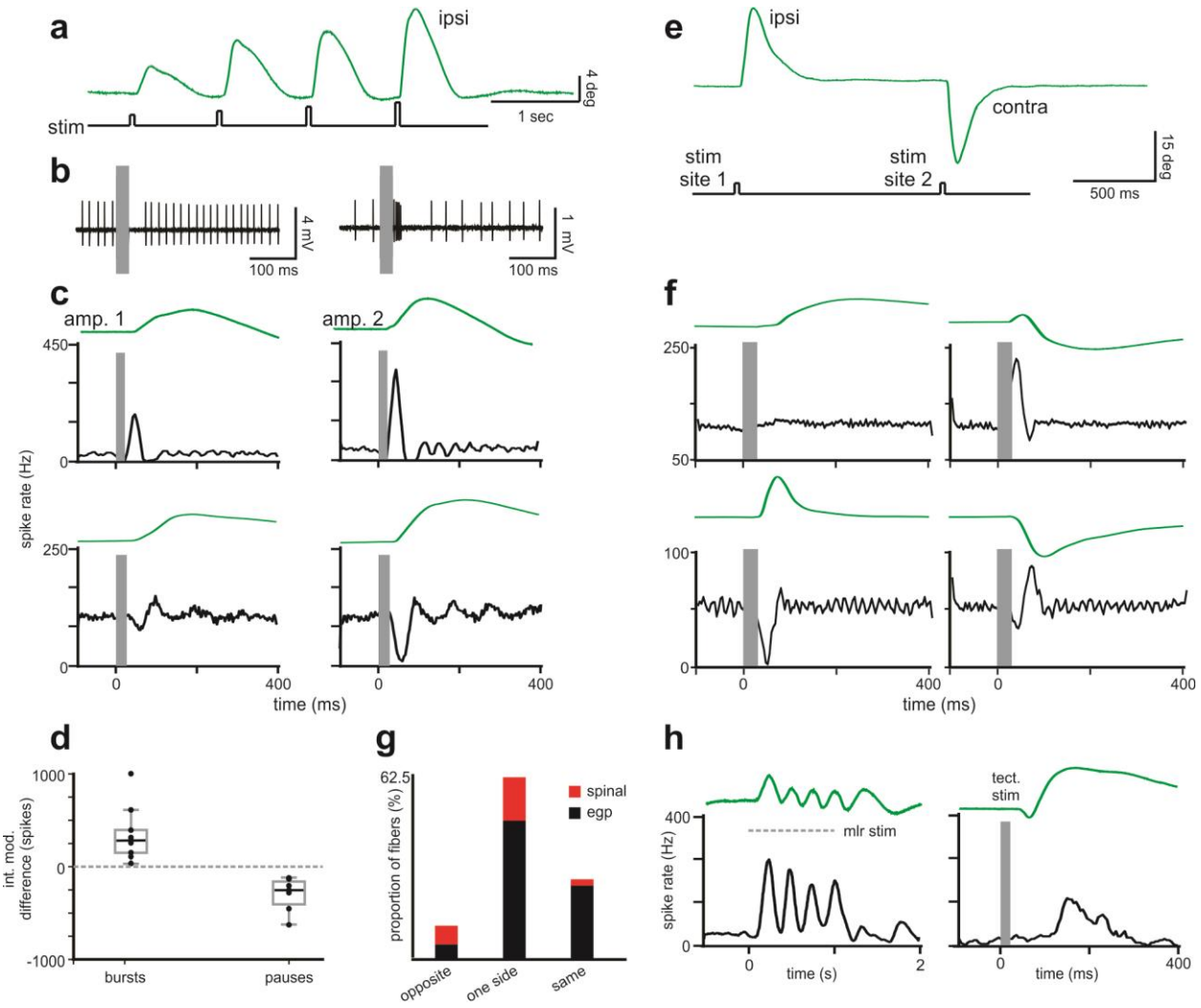


**Figure 2.4. Mossy fiber responses evoked by microstimulation of the optic tectum. (a)** Microstimulation-evoked tail movements in response to four stimulus intensities as measured by a laser displacement sensor. **(b)** Extracellular traces from two representative mossy fibers in response to tectal microstimulation. Left trace also appears in 2.4F, bottom panels; right trace also appears in 2.4C, top panels. **(c)** Smoothed spike rate histograms from two mossy fibers in response to two amplitudes of tectal microstimulation. Green traces represent tail position. Note graded bursts in top example and graded pauses in bottom example. **(d)** Box plots of integrated firing rate modulations of mossy fibers, segregated by response pattern. Integrated modulations were calculated by summing spikes over a small window following microstimulation (~100 ms). Black dots correspond to individual data points. **(e)** Tail movements evoked by microstimulation at two different sites in the optic tectum. **(f)** Smoothed spike rate histograms from two mossy fibers in response to tectal microstimulation at two sites. Notice selective response to one stimulation site in top example and opposite responses in bottom example. **(g)** Summary of mossy fiber responses to tectal microstimulation at two sites, segregated by recording location. **(h)** Smoothed spike rate histograms from a single mossy fiber responding to both MLR and tectal microstimulation. Top, green traces represent microstimulation-evoked tail displacement prior to paralysis. Gray boxes obscure microstimulation artifact

stimulus intensity (**Figure 2.4a**). We next paralyzed the fish and recorded extracellularly from mossy fibers (**Figure 2.4b**), as described above. In a subset of mossy fibers we observed activity that graded with stimulus intensity, typically in the form of brief bursts or pauses (**Figure 2.4c**). A summary of these responses is shown in **Figure 2.4d** (bursts, integrated modulation difference: 342±281 spikes, n=10 fibers, p=0.002, sign test; pauses, integrated modulation difference: -240±193 spikes, n=7 fibers, p=0.0156, sign test).

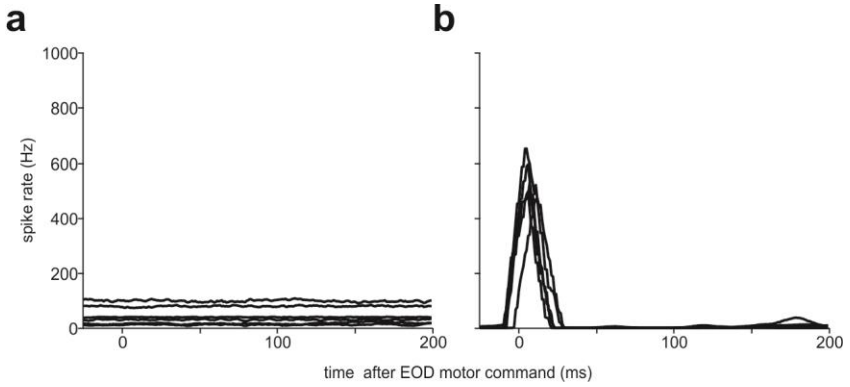


**Figure 2.5. Mossy fibers carrying movement-related CD do not exhibit EOD motor command responses. (a)** EOD motor command-triggered smoothed spike rate histograms of the six representative fibers that appear in the figures. From bottom: 2.4B, top; 2.4H; 2C; 2.4E, bottom; 2.4E, top; 2.4B, bottom. Notice no response to EOD motor command. **(b)** For comparison, five representative traces from mossy fibers with typical EOD motor command responses. Note the complete absence of baseline firing and the large bursts in response to the EOD command. These mossy fibers were also recorded extracellularly in EGp but represent an entirely distinct population from the tonically-active mossy fibers that convey corollary discharge related to movements.

From the perspective of an ELL neuron, an ipsilateral tail movement (one that brings the electric organ closer to the neuron's receptive field) will have an electrosensory consequence opposite to that of a contralateral tail movement (Sawtell and Williams 2008). Hence, in order to be useful for cancelling the electrosensory consequences of movements, corollary discharge signals must convey information that could be used to distinguish between different motor commands. To test this, we microstimulated at two sites in the tectum which reliably evoked tail movements in opposite directions (**Figure 2.4e**). We found that a majority of mossy fibers

responded either selectively to one stimulation site (**Figure 2.4f**, **top**) or oppositely to stimulation of the two sites (**Figure 2.4f, bottom**), consistent with corollary discharge signals providing a basis for distinguishing between motor commands related to different movements (opposite: n=11; same: 26; one side: n=59).

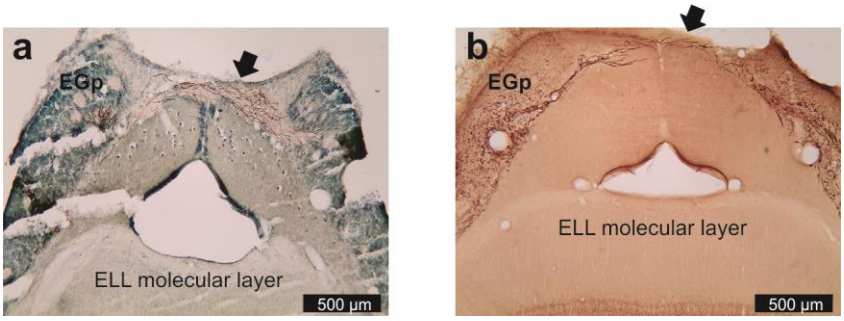


**Figure 2.6. Trajectory of an ascending spinal mossy fiber pathway to EGp. (a)** Transverse section showing labeled mossy fibers after an extracellular injection of biocytin into EGp. Mossy fibers decussate near the anterior border of ELL where they pass over the caudal lobe of the cerebellum, near the brain surface (arrow). **(b)** Previous studies have shown that spinal fibers projecting to EGp exhibit calbindin immunoreactivity (Szabo et al., 1990). A calbindin stained transverse section shows mossy fibers decussating at a similar location at the anterior border of ELL, near the brain surface. This material was taken from a previous study examining the immunocytochemistry of ELL cell types (Bell et al., 2005).

Finally, mossy fibers modulated by MLR or tectal microstimulation did not exhibit responses to the EOD motor command (**Figure 2.5**). Hence, as expected based on previous anatomical studies (Bell, Finger et al. 1981; Bell, Libouban et al. 1983; Bell, Grant et al. 1992; Bell, Dunn et al. 1995), corollary discharge signals related to movements are conveyed via separate pathways from signals related to the EOD motor command. We obtained additional insight into the anatomical origins of movement-related corollary discharge signals by recording in a superficial fiber tract at the anterior margin of EGp which contains mossy fiber axons originating from the spinal cord (**Figure 2.6**). Previous anatomical studies have shown that this pathway shares a number of similarities with the ventral spinocerebellar tract in higher vertebrates (Szabo, Libouban et al. 1979; Szabo, Libouban et al. 1990). Mossy fibers recorded in the spinal tract exhibited bursts and pauses in response to tectal microstimulation similar to

those recorded in EGp. A summary of mossy fiber responses to tectal microstimulation at two sites, segregated by recording location, is shown in **Figure 2.4g** (n=22 spinal tract fibers; n=74 EGp fibers). These results suggest that corollary discharge signals reach EGp via the spinal cord, instead of being relayed via branches of a descending motor pathway originating from the tectum. This possibility is supported as well by previous anatomical tracing studies suggesting that direct connections between EGp and the tectum or other brain centers involved in controlling movement are absent. If corollary discharge signals return to EGp from the spinal cord, it might be expected that the same fibers would relay motor command-related signals irrespective of the central origin of the commands, as has been shown for some mammalian spinocerebellar pathways, see e.g. (Jankowska, Nilsson et al. 2011). To test this, we recorded from EGp mossy fibers in two paralyzed fish in which we evoked both rhythmic movements via MLR stimulation and rapid, isolated tail movements via tectal stimulation. Fourteen of twenty-one mossy fibers modulated by MLR microstimulation were also modulated by tectal microstimulation (example in **Figure 2.4h**).

**Corollary discharge inputs to ELL neurons are plastic**

Negative images of the electrosensory consequences of the EOD described previously depend critically on the capacity to shape the effects of EOCD signals on ELL neurons via mechanisms of associative plasticity. Direct in vivo evidence for such plastic shaping of EOCD signals has been obtained by pairing EOD motor commands with dendritic spikes evoked intracellularly in medium ganglion (MG) cells (Bell, Caputi et al. 1993; Sawtell, Williams et al. 2007; Kennedy, Wayne et al. 2014). MG cells inhibit glutamatergic output neurons of ELL, occupying a position in ELL circuitry analogous to Purkinje cells in the cerebellum (Bell 2002; Bell, Han et al. 2008).

Such experiments have revealed temporally-specific depression of EOCD responses, consistent with anti-Hebbian spike timing dependent plasticity at parallel fiber-MG cell synapses documented in vitro (Bell, Han et al. 1997; Han, Grant et al. 2000). We conducted similar experiments but using tectal microstimulation at two sites to evoke motor commands related to two different movements (**Figures 2.4e and 2.7a**). We obtained whole-cell recordings from MG cells and paired a dendritic spike evoked by intracellular current injection at a fixed delay (50 or 100 ms) after microstimulation of one of the tectal sites. Subthreshold responses to microstimulation before pairing were modest, but after pairing for 5-10 minutes, we observed a response depression that was both specific to the paired microstimulation site and greatest at the paired delay (**Figures 2.7b and 2.7c**; 50 ms, n=20 pairings from 14 cells; 100 ms, n=9 pairings from 8 cells). Because pairing is restricted to the recorded cell, changes observed in these experiments likely reflect plasticity at synapses conveying movement-related corollary discharge signals to MG cells. Previous *in vitro*, *in vivo*, and modeling studies suggest that the observed response depression can be explained by removal of excitation mediated by selective weakening of parallel fiber synapses active before the dendritic spike (Bell, Han et al. 1997; Roberts and Bell 2000; Kennedy, Wayne et al. 2014). Both the temporal- and site-specificity of the response depression are notable. The former suggests that individual MG cells may possess the capacity to generate negative images of the electrosensory consequences of movements that are extended in time relative to the motor command that evokes them, while the latter suggests a capacity to generate and store multiple negative images related to different movements.

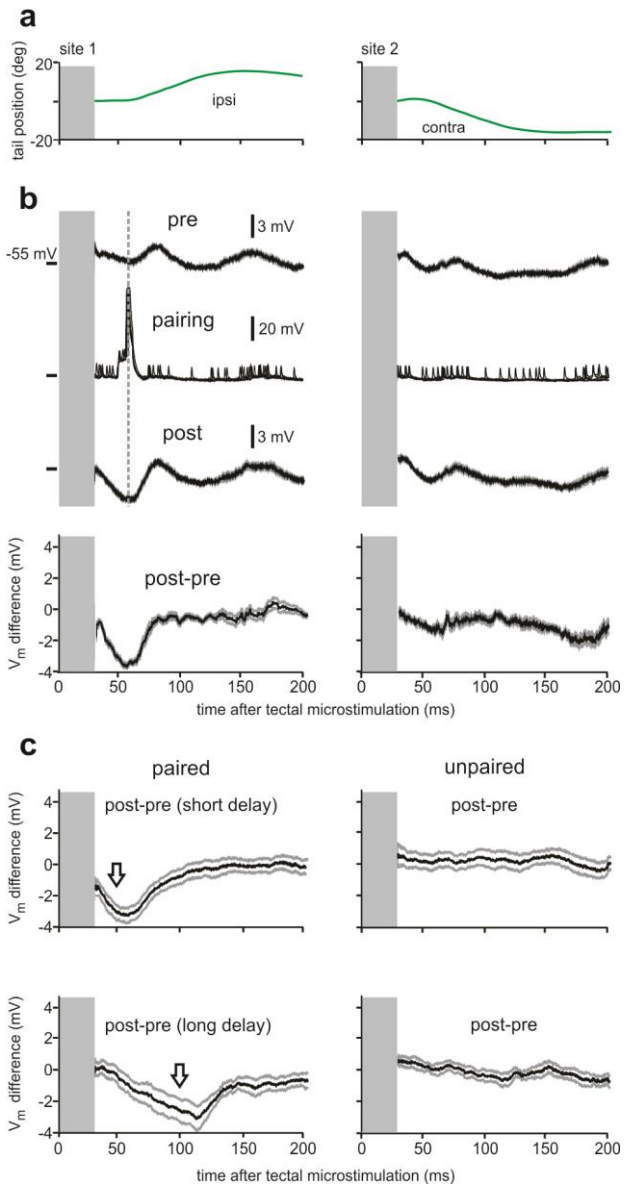


**Figure 2.7. Site- and temporally-specific plasticity of corollary discharge responses in MG cells. (a)** Tail position measured by laser displacement sensor in response to microstimulation at two sites in the optic tectum. **(b)** Traces from a representative MG cell recorded in same experiment as laser traces in **a**, showing average microstimulation-evoked synaptic responses before pairing (pre, top row), during pairing (middle row), and after pairing (post, third row). In the post and pre conditions, narrow spikes were digitally removed and membrane potentials interpolated before averaging. The middle panel shows five overlaid traces taken during the pairing period. For this cell, current injections were delivered to evoke a dendritic spike, paired at a fixed delay to microstimulation at site 1 (dotted line). The bottom panels show the difference in the average microstimulation-evoked responses before and after pairing. Note that the depression is restricted to the paired microstimulation site and greatest around the delay at which the spike was paired. **(c)** Average difference traces across cells, pooled independently of microstimulation site. Current injections were delivered at two delays relative to microstimulation (arrows) and restricted to one microstimulation site, showing both site-and temporal-specificity of the response depression. Gray outlines indicate standard error of the mean (SEM) and gray boxes obscure microstimulation artifacts.

**Negative images based on corollary discharge signals**

The most important result at the core of previous models of ELL adaptive function is that ELL neurons are capable of generating highly-specific negative images of the electrosensory consequences of the fish's own EOD. We performed experiments in order to determine whether ELL neurons could likewise generate negative images of the electrosensory consequences of movements evoked by MLR or tectal microstimulation. We simulated natural patterns of activation for the electrosensory system by delivering a brief electrical pulse (between the stomach of the fish and the tank) following each EOD motor command, mimicking the duration and timing of the fish's own EOD. We also used microstimulation of the electromotor command pathway (see **Experimental Procedures**) to achieve EOD command rates within the range of those observed in swimming fish (13Hz in our experiments). Because of the additional demands of the electrosensory stimulation, we did not monitor motor nerve activity in these experiments. Instead, we delivered brief pulses to the MLR (500 Hz, 10-15 pulses). Such stimulation reliably evoked rapid ipsilateral tail movements, similar to movements evoked by tectal stimulation.

We then paralyzed the fish and made extracellular single-unit recordings from ELL principal cells, including both putative MG cells and ELL output cells (**Figure 2.8b**) (Bell and Grant 1992; Bell, Caputi et al. 1997). Spiking responses to MLR stimulation were compared before and after a pairing period (10-15 min) during which the amplitude of a local electrosensory stimulus (ES) applied to the neuron's receptive field was smoothly graded as a function of the temporal profile of the microstimulation-evoked tail movement (**Figure 2.8a**), as measured before paralysis using a laser displacement sensor (dashed lines in **Figures 2.8, 2.9, and 2.11**). Before pairing, responses to microstimulation were small or absent. After pairing,

responses to microstimulation resembled smoothly graded negative images of the response to the ES during pairing (**Figures 2.8c and 2.8d**; n=4). Similarly, smoothly graded negative images were obtained for tectal microstimulation in separate experiments (**Figures 2.8e and 2.8f**; n=14). These results suggest that ELL neurons possess the capacity to transform brief motor commands into much longer-lasting patterns of activity that are temporally-aligned with and appropriate to cancel the electrosensory consequences of movements, i.e. negative images. Indeed, the timing of the peak modulation of mossy fibers in response to tectal microstimulation (46.98$\pm$7.63 ms, n=106 observations from n=70 fibers) is far more restricted than the peak modulation of negative images (121.21$\pm$21.85 ms, n=14 cells). Finally, the fact that negative images were similar in these two sets of experiments also suggests a general capacity to cancel the electrosensory consequences of motor commands regardless of the origins of the motor commands.

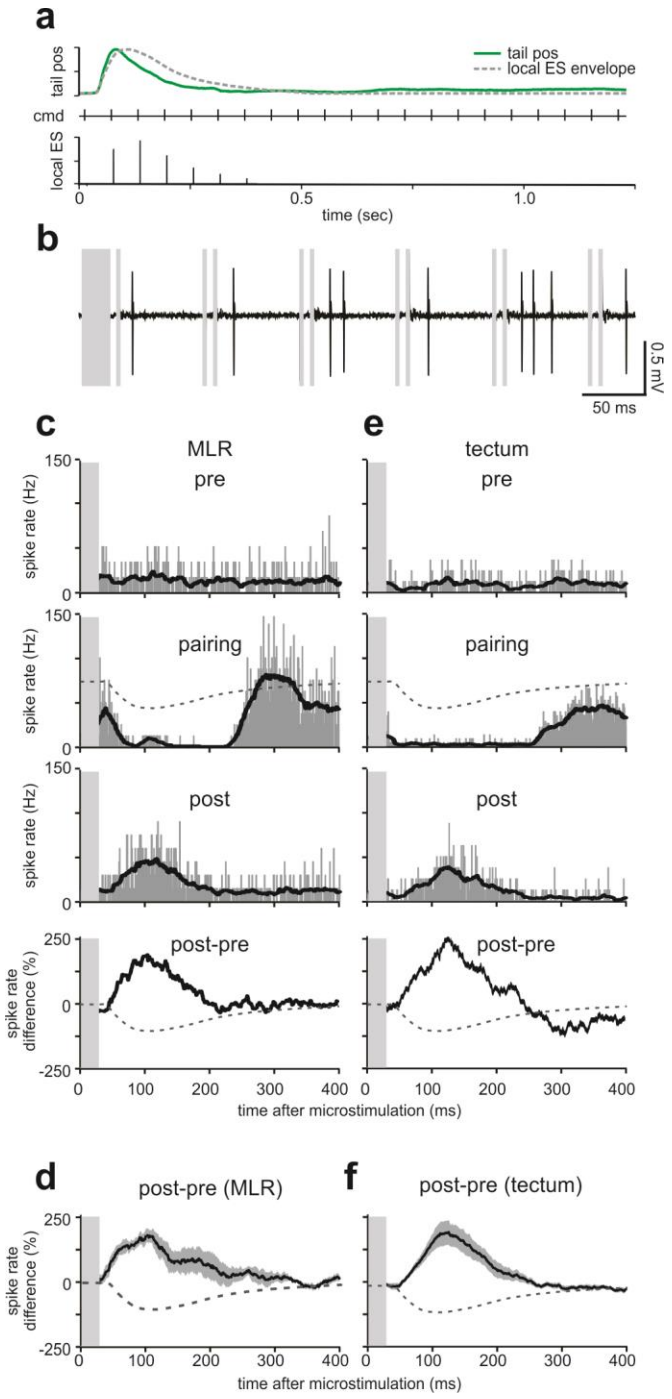


**Figure 2.8. ELL Principal cells exhibit negative images based on corollary discharge (a)** Top row, green trace: representative microstimulation-evoked tail movement measured by laser displacement sensor prior to paralysis. Top row, dotted gray trace: Waveform envelope used as look-up table for delivering local ES. Note that waveform is based on the pre-paralysis movements but is not an exact match. For purposes of pooling across fish in which movements varied in their exact time course, we created an idealized waveform closely modeled on the typical time-course of movements. Middle row: timing of EOD motor commands. Note constant rate of 13Hz due to microstimulation of the EOD command pathway. Bottom row: A local ES, placed in the receptive field of the recorded cell, was varied in amplitude according to the timing of the command and the relative value of the look-up table waveform. A constant-value global ES was delivered in conjunction with the local one, allowing for bidirectional modulation of the local EOD mimic's amplitude around a constant mean. **(b)** Representative

extracellular trace from cell depicted in 2.8C. Large gray box obscures tectal microstimulation artifact. Small gray boxes obscure electromotor command pathway microstimulation artifact (first small gray box of each pair) and global electrosensory stimulus artifact (second small gray box of each pair). **(c)** Smoothed (20 ms boxcar filter) spike rate histograms from an extracellular recording of an ELL principal cell illustrating typical response patterns as a function of time relative to microstimulation of the MLR before, (pre, top row), during (pairing, second row), and after (post, third row) pairing with a local ES (dotted gray line). Non-smoothed histograms shown in gray (1 ms bins). The difference traces in the bottom panels show the effects of pairing (after pairing minus before pairing). **(d)** Average of difference traces pooled across cells. Difference traces were constructed by subtracting the smoothed spike rate histograms. **(e)** Smoothed spike rate histogram from an extracellular recording of an ELL principal cell illustrating typical response patterns as a function of time relative to microstimulation of the optic tectum before, (pre, top row), during (pairing, second row), and after (post, third row) pairing with a local ES (dotted gray line). Non-smoothed histograms shown in gray (1 ms bins). The difference traces in the bottom panels show the effects of pairing (after pairing minus before pairing). **(f)** Average of difference traces pooled across cells. For averages shown in **d** and **f** cells were pooled to match polarity of difference trace irrespective of site or cell type. Each cell is normalized to its pre-pairing baseline firing rate. In all panels, gray outlines indicate SEM across cells and gray boxes obscure microstimulation artifacts.

The number and variety of sensory patterns evoked by movements is far greater than the sensory patterns resulting from the EOD, raising the question of the capacity of ELL neurons to generate and simultaneously store multiple negative images appropriate to cancel sensory consequences of different movements. Though testing many different movements was impractical, our preparation allowed us to ask whether ELL neurons were capable of forming two different negative images. We alternated microstimulation of the two tectal sites, and paired each with smoothly graded but opposite polarity changes in ES amplitude (**Figure 2.9a**). This mimics the natural situation in which ipsilateral versus contralateral tail movements have opposite electrosensory consequences. As in the previous results, before pairing, responses in ELL principal cells to microstimulation were small or absent. After pairing, responses to microstimulation resembled smoothly graded negative images of the response to the ES during pairing (**Figure 2.9b**). Notably, negative images were specific to the site of tectal microstimulation and bi-directional—i.e., the same neuron had the capacity to store two, opposite negative images consisting of either graded increases or decreases in firing depending on the effects of the ES during pairing (**Figure 2.9c**; n=9). Decreases in firing observed after pairing with an excitatory ES can be explained by previously described anti-Hebbian spike

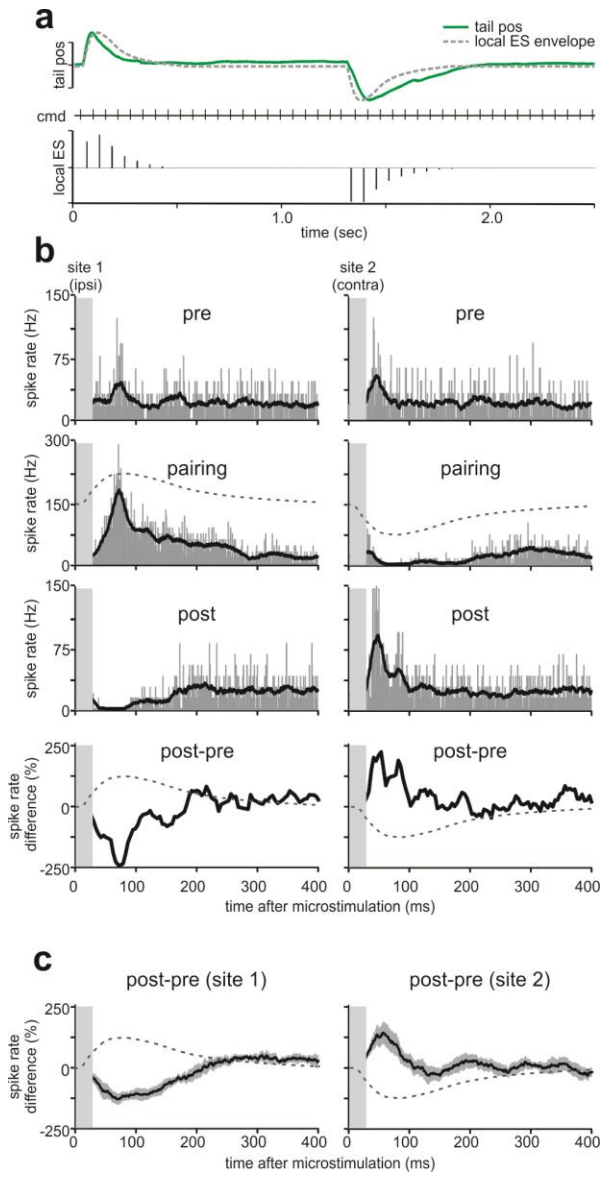


**Figure 2.9. ELL principal cells can store two different negative images in relation to different motor commands (a)** Top row, green trace: representative microstimulation-evoked tail movements measured by laser displacement sensor prior to paralysis. Top row, dotted gray trace: Waveform envelope used as look-up table for delivering local ES. Middle row: timing of EOD motor commands. Bottom row: A local ES, placed in the receptive field of the recorded cell, was varied in amplitude according to the timing of the command and the relative value of the look-up table waveform. (**b**) Smoothed spike rate histograms from an extracellular recording of an ELL principal cell illustrating typical response patterns as a function of time relative to microstimulation of the optic tectum before, (pre, top row), during (during, second row), and after (post, third row) pairing with a local ES (dotted gray line). Non-smoothed histograms shown in gray (1 ms bins). The left and right-hand columns correspond to the microstimulation sites that, before paralysis, evoked ipsilateral and contralateral tail movements, respectively. Microstimulation was delivered alternately to each site throughout the experiment. In the example shown here, site 1 was paired with an ES that excited the cell while site 2 was paired with an ES that inhibited the cell. The difference traces in the bottom panels show the effects of pairing (after pairing minus before pairing). (**c**) Average of difference traces pooled across cells showing site-specificity of pairing at site 1 and site 2. Cells were pooled to match polarity of difference trace irrespective of site or cell type. Each cell is normalized to its pre-pairing baseline firing rate. In all panels, gray outlines indicate SEM across cells and gray boxes obscure microstimulation artifacts.

timing-dependent depression at parallel fiber synapses, while increases in firing observed after pairing with an inhibitory ES can be explained by previously described non-associative potentiation at parallel fiber synapses (Bell, Han et al. 1997; Han, Grant et al. 2000).

Finally, the capacity of ELL neurons to form negative images appeared to be highly flexible and robust. Negative image magnitude did not depend strongly on whether the effect of the paired ES on the recorded neuron was the same or opposite to that which would be caused by the evoked movement under natural conditions, on cell type, or on whether the effect of the paired ES was excitatory or inhibitory (**Figure 2.10**).

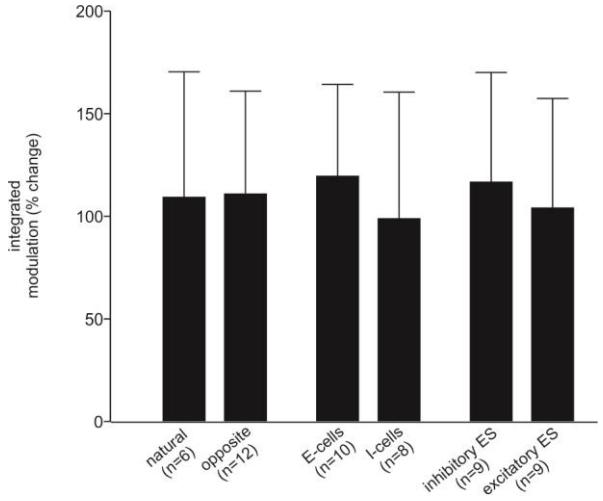


**Figure 2.10. Properties of negative images.** Data from pairing experiments with two-site tectal microstimulation pooled in three different ways. *Left:* In our experiments, we randomly assigned the relationship between the microstimulation site and the polarity of the look-up table waveform. This had the effect of establishing either a "natural" relationship, in which the local ES increased with the microstimulation site that evoked an ipsilateral movement (as would be expected to be the case for most ELL neurons under natural conditions), or an opposite relationship, in which the local ES decreased with the same microstimulation site. We found no significant difference between negative images formed with natural vs. opposite relationship (natural, % change in integrated modulation: 109±61%; opposite, % change in integrated modulation: 111±50%; p=0.95, two-sample t-test). *Middle:* ELL includes both E-cells, which are excited by an increase in ES amplitude, and I-cells, which are inhibited by the same stimulus. We found that both cell types formed robust negative images, and there was no significant difference between cell types (E-cells: 120±44%; I-cells: 99±61%; p=0.42, two-sample t-test). *Right:* ELL cells were capable of forming both excitatory and inhibitory negative images, depending on the polarity of the response evoked by the ES during pairing. We found no significant difference between negative images whether the ES excited the cell or inhibited the cell (excited: 104±53%; inhibited: 116±53%; p=0.60, paired t-test). Integrated modulations were computed by summing normalized spike rate histograms over a small window (~100 ms) and then taking the absolute value (to ease comparison of inhibitory vs. excitatory negative images). Error bars represent standard deviation.

**Negative images based on corollary discharge and proprioception require spinal input**

Given that previous studies have provided evidence for negative images based on proprioception (Sawtell and Williams 2008; Sawtell 2010), we wished to test whether negative images would still be formed based on corollary discharge signals under more natural conditions in which proprioceptive information related to movements was also available. To address this question, we induced negative images by pairing under conditions in which both corollary discharge and proprioception were activated. Tectal stimulation was delivered as before but paired with a passive displacement of the tail that matched the onset relative to tectal stimulation and time-course of the evoked movement measured prior to paralysis. Hence, in these experiments, the ES was, in principle, predictable based on both corollary discharge signals and proprioceptive signals. Comparing ELL principal cell responses to tectal stimulation alone or passive tail displacement alone before such pairings revealed that negative images were formed based on both corollary discharge and proprioceptive signals (**Figures 2.11a and 2.11b**; n=6). These results demonstrate that motor corollary discharge signals are still used even when sensory information related to movements is available, as would normally be the case.

Though our mossy fiber recordings suggest a spinal origin for corollary discharge signals, we wished to directly test whether negative images depended on ascending spinal input. In the same set of experiments described above, we injected a small volume (~1 uL) of lidocaine into the spinal cord after inducing negative images. Injections were done in a separate surgical site several centimeters from the recording site, and effectiveness was judged by disappearance of the electromotor command signal. We found that lidocaine completely abolished negative images (**Figures 2.11aand 2.11b**; n=6), without a significant change in baseline firing rate (pre-lidocaine: 14.66$\pm$8.47 Hz; post-lidocaine: 16.46$\pm$14.47 Hz, n=6, p=0.688, sign test). These

results suggest that under natural conditions negative images are formed based on both corollary discharge and proprioceptive signals conveyed to ELL via the spinal cord.

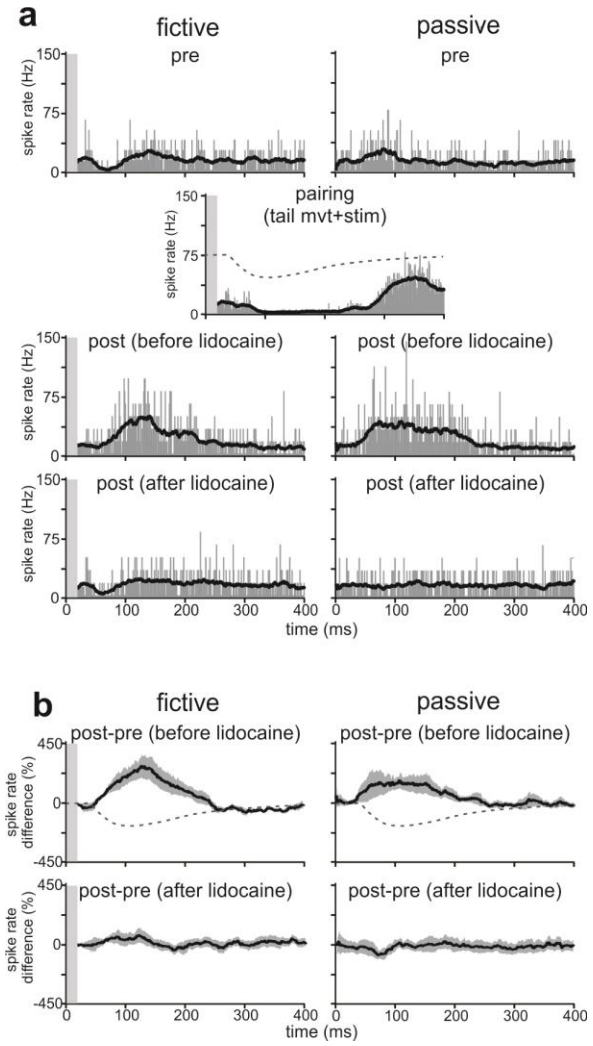


**Figure 2.11. Negative images depend on corollary discharge and proprioceptive signals conveyed by an ascending spinal mossy fiber pathway.** Negative images were induced in ELL principal cells under the conditions that mimic real movements (simultaneous rapid tail movements driven by a computer-controlled stage and tectal microstimulation), and then probed under the fictive (tectal microstimulation alone) and passive conditions (tail movements alone). **(a)** *Left column:* Smoothed spike rates from an extracellular recording of an ELL principal cell illustrating typical response patterns as a function of time relative to microstimulation of the optic tectum before, (pre, top row), during (during, second row), and after (post, third row) pairing with a local ES (dotted gray line). *Right column:* Same as left column except histograms are triggered by onset of tail movement. Non-smoothed histograms shown in gray (1 ms bins). **(b)** *Top row:* Average of difference traces pooled across cells probed under fictive (left) and passive (right) conditions. *Bottom row:* Following injection of 2% lidocaine into the spinal cord, negative images were abolished under both conditions, suggesting a spinal origin for both proprioceptive and corollary discharge signals. Error bars represent SEM across cells. Gray boxes obscure microstimulation artifacts.

**Discussion**

Here we use an advantageous model system to demonstrate that a spinal corollary discharge pathway is used to form flexible and highly-specific negative images of the sensory consequences of motor commands at the level of individual neurons. Though the capacity to generate learned predictions about the sensory consequences of movements based on plastic corollary discharge is likely critical for sensory, motor, and cognitive functions in many species, neural correlates for such predictions, as shown here, have not been well characterized in other systems.

A major finding of the present study is that, in addition to previously described EOCD signals related to highly-specialized electromotor behavior (Bell, Finger et al. 1981; Bell, Libouban et al. 1983; Bell, Grant et al. 1992; Bell, Dunn et al. 1995), ELL also receives corollary discharge signals related to movements. In contrast to EOCD signals, which merely relay the time of occurrence of the EOD, we show that movement-related corollary discharge signals convey graded information about the parameters of different types of movements (frequency in the context of rhythmic swimming and movement vigor and direction in the context of movements evoked by tectal microstimulation). The presence of varied and graded corollary discharge signals is consistent with the possibility, suggested by previous models of ELL function, that information relayed via mossy fibers and granule cells acts as a basis for generating negative images of the sensory consequences of movements via anti-Hebbian plasticity (Bell 1981; Bell, Caputi et al. 1993; Bell, Han et al. 1997; Roberts and Bell 2000). Several lines of evidence presented here, together with previous anatomical studies (Szabo, Libouban et al. 1979; Bell, Finger et al. 1981; Szabo, Libouban et al. 1990), strongly suggest that corollary discharge inputs to ELL related to tail and trunk movements originate largely, if not

exclusively, from the spinal cord. Spinocerebellar pathways conveying motor signals have been extensively studied in mammals (Oscarsson 1965; Arshavsky, Gelfand et al. 1978; Hantman and Jessell 2010; Jankowska, Nilsson et al. 2011; Fedirchuk, Stecina et al. 2013; Spanne and Jorntell 2013). The possible utility of such an ascending spinal corollary discharge in relation to negative image formation in ELL will be discussed below. Though not studied here, movements of the flexible chin appendage may also be associated with a corollary discharge (Engelmann, Nobel et al. 2009). If such signals exist they would be expected to be relayed via a separate brainstem pathway (Maler, Karten et al. 1973; Szabo, Libouban et al. 1979; Bell, Finger et al. 1981).

Though previous studies of cerebellum-like structures have provided evidence for predictions based on corollary discharge signals, these accounts have been limited to simple, highly-stereotyped behaviors, i.e. ventilation in elasmobranch fish (Bodznick, Montgomery et al. 1999) and the EOD in weakly electric mormyrid fish (Bell 1981). Whereas the EOD motor command is simple and completely stereotyped, movement motor commands are obviously more complex and diverse. Hence, a key question is whether mechanisms described previously for predicting effects of the EOD, i.e. anti-Hebbian plasticity acting on corollary discharge inputs to principal cells, are sufficient for predicting the much greater variety of sensory patterns generated by movements. Two observations suggest that the capacity for forming and storing negative images related to movement motor commands exceeds that described previously in the context of electromotor behavior and may indeed be sufficient for predicting sensory consequences of movements. First, ELL neurons form negative images based on either MLR or tectal microstimulation; i.e., predictions are formed for different movements initiated by different brain structures. Such a capacity differs from the electromotor system in which the same motor command is initiated in a stereotyped fashion from a single brain structure. Second, individual

ELL neurons are capable of simultaneously generating and storing two different negative images related to microstimulation of two distinct sites in the tectum. Though technical limitations prevented us from probing this capacity further, given the diversity of graded motor signals observed in mossy fibers together with the fact that each MG cells receives ~20,000 parallel fiber inputs and that ~30 MG cells converge onto each output cell (Meek, Grant et al. 1996; Bell, Meek et al. 2005), we expect that many more negative images could be stored.

Our results imply that ELL circuitry solves the complex problem of transforming copies of movement motor commands into a format appropriate to cancel their sensory consequences. Whereas bursts and pauses in mossy fibers evoked by tectal stimulation were stereotyped and brief, negative images in ELL neurons accurately match the temporal profiles of the fictive movements, which were substantially delayed relative to mossy fiber responses. Cancelling the effects of the fish's own EOD poses a similar problem: EOD motor command signals conveyed by mossy fibers are much briefer in duration than the effects of the EOD on passive electroreceptors (Bell and Russell 1978). EGp circuitry solves this problem by transforming stereotyped and minimally delayed EOD motor command signals conveyed by mossy fibers into granule cell responses that are more delayed and diverse (Kennedy, Wayne et al. 2014). Such granule cell responses provide a basis for sculpting temporally-specific negative images via anti-Hebbian plasticity at parallel fiber synapses onto ELL neurons. A class of excitatory interneuron, the unipolar brush cell, appears to play a key role in generating delayed responses in granule cells. The accessibility of granule cells to in vivo recordings will allow us to test whether similar mechanisms could account for the ability to predict movement consequences that are extended in time relative to motor commands.

The need to transform motor signals into a format appropriate to predict sensory input may also provide a rationale for an ascending spinal corollary discharge. Previous studies in other fish species have suggested that tonic locomotor drive from the MLR is transformed into phasic motor commands for swimming within spinal circuitry (Deliagina, Zelenin et al. 2002; Uematsu, Baba et al. 2007; Kyriakatos, Mahmood et al. 2011). Given that opposite tail movements will typically have opposite electrosensory consequences, a phasic signal returning from the spinal cord would be expected to provide a better basis for negative image formation than a tonic signal from the MLR itself. Since all tail and trunk commands are ultimately issued via the spinal cord, this suggests the intriguing possibility that, in this system at least, ascending spinal corollary discharge pathways may be sufficient for predicting the sensory consequences of a wide range of movements. These results may have implications for the functions of spinocerebellar pathways in mammals. Though it is well-established that mammalian spinocerebellar pathways convey motor signals (Oscarsson 1965; Arshavsky, Gelfand et al. 1978; Hantman and Jessell 2010; Jankowska, Nilsson et al. 2011; Fedirchuk, Stecina et al. 2013; Spanne and Jorntell 2013), roles for such pathways in predicting sensory consequences of motor commands have, to the best of our knowledge, not been clearly defined.

Real movements activate proprioception which provides an additional source of information that might be sufficient to cancel self-generated electrosensory input in the absence of corollary discharge (Bell, Grant et al. 1992; Sawtell and Williams 2008; Sawtell 2010). Our results show that both corollary discharge and proprioceptive signals are used under conditions that simulate real movements. An interesting question for future studies is how corollary discharge and proprioceptive feedback interact at the levels of mossy fibers, granule cells, and ELL principal cells, under natural conditions in which both signals are available.

Converging lines of evidence from theoretical (Wolpert, Miall et al. 1998; Anderson, Porrill et al. 2012), human behavioral (Bastian 2006; Izawa, Criscimagna-Hemminger et al. 2012), and electrophysiological investigations (Pasalar, Roitman et al. 2006; Ebner and Pasalar 2008; Brooks and Cullen 2013) suggest that the mammalian cerebellum is involved in generating internal models that predict the sensory consequences of motor commands. Internal models may have a variety of functions, from cancelling effects of self-generated sensory inputs (Cullen 2004; Angelaki and Cullen 2008) to online correction of rapid movements (Wolpert and Miall 1996). Though the existence of such internal models is widely accepted, how they are implemented in cerebellar circuitry remains largely unknown. Established roles for granule cells and parallel fiber plasticity in generating negative images in ELL (Bell 1981; Bell, Han et al. 1997; Roberts and Bell 2000; Kennedy, Wayne et al. 2014) closely resemble those proposed by leading theories of mammalian cerebellar function (Marr 1969; Albus 1971; Fujita 1982; Medina, Garcia et al. 2000; Dean, Porrill et al. 2010). In light of this correspondence, mechanisms for predicting sensory consequences of movements revealed here for the cerebellum-like circuitry of the mormyrid ELL may be expected to closely resemble those at work in the cerebellum itself.

## Experimental Procedures

### *Experimental Preparation*

All experiments performed in this study adhere to the American Physiological Society's *Guiding Principles in the Care and Use of Animals* and were approved by the Institutional Animal Care and Use Committee of Columbia University. Approximately 60 mormyrid fish (7-14 cm in length) of the species *Gnathonemus petersii* were used in these experiments. Surgical procedures

to expose EGp for recording were similar to those described previously(Sawtell, 2010). In a subset of experiments an additional anterior portion of the skull was removed to expose the optic tectum. The anesthetic (MS-222, 1:25,000) was then removed. To evoke tail movements, we targeted microelectrodes (tungsten, 0.005" diameter, 5 MOhm, 12 deg beveled tip, A-M Systems, Sequim, WA) to either the MLR, the optic tectum, or, in some experiments, to both. Continuous (40 or 100 Hz) microstimulation (50-100 uA) of the MLR evoked slow rhythmic (1-6 hz) swimming movements. Brief, high-frequency (10-15 pulses at 500 Hz) microstimulation of either the MLR or the tectum evoked rapid, isolated tail movements. When we microstimulated in two sites at the optic tectum, the anterior site evoked ipsilateral movements while the posterior site evoked contralateral movements, consistent with previous reports in goldfish (Herrero, Rodriguez et al. 1998). The fish rarely moved outside of microstimulation protocols. A laser displacement sensor (LK-503, Keyence Corporation, Woodcliff Lake, NJ) measured tail displacement from the midline (spatial precision: 50 µm; measurement delay: 2 ms). After tail movements were measured, gallamine triethiodide (Flaxedil) was given (~20 ug/cm of body length) to paralyze the fish. Paralysis blocks the effect of motor neurons on all muscles, including the electric organ, which prevents the EOD. The motor command signal that would normally elicit an EOD continues to be generated by the fish at a variable rate of 2 to 5 Hz. The EOD motor command can be measured precisely (see below). In a subset of experiments we recorded from spinal nerves to observe the motor command that would normally elicit swimming in an unparalyzed fish (see below). This preparation allows us to observe the central effects of movement-related corollary discharge in isolation from the electrosensory input that would normally result in an EOD and in isolation from the proprioceptive input that would normally occur as a result of movements.

*Electrophysiology*

The EOD motor command signal was recorded with an electrode placed over the electric organ in the tail. Spinal nerve recordings were performed as described previously for goldfish (Fetcho and Svoboda 1993). Briefly, the spinal nerves were exposed at a point rostral to the tail, but in the caudal half of the fish. A fire-polished, glass suction electrode was used to record extracellularly from the dorsal ramus of the ventral root, a nerve that innervates epaxial white musculature. Signals from the recording electrode were filtered (100 Hz high pass and 300 Hz low pass) and amplified (Warner Instruments, Hamden, CT, Model DP-311). Root burst frequency showed a clear dependence on current intensity at low current amplitudes (50-100uA).

Extracellular recordings from mossy fibers were made with glass microelectrodes filled with 2M NaCl (40-100 MOhm). Criteria for distinguishing mossy fiber recordings from other EGp units were the same as those described previously (Bell, Grant et al. 1992; Sawtell 2010). Extracellular recordings from the medial zone of ELL were made with glass microelectrodes filled with 2M NaCl (8-10 MOhm). Identification of ELL cell types was aided by previous intracellular recording and labeling studies in which characteristic EOCD and electrosensory responses were linked with cell morphology (Bell and Grant 1992; Bell, Caputi et al. 1997; Mohr, Roberts et al. 2003). Because ELL is a laminar structure, with different cell types located in different layers, recording location is also useful in identifying cell types. The laminar location of the recording electrode within ELL can be accurately judged based on characteristics of prominent EOCD- and electrosensory stimulus-evoked field potentials (Bell and Grant 1992; Bell, Grant et al. 1992). ELL cells can be broadly classified as E- or I-cells: E-cells are excited by an increase in local EOD amplitude in the center of their receptive fields, and I-cells are inhibited by such a stimulus. We recorded from I-cells located in or just above the ganglion

layer, which likely included both interneurons (MG1 cells), and efferent neurons known as large ganglion (LG) cells. We also recorded from E-cells located below the ganglion layer, which were probably efferent neurons known as large fusiform (LF) cells.

In vivo whole cell recordings from MG cells in ELL were made using methods described previously (Sawtell 2010). Electrodes (9-12 MOhm) were filled with an internal solution containing K-gluconate (122 mM), KCl (7 mM), HEPES (10 mM), $Na_2ATP$ (0.5 mM), MgATP (2 mM), EGTA (0.5 mM), and 0.5% biocytin (pH 7.2, 280-290 mOsm). No correction was made for liquid junction potentials. Only cells with stable membrane potentials more hyperpolarized than -50 mV and access resistance < 100 MOhm were analyzed. All experiments were performed without holding current, unless otherwise noted. Membrane potentials were filtered at 3-10 kHz and digitized at 20 kHz (CED Power1401 hardware and Spike2 software; Cambridge Electronics Design, Cambridge, UK).

*Dendritic Spike Pairing Experiments*

Dendritic spike pairing experiments were conducted using intracellular recordings from MG cells using methods described previously (Bell, Caputi et al. 1993; Sawtell, Williams et al. 2007; Sawtell 2010). In these experiments, we paired a brief intracellular current injection to evoke a single dendritic spike (12-15 ms; 100-600 pA) at a fixed delay to one microstimulation site that evoked tail movements prior to paralysis. The neural response to microstimulation alone was compared immediately before and after the pairing period (1-2 minutes of data were used for analysis). Cells in which resting membrane potential, access resistance, or spike height changed substantially over the course of the experiment were excluded from the analysis.

*Electrosensory Stimulus (ES) Pairing Experiments*

ES pairing experiments were conducted using extracellular recordings from ELL principal cells. Cells that did not show plasticity (roughly 15% of all recorded cells) under any condition were excluded from the analysis. This is not unexpected, as there are known non-plastic cell types in ELL (Mohr, Roberts et al. 2003).

Electrosensory responses were evoked by simultaneous global stimulation of the entire fish and local stimulation restricted to small area of the skin. Global stimuli were delivered by passing current between a small chloride silver ball inserted through the mouth in to the stomach of the fish and a second electrode placed in the water near the tail of the fish in an outside-positive configuration. The ES referred to in the paper is the modulation of the local field. Local stimuli were delivered with a bipolar stimulating electrode consisting of two small Ag-AgCl balls 5 mm apart. The electrode was held perpendicular to the skin at a distance of ~2 mm. For both global and local stimuli, brief pulses of current were delivered 4.5 ms after EOD command through the electrodes to activate electroreceptors. Absolute current strength for local stimuli ranged from 5uA-10uA while current strength for global stimuli ranged from 200-400mA. These values were chosen such that the amplitude of electrosensory-evoked field potentials could be both increased and decreased by the local stimulus, roughly mimicking the changes in EOD-evoked field potentials measured in response to tail movements in a previous study in which the natural EOD was left intact (Sawtell and Williams 2008). Small adjustments to the local amplitude were made on a cell-by-cell basis to strongly excite or inhibit the cell with minimal current. In a subset of experiments, we controlled EOD motor command rate by lowering a concentric bipolar stimulating electrode (FHC, Bowdoin, ME) into the brain along the midline in or near the axons of the precommand nucleus, which course close to the midline along the ventral surface of the

brainstem to the command nucleus (~ 5mm depth). Brief, single pulses of 0.2 ms reliably evoked an EOD motor command at low current strengths (10-20 uA), allowing experimental control over discharge frequency when necessary. We typically microstimulated the EOD command at ~13 Hz. In experiments in which spinal inactivation was performed, electrosensory stimuli were delivered at a fixed delay from the microstimulation pulse as the EOD motor command could not be measured.

In ES pairing experiments, we varied the amplitude of the local ES in the center of the recorded cell's receptive field to deliver a time-varying pattern of electrosensory stimulation based on the waveform of the tail movement recorded prior to paralysis. Since amplitude in local EOD amplitude is proportional to tail displacement for small angles, such a protocol approximates the electrosensory consequences induced by real tail movements. Microstimulation was always separated by at least 1.25 seconds. Pairing was conducted for 10-15 minutes. The neural response to microstimulation alone was compared immediately before and after the pairing period.

For the experiments conducted in **Figure 2.11**, we only microstimulated the anterior tectal site that evoked ipsilateral movements. Tail displacement was measured by a laser and then that signal was fed back into the servomotor to deliver passive tail movements that mimicked the microstimulation-evoked movement prior to paralysis. The fish's tail was lightly held between two glass rods positions posterior to the electric organ. The rods were held by a manipulator mounted to a computer-controlled servomotor (Pacific Laser Equipment, Santa Ana, CA). A partition was placed between the tail and the rest of the fish to prevent water waves from activating lateral line receptors.

In these experiments, we examined neural responses before and after pairing under two conditions: (1) *fictive*, in which we delivered microstimulation alone; (2) *passive*, in which we delivered the tail movement alone. To simulate real movements, pairing was conducted under conditions in which we delivered both the microstimulation and the tail movement simultaneously. Prior to recording, a pipette containing a solution of 2% lidocaine HCl (Sigma-Aldrich, St. Louis, MO) in 0.9% NaCl was lowered into the spinal cord at a separate surgical site several centimeters from the recording site. After inducing plasticity, a small volume of lidocaine solution (~1 uL) was injected by manual pressure into the spinal cord. The neural response was recorded continuously and data collected starting at approximately 2 min following injection. Spinal inactivation was confirmed by the disappearance of the EOD motor command.

*Data Analysis and Statistics*

Data analysis was performed offline in MATLAB (MathWorks, Natick, MA) and Spike2 (Cambridge Electronic Design). Data are expressed as mean ± standard deviation (SD), unless otherwise noted. Tests for statistical significance are noted in the text. Differences were judged to be significant at $p<0.05$.

Power spectral density functions were constructed in Spike2 by first smoothing spikes with a small Gaussian window (20 ms), then using a Fast Fourier Transform (FFT) to convert the waveform data into a power spectrum, implemented with a Hanning window.

# CHAPTER 3

# RANDOM NONLINEAR MIXTURES OF COROLLARY DISCHARGE AND PROPRIOCEPTION AS A BASIS FOR PREDICTING SENSORY CONSEQUENCES OF MOVEMENTS IN A CEREBELLUM-LIKE CIRCUIT

# CHAPTER 3: RANDOM NONLINEAR MIXTURES OF COROLLARY DISCHARGE AND PROPRIOCEPTION AS A BASIS FOR PREDICTING SENSORY CONSEQUENCES OF MOVEMENTS IN A CEREBELLUM-LIKE CIRCUIT

## Introduction

Distinguishing between patterns of sensory receptor activation due to an animal's own movements and those due to external events is vital for stable perceptions and accurate motor control (Sperry 1950; von Holst 1950). Though mechanisms for solving this fundamental problem have been explored in different brain regions in a number of model organisms (Cullen 2004; Poulet and Hedwig 2007; Crapse and Sommer 2008), important questions remain. Self-generated movements simultaneously engage motor corollary discharge signals as well as multiple sensory input streams, e.g. visual, proprioceptive, and vestibular. Though in principle both corollary discharge and sensory feedback could be used to distinguish between movement-related and external stimulation, there are few cases in which their respective roles have been extensively explored (Guthrie, Porter et al. 1983; Wang, Zhang et al. 2007; Wurtz 2008). Here we use *in vivo* electrophysiological recordings and modeling to address this issue in an advantageous model system in which circuitry and plasticity underlying the generation of cancellation signals are relatively well-understood and accessible to study.

Weakly electric mormyrid fish possess an electric organ in their tails that emits a weak electrical pulse, known as the electric organ discharge (EOD). Electroreceptors distributed over the body surface are sensitive to changes in the amplitude and waveform of the pulse. One challenge for the electrosensory system is to distinguish spatial and temporal variations in pulse amplitude and waveform due to objects in the environment from changes due to the fish's own movements. This challenge may be severe—movements alter the position of the electric organ relative to electroreceptors on the skin and thereby produce changes in electrosensory input

much larger than those associated with behaviorally relevant objects in the environment, such as invertebrate prey (Bastian 1995; Chen, House et al. 2005; Sawtell and Williams 2008; Fotowat, Harrison et al. 2013). A combination of experimental and modeling studies suggest that cancellation of predictable electrosensory inputs takes place in ELL, the first stage of central processing. ELL principal cells integrate input from electroreceptors with a variety of signals conveyed via a mossy fiber-granule cell-parallel fiber system similar to that found in the cerebellum (Bell, Han et al. 2008). These include electric organ corollary discharge (EOCD) signals related to the fish's EOD motor command, movement corollary discharge signals related to motor commands for swimming, and proprioceptive feedback conveying information about the position and movements of the body **(Figure 3.1)** (Maler, Karten et al. 1973; Szabo, Libouban et al. 1979; Bell, Finger et al. 1981; Szabo, Libouban et al. 1990; Bell, Grant et al. 1992; Sawtell 2010; Requarth and Sawtell 2013; Kennedy, Wayne et al. 2014). Anti-Hebbian spike timing dependent plasticity at parallel fiber synapses onto principal cells generates negative images that serve to cancel out components of principal cell responses that are predictable based on parallel fiber inputs (Bell 1981; Bell, Han et al. 1997; Roberts and Bell 2000; Kennedy, Wayne et al. 2014).

Previous studies of mormyrid fish have provided evidence for negative images based on proprioception in the context of passive tail displacements and for negative images based on corollary discharge in the context of fictive tail movements (Sawtell and Williams 2008; Requarth and Sawtell 2013). The goal of the present study was to understand the respective roles of corollary discharge and proprioceptive signals under more natural circumstances in which both signals are engaged. To address this issue we developed a preparation that allowed us to engage corollary discharge and proprioception either in isolation or together and to evaluate their

contributions to negative image formation. In addition, we developed a mathematical model that linked properties of negative images to the representation of corollary discharge and proprioceptive signals in mossy fibers and granule cells.

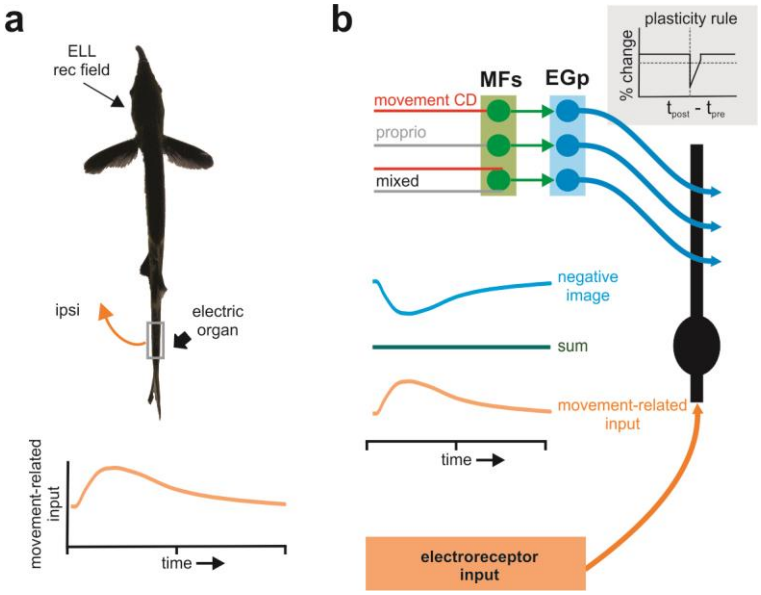


**Figure 3.1. Scheme for predicting movement consequences in ELL. (a)** For some ELL neurons (depending on the location of their receptive field on the body), self-generated changes in the electric field due to movements of the electric organ in the tail (filled arrow) are proportional to tail displacement from the midline, with tail movements towards the side of the receptive field resulting in an increase in the local electric field amplitude and an increase in electroreceptor activation. The sensory consequences of an ipsilateral tail movement as a function of time are schematized in the bottom panel. **(b)** ELL principal cells integrate electrosensory input with a variety of sensory and motor signals conveyed via a mossy fiber-granule cell pathway. Granule cells are located in an external cell mass, known as the eminentia granularis posterior (EGp) and receive excitatory mossy fiber input from a variety of sources. Previous studies have described mossy fibers conveying movement-related CD information and proprioceptive input, but whether these signals are conveyed separately in mossy fibers or are mixed is unknown. Anti-Hebbian plasticity at synapses between granule cells and ELL principal cells underlies the cancellation of predictable patterns of electrosensory input.

## Results

### Nonlinear interactions between negative images based on corollary discharge and proprioception

Changes in electrosensory input occur whenever the electric organ in the tail moves relative to electroreceptors on the skin. For movements caused by external forces such changes could be cancelled by proprioceptive feedback. On the other hand, for self-generated movements such

changes could be cancelled based on corollary discharge, proprioceptive feedback, or some combination of both. To understand how negative images are actually formed under these various circumstances, we performed a series of experiments in which we compared responses of ELL neurons before and after pairing electrosensory input under conditions in which only corollary discharge was engaged, only proprioceptive feedback was engaged, or both were engaged. To carry out these experiments, we used a previously developed "fictive" movement preparation (Requarth and Sawtell 2013). Prior to paralysis, microstimulation of the optic tectum evokes a rapid tail movement that moves the electric organ closer to the receptive field of the recorded cell. After paralysis, microstimulation evokes motor commands in the absence of movement, allowing us to monitor the effect of corollary discharge signals on neural responses in the absence of proprioceptive feedback. In addition, we can move the tail passively with a computer-controlled stage in a way that mimics the movement evoked by tectal microstimulation prior to paralysis. This setup allows us to engage corollary discharge and proprioceptive inputs either separately or together and, as described next, to control their relationship to an electrosensory stimulus.

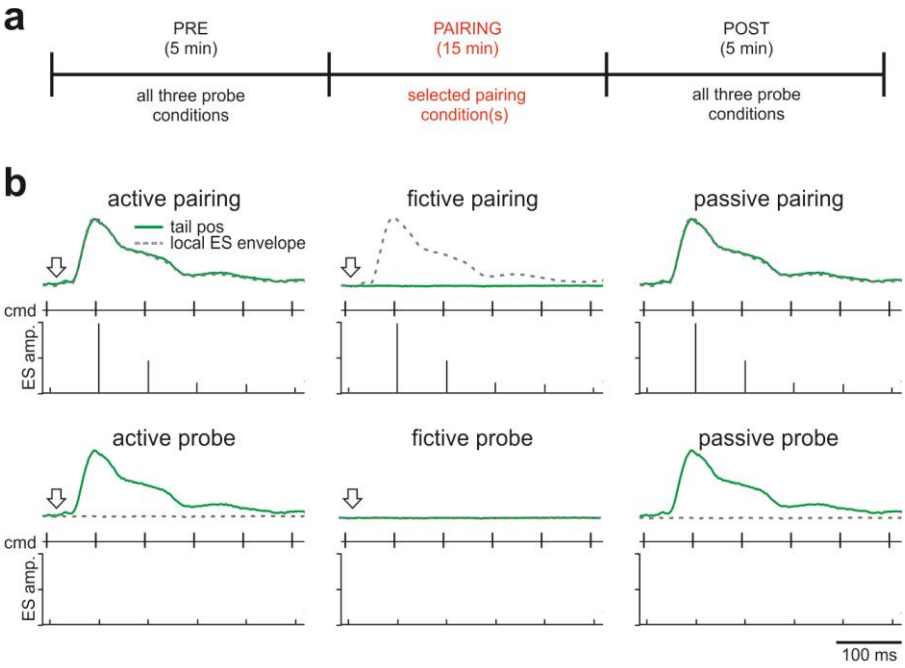


**Figure 3.2. Schematic of pairing experiment protocols.** (**a**) In all experiments, ELL principal cell responses were recorded extracellularly under three conditions (active, fictive, and passive; described below) before and after a 15-minute pairing period with an ES under one or more of these conditions. (**b**) The three conditions are as follows: *active*, in which we microstimulated the optic tectum in a paralyzed fish while delivering a rapid tail movement that matched the temporal profile of the microstimulation-evoked movement prior to paralysis; *fictive*, in which tectal microstimulation was delivered in the absence of a tail movement; and *passive*, in which a rapid tail movement was delivered without microstimulation. For each condition, during pairing the ES was modulated in a pattern that matched the temporal profile of the tail movement prior to paralysis (top row). Before and after pairing, in which the ES was unmodulated, we refer to as "probes" (bottom row). In each panel, the top green trace represents passive tail movements. The dotted gray trace is the waveform envelope used to determine the amplitude of the local ES. The middle row shows the timing of the EOD motor commands. Note constant rate of 13 Hz due to microstimulation of the EOD command pathway. The bottom row shows a local ES, placed in the receptive field of the recorded cell. The amplitude was set to the value of the envelope at the time of the command. A constant-value global ES was delivered in conjunction with the local one. The arrow, where present, represents the time of microstimulation.

We explored the interactions between corollary discharge and proprioception by recording from ELL principal cells under three conditions before and after pairing with a local electrosensory stimulus (ES). During the pairing we modulated the ES in a pattern that matched the temporal profile of the tail movement, and paired with one or more conditions (**Figure 3.2a**). We refer to conditions in which the ES was unmodulated as "probes." The pairing and probe conditions are schematized in **Figure 3.2b**. The conditions are as follows: *active*, in which we

microstimulated the optic tectum in a paralyzed fish while delivering a rapid tail movement that matched the temporal profile of the microstimulation-evoked movement measured prior to paralysis, thereby engaging both corollary discharge and proprioceptive feedback; *fictive*, in which tectal microstimulation was delivered in the absence of a tail movement, thereby engaging corollary discharge without proprioceptive feedback; and *passive*, in which a rapid tail movement was delivered without microstimulation, thereby engaging proprioceptive feedback without corollary discharge.

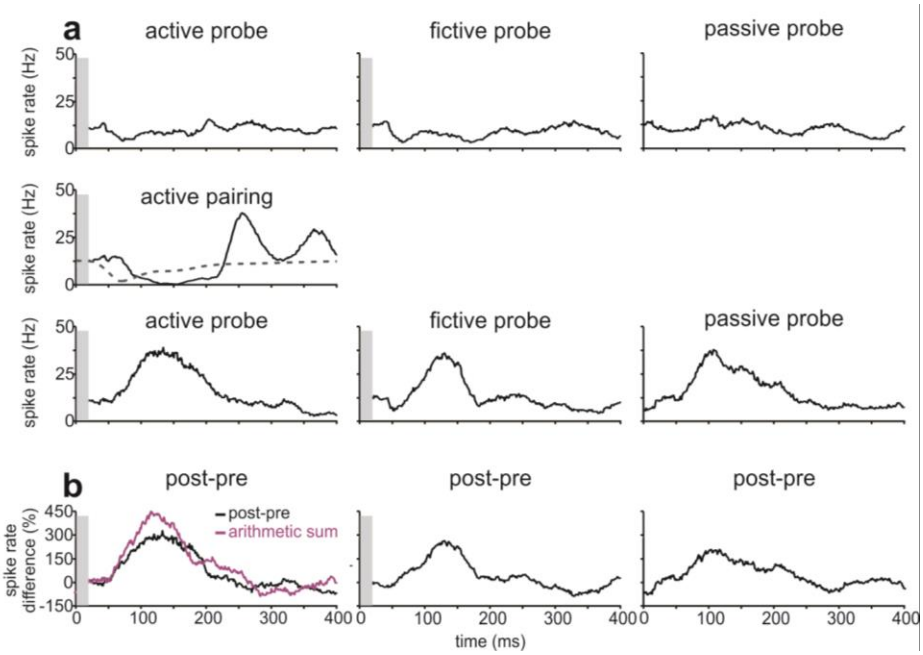


**Figure 3.3. ELL neurons exhibit negative images when paired under the active condition.** (**a**) Representative ELL neuron recorded extracellularly while being paired under the active condition. Before pairing, the neuron exhibited little response to the active, fictive, and passive probe conditions (top row). During pairing, the neuron was inhibited by an ES that was modulated in a pattern that matched the temporal profile of the tail movement prior to paralysis (middle panel). After pairing, the neuron exhibited strong responses under all three probe conditions that were opposite in polarity and roughly matched the temporal profile of the response evoked by the ES during pairing (bottom row). (**b**) Difference traces reveal negative images under all three conditions. Note that the arithmetic sum of the fictive and the passive (purple) is less than the response observed under the active condition. In all panels, gray bars obscure microstimulation artifacts.

Data from one neuron in which an ES was paired under the active condition is shown in **Figure 3.3**. Before pairing the neuron exhibited little response under active, fictive, or passive

probe conditions (**Figure 3.3a**, top row). After pairing the neuron exhibited a strong response during the active probe that was opposite in polarity and roughly matched in time to the response evoked by the ES during pairing, i.e. the change in the response (**Figure 3.3b**, post-pre) resembled a negative image of the effect of the ES during pairing. Interestingly, negative images were also observed under fictive and passive probe conditions (**Figure 3.3b**). These results suggest that both CD and proprioceptive feedback are used to generate negative images if both signals are available. Moreover, negative images based on CD and proprioceptive feedback appeared similar in their magnitude and timing. Results for all *active* pairings (n=9), along with those for pairings conducted under the *fictive* and *passive* conditions are summarized in **Figure 3.4**. Pairing under fictive or passive conditions revealed negative images for the paired condition but not for the unpaired condition (fictive, n=9; passive, n=8; **Figure 3.4b and 3.4c**). Hence negative images can be formed using either CD or proprioceptive feedback alone and do not "transfer" across modalities.

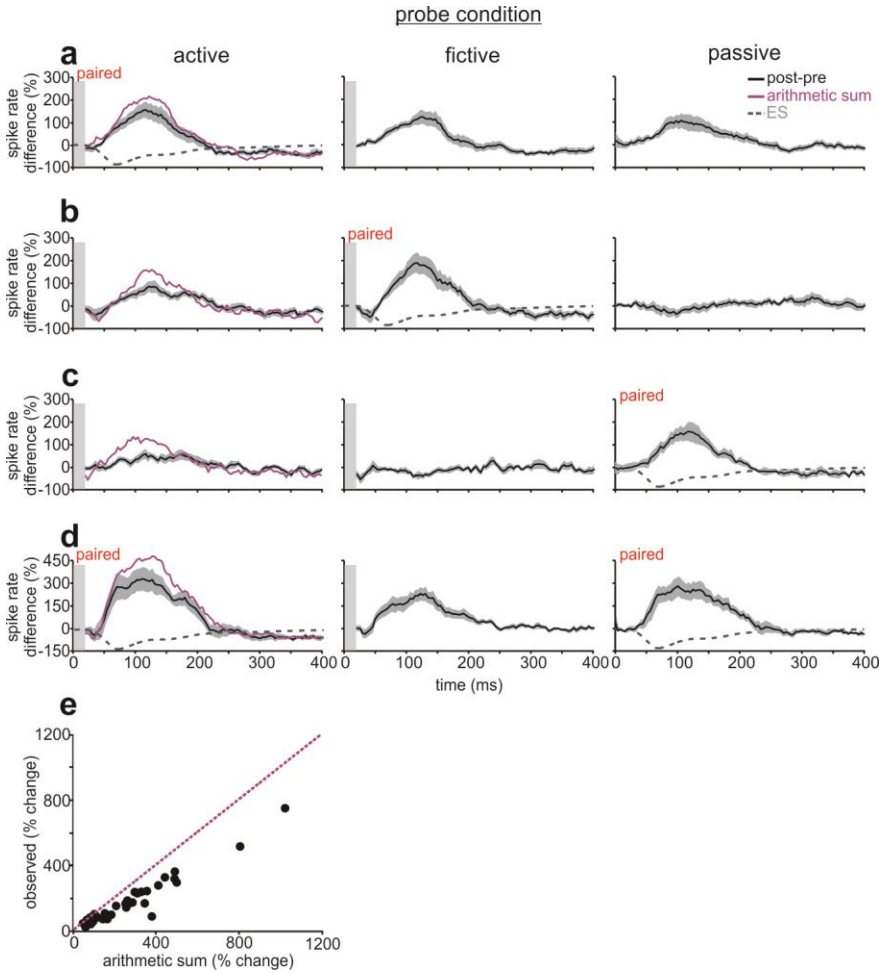


**Figure 3.4. Nonlinear interactions between CD and proprioception provide a flexible basis for negative images. (a)** *Active pairing.* Average of difference traces across ELL neurons showing effects of pairing under active conditions, during which an ES was paired with simultaneous tectal microstimulation and a rapid tail movement. *Left panel:* Difference trace measured under the paired (active) condition. *Middle panel:* Difference trace measured when probing under the fictive condition. *Right panel:* Difference trace measured when probing under the passive condition. Note that the passive and fictive contributions do not add up linearly (purple line is arithmetic sum of fictive and passive traces). **(b)** *Fictive pairing.* Average of difference traces across principal cells showing effects of pairing under fictive conditions, during which an ES was paired with tectal microstimulation alone. Note that probing under active conditions reveals a reduced negative image relative to the arithmetic sum (purple). **(c)** *Passive pairing.* Average of difference traces across principal cells showing effects of pairing under passive conditions, during which an ES was paired with a rapid tail movement alone. Note that probing under active conditions reveals a reduced negative image. **(d)** *Pairing alternately under active and passive conditions.* Average of difference traces across principal cells showing effects of pairing under active and passive conditions, during which an ES was alternately paired with rapid tail movements alone followed by simultaneous rapid tail movements and microstimulation. These conditions approximate situations in which changes in electrosensory input occur both as a result of self-generated tail movements and tail movements due to external forces. Note that similar negative images were formed in both trained conditions (left- and rightmost panels) despite a robust contribution from CD signals (middle panel). **(e)** Scatterplot of all recorded cells, plotting the observed response under the active condition vs. the arithmetic sum of the fictive and passive conditions. Note that nearly all dots lie below the unity line (dotted purple). In all panels, gray outlines indicate s.e.m across cells and gray bars obscure microstimulation artifacts.

Unexpectedly, we found that when both the paired and unpaired signals were engaged (**Figure 3.4**, active probes) negative images were reduced, i.e. negative images observed under the active condition were less than the arithmetic sum of the responses observed under the passive and fictive conditions (fictive, arithmetic: 199±113% change in integrated modulation, observed: 117±58% change in integrated modulation, n=9, p=0.027; passive, arithmetic: 168±106% change in integrated modulation, observed: 85±55% in integrated modulation, n=8, p=0.0035, paired t-test) (**Figure 3.4b-d, left panels**). Hence the presence of the unpaired signal suppresses the negative images based upon the paired signal.

Nonlinear interactions could provide the flexibility required for generating negative images based on different but overlapping sets of signals, e.g. CD and proprioception under active conditions and proprioception alone under passive conditions. Such a capacity might be functionally relevant, because a given change in the position of the electric organ relative to electroreceptors will have the same electrosensory consequence regardless of whether it is self-generated (engaging both corollary discharge and proprioception) or due to external forces (engaging proprioception alone). To address this possibility, we performed an additional series of experiments in which we paired the ES alternately under active and passive conditions. ELL neurons exhibited a capacity to form similar negative images based on corollary discharge and proprioception (active probe, **Figure 3.4d**) or on proprioception alone (passive probe, **Figure 3.4d**). Moreover, as expected for a nonlinear system but not a linear one, probing under fictive conditions revealed a contribution from CD signals (**Figure 3.4d, middle panel)**. Also consistent with a nonlinear system, the scatter plot of all recorded cells depicted in **Figure 3.4e** shows that the arithmetic sum of the fictive and passive conditions is consistently less than the observed response during the active conditions (arithmetic: 277±214% change in integrated modulation,

observed: 178±149% change in integrated modulation, n=34, p<0.0001, paired t-test). Therefore, nonlinear interactions between proprioceptive and corollary discharge signals appear to provide a flexible basis for generating negative images of the electrosensory consequences of movements, irrespective of how the movements are generated.

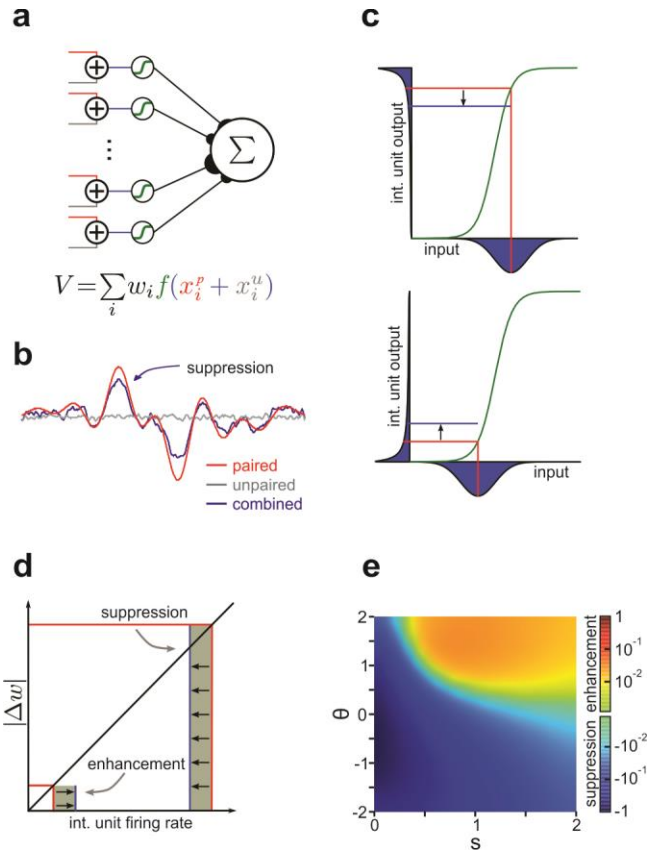


**Figure 3.5. Network model with randomly combined inputs and nonlinear processing. (a)** Model schematic. The paired (red) and unpaired (gray) inputs are added and passed through an intermediate layer containing a sigmoid nonlinearity (green). The network output is the weighted sum of the outputs of the intermediate layer units. **(b)** Simulation results when the network fits an arbitrary function with only the paired inputs active, but is tested in three cases: paired inputs only (red), unpaired inputs only (gray), and both inputs combined (blue). The unpaired input suppresses the network's learned response to the paired input. **(c)** Interaction between the paired and unpaired inputs to an intermediate layer unit, with a sigmoid nonlinearity (green). The paired input value and resulting output are indicated by vertical and horizontal red lines, respectively. For the given paired input value, the distributions (over values of the unpaired input) for the combined input (x-axis) and resulting output (y-axis) are shown in blue. The blue line indicates the mean output in the combined case. *Top:* When the paired input falls within the concave region of the nonlinearity (above the threshold), the output distribution is skewed such that the mean combined output is below the response to the paired input alone. *Bottom:* When the paired input falls within the convex region of the nonlinearity (below the threshold), the output distribution is skewed such that the mean combined output is above the response to the paired input alone. **(d)** Contributions of the intermediate layer interactions shown in (C) to network output. The contribution to the change in network output (shaded area) is given by the product of the change in weight and the firing rate. Because the magnitude of the learned weight change is proportional to the firing rate, the suppression of high firing rates by the unpaired input has a larger effect on the network's learned response than the enhancement of low firing rates. **(e)** Parameter dependence of suppression/enhancement effects.

The effect of suppression is stronger and favored for either low thresholds ($\theta$) and/or narrow nonlinearity widths (s). The threshold and width are in units of the paired input standard deviation, with a threshold value of zero corresponding to the mean of the training input distribution. Values are plotted relative to the maximum effect magnitude on a logarithmic scale (see Experimental Procedures).

### Explanation of nonlinear interactions by a simple network model

We used the properties described above—suppression of the paired response by the unpaired input, lack of transference, and sub-linear combination of inputs—to constrain a simple network model of negative image formation (**Figure 3.5a**). The model includes both paired (red) and unpaired (gray) inputs, which are combined in an intermediate layer. The firing rate of each intermediate layer unit is determined by applying an input-output function to the sum of its inputs. The network's output is then given by the weighted sum of the intermediate layer units' firing rates. Considered in relation to ELL circuitry, each set of input signals represents proprioception and CD, the activity of the intermediate layer represents the coding of the inputs in GCs, and the output layer represents an ELL principal cell.

To simulate the experimental pairing protocol, we trained the network output to fit an arbitrary function by least mean-squared learning of the weights (**Figure 3.5b;** see Methods). To mimic the different conditions during training and probing, we trained the network using only one set of inputs, then testing in three cases: paired inputs only, unpaired inputs only, and both inputs combined. These conditions mimic the experiments in **Figure 3.4b or 3.4c**, allowing us to investigate the conditions under which the network exhibited the experimentally observed properties of (1) lack of transference across input modalities, and (2) suppression of the negative image by the unpaired response.

For the network to exhibit a lack of transference, as observed in the negative images, the signals provided by the two sets of inputs to a given intermediate layer unit must be on average

uncorrelated with each other. That is, an intermediate layer unit cannot preferentially receive similarly tuned paired and unpaired inputs. For the network to exhibit the observed sub-linear addition of the responses to the paired and unpaired inputs, the network must contain a nonlinearity after the paired and unpaired inputs are combined in the intermediate layer; otherwise, the response to the combined inputs would simply be the sum of the responses to the individual inputs. We therefore simulated the pairing and probing procedures as follows: the paired and unpaired inputs were uncorrelated, and a sigmoid input-output function was applied at the intermediate layer units (**Figure 3.5b**). This network clearly recapitulates both the lack of transference from paired response to unpaired response, and the suppression of the paired response by the unpaired inputs.

| | | granule cell | | | | | |
|---|---|---|---|---|---|---|---|
| | | 1 | 2 | 3 | 4 | 5 | 6 |
| parameters (sp/cmd) | A (sp/cmd) | 1.86 | 3.55 | 2.01 | 6.19 | 3.94 | 2.49 |
| | θ (pA) | 35.2 | 13.8 | 9.42 | 10.9 | 15.1 | 11.9 |
| | s (pA) | 7.78 | 1.46 | 0.497 | 1.31 | 3.61 | 1.85 |
| | $V_{50}$ (mV) | 16.0 | 13.6 | 16.0 | 14.8 | 9.66 | 7.54 |
| parameters (inst. firing rate) | A (Hz) | 165.7 | 136.2 | 90.6 | 192.9 | 204.9 | 121.4 |
| | θ (pA) | 35.2 | 11.2 | 9.37 | 11.0 | 11.2 | 11.9 |
| | s (pA) | 7.78 | 1.46 | 0.497 | 1.31 | 3.61 | 1.85 |
| | $V_{50}$ (mV) | 16.0 | 13.6 | 16.0 | 14.8 | 9.66 | 7.54 |

**Table 3.1. Fit parameters for GC input-output functions.** Input-output responses (e.g., **Figure 7A**) for six GCs were fit to a sigmoid nonlinearity (see equation (3) in Methods). Spikes/cmd refers to the number of action potentials observed up to 60 ms following the EOD motor command. The lower half of table lists parameters when peak instantaneous firing rate was calculated rather than spikes/cmd. Note qualitative similarity.

To explore the origin of the suppressive effects, we examined the interaction among the paired input value, the unpaired input distribution, and the parameters of the nonlinearity (**Figure 3.5c)**. When the paired input falls in the concave region of the nonlinearity, the firing rate

distribution during the combined case is skewed such that the mean of the distribution is less than the response to the paired input alone (**Figure 3.5c**, top panel), consistent with Jensen's inequality. Therefore, when the paired input is combined with the unpaired input distribution, there will be on average a reduction in the firing rate of the intermediate layer unit, which contributes to suppression of the learned response. The opposite case, in which the nonlinearity threshold is high relative to the value of the paired input, results on average in an increase in the firing rate of the intermediate layer unit (**Figure 3.5c,** bottom panel**)**, which contributes to enhancement of the learned response. Because the output unit receives a large number of inputs from the intermediate layer, the law of large numbers justifies focusing on the average change in an intermediate layer unit's output due to the addition of the untrained input.

For a given input pattern to the network, some intermediate layer units receive strong input above the threshold, and others receive weak input below the threshold. Whether there is net suppression or net enhancement depends upon the distribution of paired inputs relative to the distribution of thresholds. However, if the magnitude of the synaptic weight change is proportional to the input firing rate, as suggested by previous experimental and theoretical studies (Roberts and Bell 2000) the reduction of high firing rates by the unpaired input will have a larger effect on the network's output than the enhancement of low firing rates (**Figure 3.5d**). As a result, suppression rather than enhancement occurs in a large region the parameter space for the width and threshold of the nonlinearity (**Figure 3.5e**; see Methods). Furthermore, even for parameters that favor enhancement, the effect of this enhancement is substantially less than that of suppression in other parameter regions. This last point is important because granule cell populations exhibit a distribution of thresholds (Kennedy, Wayne et al. 2014) and non-linearity widths (See **Table 3.1**).

Overall, this theoretical account suggests that all of the observed properties of negative images observed experimentally can be explained by a simple network architecture, inspired by ELL circuitry, in which CD and proprioceptive inputs are coded as random nonlinear mixtures before the strength of these inputs is adjusted at the level of the principal cells.

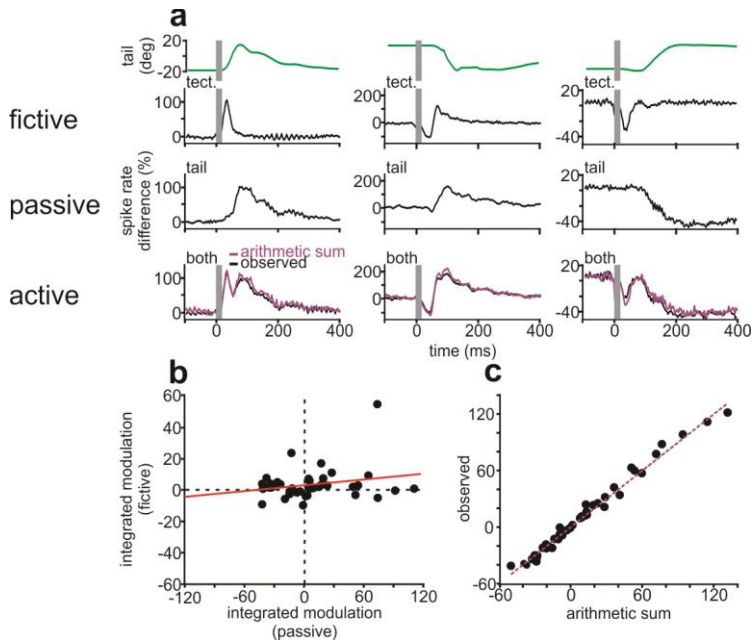


**Figure 3.6. Linear mixing of proprioceptive and CD information in MFs (a)** Difference traces of smoothed spike rate histograms from extracellular recordings of three representative MFs recorded in EGp under fictive (top row), passive (middle row), and active (bottom row) conditions. Tail position is shown above recordings in green. The arithmetic sum of the integrated spike rate modulations under passive and fictive conditions is plotted in purple. **(b)** Scatterplot of integrated modulations under passive conditions plotted against integrated modulations under fictive conditions (n=42 fibers). Note lack of correlation. **(c)** Integrated modulations of MFs under active conditions plotted against the arithmetic sum of the integrated modulations during passive and fictive conditions. Note that the modulations appear to sum linearly, falling near the unity line (purple).

## Mixtures of proprioceptive and corollary discharge signals conveyed by a spinal mossy fiber pathway

The model described above suggests that corollary discharge and proprioceptive information should be represented as random, nonlinear mixtures in order to explain properties of negative images. We asked how these signals are actually represented, beginning at the level of the mossy

fiber inputs to granule cells. Previous studies have shown that a spinal mossy fiber pathway to EGp conveys proprioceptive information, including tail position signals, and also corollary discharge signals (Szabo, Libouban et al. 1990; Requarth and Sawtell 2013). However, it is not known whether proprioception and corollary discharge are mixed at the spinal level in mormyrid fish, as shown for some mammalian spinocerebellar pathways. To test this we used high-resistance microelectrodes to record extracellularly from putative mossy fiber axons in EGp and in a superficial fiber tract that decussates at the anterior margin of EGp and contains mossy fiber axons originating from the spinal cord (Szabo, Libouban et al. 1990). We characterized mossy firing responses under conditions identical to the active, fictive and passive conditions used to study negative images. Previous studies have demonstrated position coding in EGp mossy fibers in the context of static displacement of the tail and/or trunk, suggesting that responses described here under passive conditions are not simply due to touching the tail (Bell, Grant et al. 1992; Sawtell 2010). The three examples in **Figure 3.6a** are typical of the responses we observed. The same MFs showed short-latency bursts or pauses under fictive conditions (**Figure 3.6a, first row**) along with either excitatory or inhibitory responses that tracked tail position under passive conditions (**Figure 3.6a, second row**). Hence, corollary discharge and proprioceptive information are mixed in individual mossy fibers. Furthermore, we found that that bursts or pauses caused by tectal stimulation could be mixed with excitatory or inhibitory proprioceptive responses. The lack of correlation ($R^2$=0.054, n=42; **Figure 3.6b**) between integrated firing rate modulations under fictive versus passive conditions is consistent with random mixing of CD and proprioceptive signals in MFs, as suggested by our modeling. However, in contrast to model requirements, the combination of CD and proprioceptive signals in MFs is strikingly linear ($R^2$=0.99, n=42; **Figure 3.6c**), with no significant difference between the arithmetic sum and the

observed response under active conditions (arithmetic: 11.3±41.9% change in integrated modulation; observed: 12.4±42.7% change in integrated modulation; p=0.28, sign test). Thus, the mixing in MFs in not sufficient to account for the observed nonlinear interactions in the negative images.

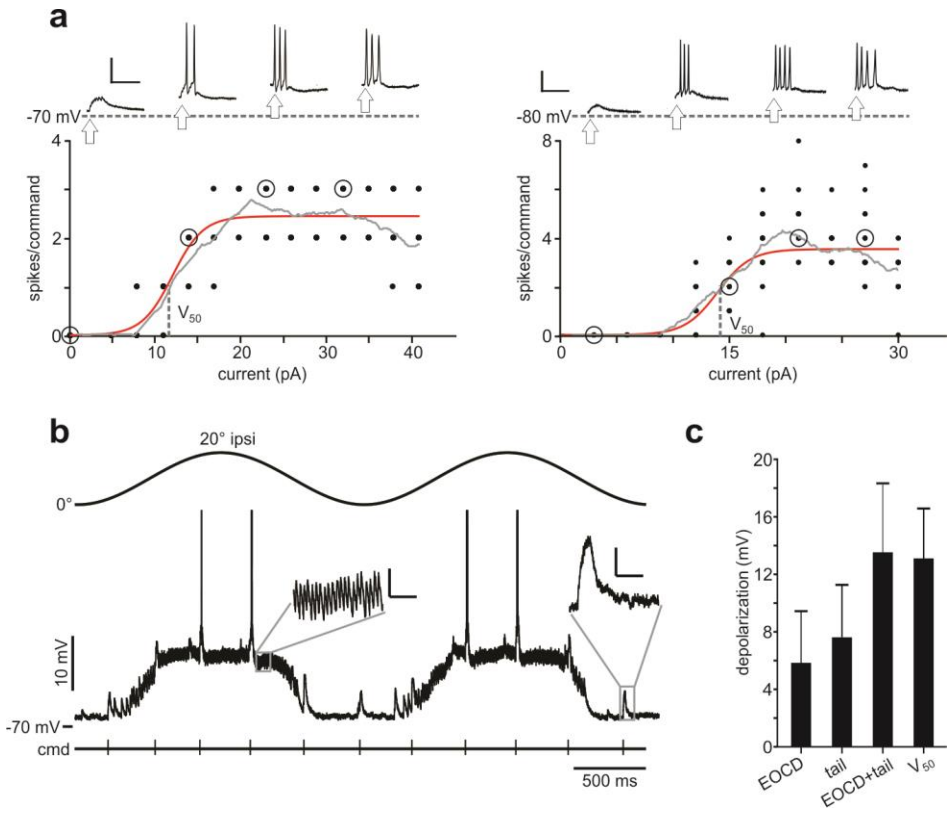


**Figure 3.7. Evidence for nonlinear recoding in GCs. (a)** *In vivo* whole-cell recording from two GCs, illustrating typical responses to intracellular current injections. The number of spikes fired per EOD motor command is plotted as a function of current injection along with a sigmoid fit (red), and a moving boxcar average (gray). *Above:* Representative command-locked responses at varying levels of injected current (corresponding to the open circles along the fitted input-output curve) plotted above resting membrane potential (gray dotted line). The time of the command is indicated by arrows. Scale bars: 20 mV, 25 ms. (**b**) Trace from a representative GC in which tail movements resulted in depolarization and action potential firing at a preferred position. Action potential firing is restricted to the range of preferred positions over which EPSP summation and depolarization occurs. Note the two clearly defined inputs, seen more clearly in insets. Note that the tonically-active EPSPs related to tail position sum with the EOCD input to provide the additional depolarization to push the cell above threshold. Inset scale bar: 2 mV, 30 ms. **(C)** Depolarizations due to naturally occurring MF inputs compared the depolarization ($V_{50}$) caused by current injection at half-maximum values.

## Evidence for nonlinear recoding of mossy fiber inputs in granule cells

Signals conveyed by mossy fibers are recoded in granule cells before they reach ELL principal cells. Hence, nonlinear recoding could occur in granule cells, as suggested also by theories of mammalian cerebellar function (Marr 1969; Albus 1971). One way for GCs to fulfill the specific requirements suggested by our modeling would be for mossy fiber inputs to drive granule cells into a concave, i.e., saturating, region of their input-output curves. As a first step towards evaluating this possibility, we recorded from EGp granule cells *in vivo* and measured action potential firing as a function of injected current. Previous studies have shown that most EGp granule cells (~75%) receive mossy fiber input related to the EOD motor command, typically in the form of a stereotyped high-frequency (~800 Hz) burst of 6-10 action potentials (Bell, Grant et al. 1992; Kennedy, Wayne et al. 2014). Consistent with this, all six granule cells recorded here received a prominent depolarization related to the EOD motor command and for all but the largest current injections, action potentials were caused by the temporal summation of depolarizations due to current injection and those due to the EOD command input (**Figure 3.7a, top traces**). For this reason, and because all input to the active electrosensory system is processed in relation to the EOD command, we analyzed action potential firing within a small time window after the EOD command. Relationships between injected current and GC spiking were well-fit by sigmoid functions (n=6, **Table 3.1**) and showed clear signs of saturation in response to small amounts of injected current (i.e., no increase in command-locked spiking for several current steps). Results were similar when we analyzed maximum spike frequency instead of the number of spikes per command (**Table 3.1**).

To ask whether depolarization due to naturally occurring MF inputs could drive granule cells into a saturating region of their input-output curves, we turned to a large existing dataset of 230 GCs recorded in an awake, paralyzed preparation similar to that used in the present study.

Though responses to tectal microstimulation were not obtained in these experiments, 45 granule cells received proprioceptive MF input, as judged by a prominent EPSP whose rate of occurrence was strongly modulated by passive tail movement. Tail movements in these studies were of similar amplitude but substantially slower (0.1-0.5 Hz) than those used in the present study. Thirty-six of these GCs also exhibited a second, distinct EPSP waveform time-locked to the EOD motor command (**Figure 3.7b**), consistent with a previous report of multimodal integration of proprioceptive and EOCD inputs in a majority of GCs (Sawtell 2010). The combined depolarization due to proprioceptive and EOCD MF inputs are similar in magnitude (13.4$\pm$4.7 mV, n=36; **Figure 3.7c**) to the depolarizations occurring at the half-maximum point (12.9$\pm$3.5 mV, n=6; **Figure 3.7c**) of the GC input-output curves. These results suggest that depolarizations due to naturally occurring inputs could drive granule cells into a saturating region of their input-output curves.

**Discussion**

A central finding of the present study is that both motor corollary discharge and proprioceptive feedback are used to generate negative images under conditions approximating self-generated tail movements. The observation that negative images based on corollary discharge and those based on proprioceptive signals are roughly equivalent is remarkable given the very different nature of the two signals (i.e. motor versus sensory). With respect to corollary discharge, our results and those of a previous study (Requarth and Sawtell 2013) indicate that bursts and pauses in mossy fibers evoked by tectal microstimulation are stereotyped and brief. In contrast, negative images observed after fictive pairings (in which only corollary discharge signals are engaged) accurately match the temporal profiles of the fictive movements, which are

substantially delayed relative to mossy fiber responses. A possible solution to this problem is suggested by a recent study demonstrating that EGp circuitry transforms stereotyped and minimally delayed electric organ corollary discharge signals into more delayed and temporally diverse granule cell responses (Kennedy, Wayne et al. 2014). With respect to proprioception, it has been sometimes assumed that proprioception is too inaccurate or delayed to effectively cancel unwanted sensory consequences of movements (Wang, Zhang et al. 2007; Wurtz 2008). Negative images observed here after passive pairings (in which only proprioceptive signals are engaged) suggest that this is not always the case and provide an example of the use of one stream of sensory information to cancel another.

Inferences from our results to conditions of natural self-generated movements depend on the assumption that proprioceptive responses observed in response to passive displacements in paralyzed fish are similar to those that would occur during self-generated movements. This question is difficult to address experimentally because responses observed during self-generated movements could also be due to motor signals. Nevertheless, we have recorded EGp mossy fibers in unparalyzed fish during tectal microstimulation and observed firing rate modulations that track position (similar to passive responses observed here in paralyzed fish) during both active and passive movements (unpublished observations). Though not definitive, these observations suggest that proprioceptive coding is not radically altered under paralyzed conditions. Several additional lines of evidence suggest that responses we observed in paralyzed fish are reflective of those that would occur as a result of natural movements. First, proprioception in fish (in locomotor muscles at least) is likely mediated by free endings in muscle tissue and tendons rather than by a more elaborate muscle spindle (Barker, Hunt et al. 1974; Bone 1979; Srivastava 1979). The lack of muscle spindles implies that fish do not possess

any functional or anatomical equivalent of the independent efferent control over proprioceptors exerted by the gamma motoneurons, as described in mammals (Boyd 1980; Hulliger 1984). Our finding that effects of tectal stimulation and passive tail displacements sum linearly in mossy fibers is consistent with the absence of efferent control.

Though the capacity to generate negative images based on two separate streams of information may reduce uncertainty and allow for more accurate or robust sensory cancellation, it also poses a potential problem. For a river-dwelling fish, the same change in body position may result from motor commands, external forces or combinations of both. Though a linear system, in which CD and proprioceptive inputs are simply added, could not effectively utilize both streams under these conditions, our results suggest that ELL neurons are capable of generating equivalent negative image based on CD and proprioception or proprioception alone. A simple network model was used to explore how this was possible. The key insight that emerged is that a model in which CD and proprioceptive inputs are represented as random, nonlinear mixtures fully accounts for properties of negative images observed in vivo, including the capacity to generate the same negative image based on CD and proprioception or proprioception alone. Such mixed nonlinear coding appears to be useful in a variety of contexts, from sensorimotor transformations to cognitive tasks (Zipser and Andersen 1988; Pouget and Sejnowski 1997; Mante, Sussillo et al. 2013; Rigotti, Barak et al. 2013).

Though coding of movement-related corollary discharge (Requarth and Sawtell 2013) and proprioceptive information have been described previously for mossy fibers in the mormyrid EGp, it was not known whether corollary discharge and proprioceptive signals were mixed in the same mossy fibers. Our results clearly demonstrate that mixing indeed occurs and appears to be random, in that no systematic relationship was observed between the characteristics of the

sensory and motor responses observed within the same fibers. Our experimental setup makes it impossible for us to estimate the prevalence of such mixing in mossy fibers because we may have easily missed proprioceptive responses in some mossy fibers (by failing to move the appropriate part of the body) or corollary discharge responses (by failing to stimulate the appropriate motor commands). Our results also do not speak to the possibility that additional mixing may occur in granule cells. Mixing of sensory and motor signals in spinocerebellar neurons, as shown here for mormyrid fish, has been extensively studied in vertebrates (Oscarsson 1965; Arshavsky, Gelfand et al. 1978; Hantman and Jessell 2010; Jankowska, Nilsson et al. 2011; Fedirchuk, Stecina et al. 2013; Spanne and Jorntell 2013). The population of mixed mossy fibers recorded here likely corresponds to an ascending lateral column system in the mormyrid spinal cord that shares a number of anatomical similarities with the mammalian ventral spinocerebellar tract (Szabo, Libouban et al. 1990). Most accounts of the function of such mixing in mammalian systems have posited some specific logic underlying interactions between sensory and motor signals (Lundberg 1971; Spanne and Jorntell 2013). Our results suggest a simpler, though not mutually exclusive, view in which such mixtures are components of a random basis that could allow for flexible predictions based on either sensory or motor signals. Though the linear interactions observed between sensory and motor responses in mossy fibers is consistent with highly linear properties of mossy fiber neurons described in mammals (Kolkman, McElvain et al. 2011), such linear mixing alone clearly does not fulfill the requirements for nonlinear input combinations suggested by our network model.

Nonlinear recoding of MF inputs in GCs is a key feature of theoretical accounts of mammalian cerebellar cortex (Marr 1969; Albus 1971) and has received experimental support in the form of brief, action potential bursts observed in some *in vitro* and *in vivo* studies of

mammalian cerebellar granule cells (Chadderton, Margrie et al. 2004; Barmack and Yakhnitsa 2008; Ruigrok, Hensbroek et al. 2011). Our network model suggests that such nonlinear recoding, together with random mixing already observed at the level of spinal mossy fibers, can fully account for nonlinear interactions between corollary discharge and proprioception observed in ELL neurons. Additional sites and mechanisms for nonlinear processing within ELL are possible, e.g. normalization of granule cell output via Golgi cell inhibition (Marr 1969; Albus 1971; Crowley, Fioravante et al. 2009; Rothman, Cathala et al. 2009). Though we do not exclude those possibilities, we focus here instead on the straightforward possibility that depolarization due to excitatory mossy fiber inputs under conditions of negative image formation is sufficiently strong to push granule cells into the concave, i.e., saturating, region of their input-output functions. Strong depolarization observed in EGp granule cells reported on here is due in part to previously described multimodal integration of spinal/proprioceptive and EOD command mossy fiber inputs (Sawtell 2010). Since the timing of the EOD motor command is independent of the fish's movements (Toerring and Moller 1984), EOD command input simply acts as an additional source of depolarization that will summate with depolarization due to spinal mossy fiber input conveying proprioceptive and movement-related corollary discharge signals. Though our analysis suggests that such depolarization may be sufficiently strong to drive some granule cells towards saturation, this is unlikely to be the case for all granule cells. Indeed, depolarization due to activation of both proprioceptive and EOD command input is subthreshold for some recorded granule cells (Sawtell 2010).

The observation that interactions between proprioceptive and corollary discharge are consistently sublinear could be explained if strongly activated granule cells, i.e. those operating near saturation, make a dominant contribution to negative images. Our network model offers an

explanation for why this may be the case. Nonlinear interactions between corollary discharge and proprioceptive signals observed in the context of negative images are believed to reflect granule cell inputs that have undergone synaptic plasticity. If, as assumed in previous work in this (Roberts and Bell 2000) and other systems (Abbott and Nelson 2000), such plasticity is proportional to granule cell firing rate, the most active granule cells will, indeed, provide the greatest contribution to learned changes in the network output (**Fig. 3.5e)** . Though the relationship between granule cell firing rate and plasticity in principal cells has not been examined in mormyrid fish, *in vitro* studies of weakly electric gymnotiform fish have shown that burst firing is required to induce long-term synaptic depression in ELL principal cells and that the magnitude of LTD is greater for larger bursts (Harvey-Girard, Lewis et al. 2010). Such a nonlinear plasticity rule would exaggerate the suppressive effects predicted by our model.

Previous *in vivo*, *in vitro*, and modeling studies of weakly electric mormyrid fish have provided a relatively complete mechanistic account of how copies of motor commands related to the fish's stereotyped EOD pulse are used to cancel self-generated electrosensory inputs (Bell 1981; Bell, Han et al. 1997; Roberts and Bell 2000; Kennedy, Wayne et al. 2014). The present study suggests that mechanisms of negative image formation are quite general in that they operate on a variety of sensory and motor signals and may perform more complex functions, i.e. predicting the sensory consequences of movements. Our results also show how interactions between input coding, explored here at the levels of mossy fibers and granule cells, and plasticity are critical for shaping the output of an adaptive neural circuit.

**Experimental Procedures**

*Experimental Preparation*

All experiments performed in this study adhere to the American Physiological Society's *Guiding Principles in the Care and Use of Animals* and were approved by the Institutional Animal Care and Use Committee of Columbia University. Mormyrid fish (7-14 cm in length) of the species *Gnathonemus petersii* were used in these experiments. Surgical procedures to expose EGp for recording were similar to those described previously (Sawtell, 2010). An additional anterior portion of the skull was removed to expose the optic tectum. The anesthetic (MS-222, 1:25,000) was then removed. To evoke tail movements, we targeted microelectrodes (tungsten, 0.005" diameter, 5 MOhm, 12 deg beveled tip, A-M Systems, Sequim, WA) to a site in the anterior portion of the optic tectum that evoked ipsilateral movements, consistent with previous reports in goldfish (Herrero, Rodriguez et al. 1998). Brief, high-frequency (10-15 pulses at 500 Hz) microstimulation evoked rapid, isolated tail movements. A laser displacement sensor (LK-503, Keyence Corporation, Woodcliff Lake, NJ) measured tail displacement from the midline (spatial precision: 50 μm; measurement delay: 2 ms). After tail movements were measured, gallamine triethiodide (Flaxedil) was given (~20 ug/cm of body length) to paralyze the fish. Paralysis blocks the effect of motor neurons on all muscles, including the electric organ, which prevents the EOD. The motor command signal that would normally elicit an EOD continues to be generated by the fish at a variable rate of 2 to 5 Hz. The EOD motor command can be measured precisely (see below). This preparation allows us to observe the central effects of movement-related corollary discharge in isolation from the electrosensory input that would normally result in an EOD and in isolation from the proprioceptive input that would normally occur as a result of movements.

To engage proprioceptive feedback, tectal microstimulation-evoked tail displacement was measured by a laser and then that signal was fed back into the servomotor to deliver passive tail movements that mimicked the microstimulation-evoked movement prior to paralysis. The fish's tail was lightly held between two glass rods positioned posterior to the electric organ. The rods were held by a manipulator mounted to a computer-controlled servomotor (Pacific Laser Equipment, Santa Ana, CA). A partition was placed between the tail and the rest of the fish to prevent water waves from activating lateral line receptors.

*Electrophysiology*

The EOD motor command signal was recorded with an electrode placed over the electric organ in the tail.

Extracellular recordings from the medial zone of ELL were made with glass microelectrodes filled with 2M NaCl (8-10 MOhm). Identification of ELL cell types was aided by previous intracellular recording and labeling studies in which characteristic EOCD and electrosensory responses were linked with cell morphology (Bell and Grant 1992; Bell, Caputi et al. 1997; Mohr, Roberts et al. 2003). Because ELL is a laminar structure, with different cell types located in different layers, recording location is also useful in identifying cell types. The laminar location of the recording electrode within ELL can be accurately judged based on characteristics of prominent EOCD- and electrosensory stimulus-evoked field potentials (Bell and Grant 1992; Bell, Grant et al. 1992). ELL cells can be broadly classified as E- or I-cells: E-cells are excited by an increase in local EOD amplitude in the center of their receptive fields, and I-cells are inhibited by such a stimulus. We recorded from I-cells located in or just above the ganglion layer, which likely included both interneurons (MG1 cells), and efferent neurons known as large

ganglion (LG) cells. We also recorded from E-cells located below the ganglion layer, which were probably efferent neurons known as large fusiform (LF) cells.

Extracellular recordings from mossy fibers were made with glass microelectrodes filled with 2M NaCl (40-100 MOhm). Criteria for distinguishing mossy fiber recordings from other EGp units were the same as those described previously (Sawtell 2010).

*In vivo* whole cell recordings from GCs in EGp were made using methods described previously(Sawtell, 2010). Electrodes (9-12 MOhm) were filled with an internal solution containing K-gluconate (122 mM), KCl (7 mM), HEPES (10 mM), $Na_2ATP$ (0.5 mM), MgATP (2 mM), EGTA (0.5 mM), and 0.5% biocytin (pH 7.2, 280-290 mOsm). No correction was made for liquid junction potentials. Only cells with stable membrane potentials more hyperpolarized than -50 mV and access resistance < 100 MOhm were analyzed. All experiments were performed without holding current, unless otherwise noted. Membrane potentials were filtered at 3-10 kHz and digitized at 20 kHz (CED Power1401 hardware and Spike2 software; Cambridge Electronics Design, Cambridge, UK).

*Electrosensory Stimulus (ES) Pairing Experiments*

ES pairing experiments were conducted using extracellular recordings from ELL principal cells. Cells that did not show plasticity (roughly 15% of all recorded cells) under any condition were excluded from the analysis. This is not unexpected, as there are known non-plastic cell types in ELL(Mohr et al., 2003).

Electrosensory responses were evoked by simultaneous global stimulation of the entire fish and local stimulation restricted to small area of the skin. Global stimuli were delivered by passing current between a small chloride silver ball inserted through the mouth into the stomach

of the fish and a second electrode placed in the water near the tail of the fish in an outside-positive configuration. The ES referred to in the paper is the modulation of the local field. Local stimuli were delivered with a bipolar stimulating electrode consisting of two small Ag-AgCl balls 5 mm apart. The electrode was held perpendicular to the skin at a distance of ~2 mm. For both global and local stimuli, brief pulses of current were delivered 4.5 ms after EOD command through the electrodes to activate electroreceptors. Absolute current strength for local stimuli ranged from 5uA-10uA while current strength for global stimuli ranged from 200-400mA. These values were chosen such that the amplitude of electrosensory-evoked field potentials could be both increased and decreased by the local stimulus, roughly mimicking the changes in EOD-evoked field potentials measured in response to tail movements in a previous study in which the natural EOD was left intact (Sawtell and Williams 2008). Small adjustments to the local amplitude were made on a cell-by-cell basis to strongly inhibit the cell with minimal current. In a subset of experiments, we controlled EOD motor command rate by lowering a concentric bipolar stimulating electrode (FHC, Bowdoin, ME) into the brain along the midline in or near the axons of the precommand nucleus, which course close to the midline along the ventral surface of the brainstem to the command nucleus (~ 5mm depth). Brief, single pulses of 0.2 ms reliably evoked an EOD motor command at low current strengths (10-20 uA), allowing experimental control over discharge frequency when necessary. We typically microstimulated the EOD command at ~13 Hz.

In ES pairing experiments, we varied the amplitude of the local ES in the center of the recorded cell's receptive field to deliver a time-varying pattern of electrosensory stimulation based on the waveform of the tail movement recorded prior to paralysis. Since change in local EOD amplitude is proportional to tail displacement for small angles, such a protocol

approximates the electrosensory consequences induced by real tail movements. Tectal microstimulation was always separated by at least 1.25 seconds. Pairing was conducted for 10-15 minutes. The neural response to tectal microstimulation and/or tail displacement was compared immediately before and after the pairing period.

*Computational Model and Analytical Results*

Our simulated network consisted of an intermediate layer of N = 2,000 units with a sigmoid nonlinear input-output function $f_{s,\theta}(x) = 1/(1 + \exp\left(\frac{\theta - x}{s}\right))$ with threshold (i.e. half-maximum point) $\theta = 0$ and scale $s = 0.2$. Each unit received "paired" and "unpaired" inputs, $x_i^p(t)$ and $x_i^u(t)$, which were determined as follows. For each intermediate layer unit, we selected two functions randomly, independently, and uniformly from the set $\{\cos 2\pi kt,\ \sin 2\pi kt; k = 1,2,\ldots,50\}$. Each selected function was then independently designated as "paired" or "unpaired" with equal probability. The input $x_i^p(t)$ was then set as the sum of the (up to two) "paired" functions, and the input $x_i^u(t)$ was then set as the sum of the (up to two) "unpaired" functions. Throughout, the weights were trained under the conditions that only the paired inputs $x_i^p$ were active and the unpaired inputs $x_i^u$ set to zero, such that the network output, define as the sum of the nonlinear units with weights $w_i$, was given by

$$V(t) = \sum_{i=1}^{N} w_i f_{s,\theta}\left(x_i^p(t)\right). \qquad (1)$$

Under these conditions, plasticity was simulated by setting the weights $w_i$ to minimize the expected least squared error between the network output $V(t)$ and the target function $h(t)$, with $t$ ranging over the interval [0, 1] to represent time after movement motor command. Assuming the individual units to be noisy, the expected least-squares error is obtained by setting the weights $w$ as follows:

$$\mathbf{w} = \left(\int_0^1 \mathbf{r}(t)\mathbf{r}^T(t)\,dt + \Sigma\right)^{-1} \int_0^1 \mathbf{r}(t)h(t)dt \qquad (2)$$

where Σ is a diagonal matrix with entries equal to the trial-to-trial variance of each nonlinear unit's output. In our simulations, we set the diagonals of the noise matrix as $\Sigma_{ii} = 10$.

Once the weights were determined, we calculated the network output under three probe conditions: first, with just the paired input present, given by equation (1); second, with just the unpaired inputs $V(t) = \sum_{i=1}^{N} w_i f_{s,\theta}\left(x_i^p(t)\right)$; and third, with the two inputs combined $V(t) = \sum_{i=1}^{N} w_i f_{s,\theta}\left(x_i^p(t) + x_i^u(t)\right)$. The plotted results were averages of 15 repeated simulations with different randomly chosen input functions and labels provided to each nonlinear unit.

To analyze the parameter dependence of the observed suppression effect (**Fig 3.5e**), we considered learning rules in which the magnitude of the weight change is proportional to the presynaptic firing rate during learning. For simplicity, we considered learning a single time point (i.e. no *t* dependence) with the input values $x^p$ and $x^u$ independently distributed as Gaussian variables with zero mean and unit variance. In this case, the output enhancement/suppression, given as the product of the weight change magnitude $|\Delta w| \sim f_{s,\theta}(x^p)$ and the difference in firing rates $f_{s,\theta}(x^p + x^u) - f_{s,\theta}(x^p)$, has the following expectation value:

$$E(s,\theta) = C\int_{-\infty}^{\infty}\int_{-\infty}^{\infty} e^{-\frac{(x^p)^2+(x^u)^2}{2}}\left(f_{s,\theta}(x^p + x^u) - f_{s,\theta}(x^p)\right)f_{s,\theta}(x^p)dx^p dx^u\,,$$

with the proportionality constant $C$ depending on the learning rate and duration of pairing. We plotted the above expression with $C$ set to normalize the maximum magnitude of the above expression to unity.

*Data Analysis and Statistics*

Data analysis was performed offline in MATLAB (MathWorks, Natick, MA) and Spike2 (Cambridge Electronic Design). Data are expressed as mean ± standard deviation (SD), unless otherwise noted.

We constructed GC input-output curves as follows. After obtaining a stable whole-cell configuration, small amounts of current were injected into cells in 5-sec steps. Spikes were counted from 0-60 ms following the EOD motor command. Spikes were rarely observed outside of this window except at the highest currents. Data were used to fit to a sigmoid input-output function defined by the following equation:

$$f_{s,\theta}(x) = \frac{A}{1+e^{\frac{-(x-\theta)}{s}}} \quad (3)$$

where *f(x)* equals either spike count per command or instantaneous firing rate as a function of current injection amplitude, *x* equals current step value, $\theta$ is half-maximum point in pA and *s* reflects the inverse of the steepness of the sigmoid. All fit parameters are collated into **Table 1**.

We constructed a current vs. voltage curve by measuring the mean change in membrane potential due to current injection. $V_{50}$ is the membrane depolarization corresponding to the fitted half-maximum point current injection. EOCD amplitude was calculated by taking an EOD motor command-triggered waveform average prior to current injection, while the cell was resting. Peak EOCD voltage minus resting membrane potential was taken as EOCD amplitude. Resting membrane potential was also calculated from this waveform average, at a time point just prior to the EOD motor command. Tail depolarization was calculated by finding the maximum depolarization caused by tonic EPSPs and comparing that to resting membrane potential. EOCD+tail is simply the arithmetic sum of those two calculated values.

Integrated modulations were computed by summing over a small window (200 ms) following tectal microstimulation or onset of tail movement. Values are expressed in percent change from baseline firing rate.

Tests for statistical significance are noted in the text. Differences were judged to be significant at $p<0.05$.

# CHAPTER 4

# DISCUSSION AND FUTURE DIRECTIONS

# CHAPTER 4: DISCUSSION AND FUTURE DIRECTIONS

## Discussion

This thesis demonstrated how a cerebellum-like structure, the electrosensory lobe (ELL) of mormyrid fish, uses corollary discharge (CD) (Chapter 2) and combinations of CD and proprioception (Chapter 3) to predict the electrosensory consequences of swimming movements. In Chapter 2, we showed that a spinal CD pathway is used to form flexible and highly-specific negative images of the sensory consequences of motor commands at the level of individual neurons. We showed that ELL receives CD signals related to movements and that mechanisms described previously for predicting the effects of the electric organ discharge (EOD), i.e. anti-Hebbian plasticity acting on CD inputs to principal cells, are sufficient for predicting the sensory consequences generated by simple swimming movements. In Chapter 3, we found that both CD and proprioceptive feedback are used to generate negative images under conditions approximating self-generated tail movements. We found that mossy fibers (MFs) originating in the spinal cord carry random mixtures of CD and proprioceptive signals, and that properties of granule cells (GCs) observed in vivo are consistent with nonlinear recoding of these signals. We developed a simple network model to show that random, nonlinear mixtures of CD and proprioceptive signals can account for properties of negative images observed in vivo.

In this chapter, I will discuss how the work in this thesis relates to broader issues in neuroscience. The mechanisms for predicting sensory events are of general importance to a variety of fields. Here, I have chosen a few cases in which relevance of the fish is clear, but this is by no means an exhaustive list. First, I will consider how the work described here bears on an

ongoing debate in the cerebellar field: does the cerebellar circuitry act as a forward model, a type of internal model that can predict the sensory consequences of motor commands? What is the evidence to support the cerebellum as a forward model? And how might such a forward model be implemented in cerebellar circuitry? Insights from electric fish may shed light on these issues by considering how a forward model could be implemented in a cerebellum-like structure.

Motor commands are not the only way to predict the sensory consequences of movements. Second, I will consider how one stream of sensory information can serve as a predictive signal to cancel another stream of sensory information. Finally, I will consider how the mechanisms for generating temporally-specific negative images relate to temporal processing in general, and specifically within the context of eyelid conditioning in the cerebellum.

The final section will describe future experiments based on the work in this thesis.

*Cerebellum and forward models*

The results presented in Chapter 2, along with previous studies in cerebellum-like structures, have provided evidence for CD-based sensory predictions. However, the work described here was limited to a small set of movements, i.e., two simple tail movements in opposite directions. Previous accounts were limited to a highly-stereotyped behavior, the EOD (Bell 1981; Bell, Han et al. 1997; Roberts and Bell 2000; Kennedy, Wayne et al. 2014). A critical question is whether the kind of mechanism described for predicting the effects of the mormyrid EOD or tail movements—i.e., anti-Hebbian plasticity acting on CD inputs to principal cells—is sufficient for predicting the much greater variety of sensory patterns generated by movements. There are numerous lines of evidence, detailed below, that indicated that the

cerebellum may also make predictions about the sensory consequences of movements. It is possible that the similar mechanisms underlying sensory predictions in ELL could also underlie those in the cerebellum.

It has been proposed that the cerebellum may play a key role in adaptive and predictive motor control. Predictive control allows past experience to influence an action. For example, knowing whether a cup is full or empty before picking it up influences how much force is applied to the grasp, and once the cup is grasped, it changes the dynamics of the arm movements. Experimental evidence supports that the cerebellum is probably involved in such predictive control (Bastian 2006). Several studies, for example, indicated that predictive control is deficient in cerebellar patients, who respond to unpredictable perturbations of movements but do not adapt to predictable perturbations (Smith and Shadmehr 2005; Morton and Bastian 2006).

Theoretical accounts of predictive control posit roles for at least two types of models, forward and inverse models (Wolpert, Miall et al. 1998). Forward models, generally speaking, take as input the current state of the body together with copies of motor commands and provide, as output, an estimate of the new state of the system. For example, a forward model of the arm might predict the proprioceptive signals that arise from a particular change in joint angles and velocities. An inverse model takes as inputs the goal of an action together with information about the current state of the system and provides, as output, the motor commands that will achieve the goal. Both types of models must be able to adapt to changes in the action or in the system—such as the load induced by moving the arm with a cup in hand.

Why is there a need for forward models? They apparently reproduce signals about movement that are already available from other sensory systems, such as proprioception. One plausible explanation is that feedback from the periphery is slow. For example, in eye

movements proprioceptive delays may be up to a hundred milliseconds whereas saccades can occur much faster (Wang, Zhang et al. 2007). Visual feedback is even slower, and does not inform the brain about changes in muscle forces or joint angles required to correct for movement errors. A forward model can provide this missing feedback information in real time. In addition, sensory information may provide an additional, independent source of inflow to forward models to develop an optimal estimation of the state of the body.

But where do such forward models exist and how are they implemented? What is required of a forward model are the sensory consequences that result from an action, not simply the motor command itself. Is there any evidence that elements in the cerebellum generate such signals? A 2006 study by Pasalar, et al. (Pasalar, Roitman et al. 2006) found evidence that Purkinje cells provide a kinematic representation of arm movements, i.e., position, direction, and velocity. Such a representation is consistent with Purkinje cells representing predictions about the upcoming motor state of the system, i.e., a forward model, and inconsistent with an inverse model in the cerebellum because Purkinje cell firing did not encode information about motor commands. To distinguish between a forward and inverse model, the authors designed a task in which they asked monkeys to make the same movements in environments with different dynamics. Specifically, the authors trained monkeys to use a manipulandum to control a cursor on a screen and track a stimulus moving in a circular manner. They then altered the forces required to move the manipulandum, changing the forces on the hand required to continue to track the cursor. Rather than encode some aspect of muscle force, Purkinje cell output only depended on position, direction, and velocity of the hand movement—independent of the force-field conditions. Indeed, consistent with generating sensory predictions of a movement, previous studies (Coltz, Johnson et al. 1999; Roitman, Pasalar et al. 2005) showed that the discharge of

Purkinje cells in similar tracking tasks led arm kinematics by around 100 milliseconds. Taken together, these results indicated that Purkinje cells could be generating a forward model of the upcoming motor state, which would be useful for rapid motor control. Thus, the authors suggest that the cerebellum, rather than generate motor commands, outputs predictions of the sensory consequences of motor commands. Such a function is similar to what we found ELL does in the context of swimming movements.

Results from human behavioral studies also implicate the cerebellum in generating forward models. A 2012 study by Izawa, et al. (Izawa, Criscimagna-Hemminger et al. 2012) found evidence that the cerebellum appears critical for learning to predict the visual sensory consequences of motor commands. The authors perturbed the relationship between displacement of the hand and displacement of the cursor while asking control and cerebellar patients to do two tasks. In the first task, the subjects were asked to move the cursor to goals near a previously trained target. Both cerebellar patients and controls were able to alter their motor commands in response to the trained target and generalize this to neighboring targets (inconsistent with the cerebellum acting as an inverse model that associates the goal of the movement with the motor commands to achieve that goal). Then, in a second task, they asked subjects to self-select a movement without an explicit target and then report where they believed their hand had moved to. In healthy people, the perturbation training induced larger shifts in predicted sensory consequences of the motor command than in people with cerebellar damage. This result is consistent with cerebellum acting as a forward model that predicts the sensory consequences of motor commands. Again, the output—a sensory prediction—is similar to the output of ELL in the context of swimming movements.

In short, this electrophysiological and behavioral work is reminiscent of the work described in this thesis in that what are essentially forward models are computed in cerebellum-like structures in mormyrid fish. That is, feedforward CD signals are used to generate a prediction about the expected sensory input pattern following a motor command. Given that there are similar cell types, circuitry, and plasticity in the cerebellum and cerebellum-like structures, is it possible that the mechanisms underlying the work described above are similar to those described in electric fish? One objection with previous work in electric fish is that the mechanisms were worked out within the context of the highly-specialized EOD motor command. However, the work described in this thesis, in which ELL predicts the sensory consequences of movements, suggests that the mechanisms are indeed far more general.

*Predicting one stream of sensory information with another*

In Chapter 3, we showed that ELL can generate negative images of the electrosensory consequences of movements based on proprioceptive feedback. This brings up the interesting question of predicting one stream of sensory input with another. Such a capacity would be consistent with cerebellum-like structures acting as an adaptive filter, a signal processing device that decorrelates any inputs with a teaching or error signal. Such a device would be capable of sensory cancellation, and indeed, the cerebellum itself has been proposed to act as an adaptive filter (Fujita 1982; Dean, Porrill et al. 2010), although direct experimental evidence is lacking. As detailed below, there is convincing evidence that cerebellum-like structures in other fish act as adaptive filters, generating predictions on the basis of other sensory inputs.

In the gymnotid ELL (Bastian 1995; Bastian 1996), the tail poses the same challenge for the electrosensory system as in mormryids; that is, during a tail bend, electroreceptors on one side of the body are strongly affected by the EOD whereas those on the other side are less strongly affected. Such changes would probably interfere with perception. In 1996, Bastian (Bastian 1996) showed that two types of predictive sensory signals can be used to generate negative images—proprioceptive signals and global electrosensory stimuli. In the case of proprioceptive signals, the author recorded from ELL principal cells while pairing an electrosensory stimulus with a fixed phase of a tail bend. The tail bend alone initially had little effect on the cells, but after pairing, the tail bend alone evoked responses in the cells that were negative images of the electrosensory-evoked response. As in the work described in this thesis, these negative images were probably based on proprioceptive inputs. A role for predictive inputs from the same sensory modality was demonstrated by modulating a global electrosensory stimulus in a way that mimicked the voltage changes caused by a tail movement. They then paired a local electrosensory stimulus at a fixed phase with the global modulation. ELL cells now responded to global electrosensory stimulation with negative images of the effects of the local electrosensory stimulus.

Similar adaptive processing has been observed in the elasmobranch dorsal octaval nucleus (DON), a cerebellum-like structure at the first stage in the passive electrolocation system (Montgomery and Bodznick 1994; Bodznick, Montgomery et al. 1999). Elasmobranch electroreceptors are very sensitive to electric fields, but respond vigorously to electric fields created by the fish's own ventilation (Montgomery 1984). Principal cells of the DON do not respond to the fish's own ventilation (Montgomery 1984). The cancellation of responses is probably due to negative images. This was demonstrated by pairing electrosensory stimuli to the

receptive field of DON cells with a specific phase in the ventilatory cycle. Before pairing, the cells had little response to ventilation, but after pairing, ventilation evoked strong responses in the cells that were opposite to the effects of the paired electrosensory stimulus. Similar to the gymnotid ELL, the elasmobranch DON was able to generate negative images based on either proprioceptive or global electrosensory signals (Montgomery 1984). (Pertinent to the present study, the DON was also able to use motor corollary discharge signals to form negative images.) Taken together, these results indicate that cerebellum-like structures can take a variety of signals and generate sensory predictions. Such a capacity is expected for an adaptive filter, which would not make a distinction between sensory modalities or between sensory and motor inputs. Consistent with this, we found in Chapter 3 that ELL is indifferent to the modality of the signals used as a basis for negative images, and, in fact, it appears that proprioceptive and motor signals are already randomly mixed at the level of MFs.

Such predictions of one sensory stream based on another are not limited to cerebellum-like structures. The cerebellum may also do so. In eyelid conditioning, for example, the timing of one sensory signal, an air puff or electrical shock to the eye is predicted from another sensory signal, a tone (Kim and Thompson 1997). It is thought that the air puff or electric shock is signaled by the climbing fiber whereas the mossy fibers carry information about the tone. Another example is in cerebellar modulation of the vestibulo-ocular reflex. In this case, the prediction of one sensory stimulus, retinal slip, is done by another sensory stimulus, vestibular signals. It is thought that retinal slip is signaled by the climbing fiber (Maekawa and Simpson 1972) whereas vestibular signals are conveyed by mossy fibers (Lisberger and Fuchs 1974).

*Temporal processing*

It has long been postulated that the cerebellum is involved in timing. Are studies in ELL relevant to these mechanisms? Studies of delay in classical eyelid conditioning suggest that they may be. There are clear analogies between the generation of temporally specific negative images and the learning of adaptively timed responses in eyelid conditioning (Medina, Garcia et al. 2000). Eyelid conditioning pairs a conditioned stimulus, such as a tone, with an unconditioned stimulus, such as an air puff to the eye. Initially, there is only a reflexive response to the air puff but after training of a few hundred trials, the tone will elicit an eyelid closure. Eyelid conditioning is very sensitive to the time interval between the onset of the tone and the air puff. For example, there is little or no learning when the interval is less than 100 milliseconds, learning peaks for intervals of 150-500 milliseconds, and gradually falls off for longer intervals (Schneiderman and Gormezano 1964; Smith, Coleman et al. 1969). Conditioned responses are very precisely timed, peaking at the time when the air puff is anticipated (Mauk and Ruiz 1992).

In circuit terms, the tone is conveyed to the cerebellum via MFs (Aitkin and Boyd 1978; Lewis, Lo Turco et al. 1987), the air puff is conveyed via climbing fibers (McCormick, Steinmetz et al. 1985; Mauk, Steinmetz et al. 1986; Sears and Steinmetz 1991), and output from a cerebellar nucleus drives expression of the eyelid closure (McCormick, Clark et al. 1982; McCormick and Thompson 1984). MFs synapse onto cerebellar nuclei both directly and also indirectly via the cerebellar cortex. In the cerebellar cortex, MFs synapse onto much more numerous GCs, whose axons provide parallel fiber input to Purkinje cells. Purkinje cells also receive climbing fiber input from the inferior olive. Purkinje cells provide inhibitory input to cerebellar nuclei cells. Climbing fiber activity, induced by the air puff, decreases parallel fiber synapses via long-term depression (LTD) (Ito 2001), causing Purkinje cell activity during the

tone to decrease. Because Purkinje cells are inhibitory, the transient pause in their activity increases the output of cerebellar nucleus neurons, driving eyelid closure (Heiney, Kim et al. 2014).

But how is the transient activity decrease leaned by Purkinje cells appropriately timed? Models of the cerebellum (Medina, Garcia et al. 2000; Medina and Mauk 2000) propose that activity of the GC layer is key. GC activity must vary in time such that different GCs are active at different times during the tone. Such response patterns are critical for generating appropriately timed responses because they would allow LTD to occur only for those parallel fiber synapses that are active when the air puff is presented. In addition, GC activity at different times allows for long-term potentiation (LTP) to occur at parallel fiber synapses, resulting in a large increase in Purkinje cell firing, allowing for suppression of short-latency responses. This birdirectional, reversible plasticity is reminiscent of the nature of plasticity in ELL, in which these features are critical for adaptive processing.

A number of models of GC activity have been proposed that fulfill the requirement that GCs are active at different times. As detailed by Medina and Mauk (Medina and Mauk 2000), there are at least three popular models for timing. The first, the tapped-delay-line model, assumes that the tone engages different input elements in sequence. A second model, the spectral model, assumes that GCs have a variety of time constants such that parallel fiber synapses are active at different times after the tone. A third model, the oscillatory model, assumes that GCs activated by the tone oscillate with different frequencies. The combination of GCs active at any one point in time is unique, with the timing arising because particular combinations of cells are weakened through LTD by the air puff-activated climbing fiber input. Results from a computer simulation suggested that dynamic interactions between MFs, Golgi cells, and GCs give rise to GCs that are

active at different times during the tone (Medina, Garcia et al. 2000). Although clearly in this simulation Golgi cells played a critical role in generating such temporally diverse responses, direct experimental evidence is lacking. Regardless of the exact nature of GC responses, the upshot of these models is that GC responses serve as a temporal basis that is sculpted by bidirectional plasticity, allowing for adaptively timed responses. Such a capacity is very similar to mechanisms in ELL, as detailed below.

When ELL generates temporally-specific negative image, it faces similar challenges to those the cerebellum faces in eyelid conditioning. In this case, the system must transform brief, minimally delayed electric organ corollary discharge (EOCD) signals conveyed by MFs into a temporally-expanded basis because the sensory consequences of the fish's own EOD on its passive electroreceptors can last for several hundred milliseconds. As in the cerebellum, MF input is first transformed by GC circuitry before synapsing onto downstream principal neurons. If different GCs are not active at different times relative to the EOD motor commands, then associative plasticity at specific delays relative to the command would not be possible. Although previous models of ELL assumed a tapped-delay-line model of GC activity (Roberts and Bell 2000), recent work (Kennedy, Wayne et al. 2014) has shown a role for a GC layer interneuron, the unipolar brush cell (UBC). In vivo recordings demonstrated that UBCs apparently take brief MF input and generate temporally diverse and delayed responses that are faithfully recoded in GCs. These responses are highly non-uniform, unlike a delay line model, although the concept is similar—GC responses that are active at different times throughout the EOD cycle or eyelid delay period. This role for UBCs is in contrast to models of the cerebellum in which Golgi cell inhibition is thought to create the temporally diverse responses required by eyelid conditioning. Although it should be noted that the mechanisms are by no means mutually exclusive, as roles

for Golgi cells and UBCs in the cerebellum have yet to be directly explored. Whatever the exact mechanism, this capacity for learning timed relationships could be useful not only for predicting the sensory consequences of the EOD or eyelid conditioning, but also for predicting the sensory consequences of movements, as suggested by the work here. Our results showed brief bursts and pauses in MFs carrying CD information, yet long-lasting negative images extending several hundred milliseconds in time were observed. The mechanisms for temporal expansion may be similar, and could be tested in future work.

## Future Directions

### *Future directions related to Chapter 2: Generalization experiments*

The issue of whether the brain uses internal models has been studied extensively in behavioral experiments in human motor control. For example, an approach to study motor adaptation is to change the mechanical environment of the body so that the subject must adapt the motor control system to perturbed dynamics of the system. These experiments ask the subject to reach for a target while perturbing that motion with a load or a force-field (Lacquaniti, Soechting et al. 1982; Lackner and Dizio 1994). Eventually, the subjects adapt to the new environment. Upon removal of the perturbation, however, aftereffects are seen that persist for some time and are specific to the magnitude of the perturbation; specifically, the subjects err in the opposite direction of the perturbation. Such adaptation and aftereffects are reminiscent of cancellation and negative images in fish.

But how is the existence of an internal model investigated? In one interesting study, Shadmehr and Mussa-Ivaldi (Shadmehr and Mussa-Ivaldi 1994) investigated motor adaptation in a force-field to ask how the nervous system adapts. They concluded that the nervous system

forms an internal model of the arm dynamics in the modified environment. The authors reasoned that the adaptation was due to an internal model rather than a "look-up table," because the subjects were able to transfer the learning to another workspace (where performing the same reaching task required different joint configurations). That is, the adaptation "generalized" beyond the training conditions—consistent with the construction of an internal model of the new dynamics. However, despite extensive work, these behavioral results and theoretical conjectures have yet to receive a satisfactory mechanistic explanation at the level of neural circuits.

Motivated by this "generalization" genre of human behavioral experiments, analogous negative image experiments can be performed in fish, with analysis at the level of neural circuits. These experiments can be performed in a number of ways. Here, I will describe three possible sets of experiments: probing generalization in the context of microstimulation of the mesencephalic locomotor region (MLR), microstimulation of the optic tectum, and with passive movements of the tail.

To test generalization in the context of MLR microstimulation, we would take advantage of one of our fictive preparations presented in Chapter 2. Briefly, in this preparation we evoked rhythmic swimming movements by continuous microstimulation of the MLR, which evoked swimming in the 1-6 Hz range. The frequency of swimming movements clearly graded with stimulus intensity. After characterizing the movements evoked by microstimulation, we paralyzed the fish and monitored motor commands directly by recording from motor nerves that exit in the ventral root of the spinal cord. In our preparation, nerve recordings revealed rhythmic bursts of activity, the frequency of which graded with stimulus intensity, comparable to swimming frequencies prior to paralysis.

Can ELL neurons use movement-related CD to generate negative images of the electrosensory consequences of rhythmic swimming movements? If so, do those negative images generalize to multiple swimming frequencies? To test this directly, we would perform a pairing experiment analogous to those performed in Chapter 2. As before, we would simulate natural patterns of activation for the electrosensory system by delivering a brief electrical pulse (between the stomach of the fish and the tank) following each electric organ motor command. Then, we would paralyze the fish and make extracellular single-unit recordings from ELL principal cells. We would smoothly grade the amplitude of a local electrosensory stimulus applied to the neuron's receptive field as a function of a smoothed ventral nerve signal. This would have the effect of approximating the electrosensory consequences of the swimming movement prior to paralysis. We would then compare spiking response before and after a pairing period of 10-15 minutes. We would expect to see ELL neurons exhibit rhythmically modulated negative image responses locked to the motor nerve signal. Such an experiment would address whether ELL neurons can use movement-related CD to generate negative images of the electrosensory consequences of rhythmic swimming movements.

To test whether these negative images generalize to multiple swimming frequencies, we could simply modify the pairing experiment above. In this case, we would probe the spiking activity of an ELL neuron at three microstimulation intensities (which evoked three different rhythmic swimming frequencies prior to paralysis). Then, we would pair a local electrosensory stimulus with one of the microstimulation intensities. Finally, we would probe again at all three microstimulation intensities. If the effects generalize, we would expect that negative images were formed regardless of the probed microstimulation frequency. Such a capacity to generalize

would be useful, as the sensory consequences of every swimming movement would not have to be experienced to be predicted.

Another experiment in this spirit would be to test generalization in the context of tectal microstimulation. This experiment would be set up as above except tectal microstimulation would be used to evoke rapid tail movements. We would develop a microstimulation protocol that allowed us to vary parameters of the movement, such as position and velocity, independently. Indeed, varying stimulus parameters has been shown to vary movement characteristics of the tail in goldfish (Herrero, Rodriguez et al. 1998) when stimulating the tectum, and the eye in primates (Van Opstal, Van Gisbergen et al. 1990) when stimulating in the superior colliculus. In our case, for example, prior to paralysis, we would generate one movement that had a high velocity but small position deviation, another movement with the same velocity but a larger position deviation, and one movement with a low velocity and a high position deviation. Then we would then paralyze the fish and examine spiking activity in ELL neurons in response to all three microstimulation protocols. We would then pair a local electrosensory stimulus with one of the microstimulation protocols and again probe all three. Can the fish learn the different components of the movements? That is, does learning information about velocity, for example, generalize to all velocities? Does information about position generalize to all positions? Such a capacity would be useful as the sensory consequences of every swimming movement would not have to be experienced to be predicted.

A final experiment would be to test generalization in the context of proprioceptive movements. These experiments are quite simple: We would pair an electrosensory stimulus with a restricted range of tail movements and then probe at a much greater range. Interestingly, whether or not the fish can form negative images outside of the paired region may be able to be

traced back to the nature of the predictive signals. MFs conveying information from stretch receptors encode the position of body segments with great fidelity. These signals are transformed into tuning curves in GCs. Are these tuning curves relatively narrow or wide? Narrow tuning curves may imply that the fish can form highly-specific negative images, but that do not generalize outside of the paired region. Wide tuning curves may imply that the negative images do generalize. Indeed, Shadmehr and Mussa-Ivaldi (Shadmehr and Mussa-Ivaldi 1994) propose that the elements with which the nervous system formed an internal model of environmental forces must have had wide receptive fields, producing a response for areas of the workspace outside of the trained region. In our case, we know what these elements are: the GCs. Are wide receptive fields, in these contexts, all that is needed for generalization to occur? This would imply that a relatively simple mechanism may contribute to the complex phenomenon of generalization.

*Future directions related to Chapter 2: Motor coding*

Another avenue of inquiry related to Chapter 2 is to further investigate the responses of MFs and GCs in response to movements. The capacity of internal models may greatly depend upon the structure of their inputs. Movement-related information includes both CD and proprioceptive feedback. Proprioceptive feedback conveyed by MFs has been somewhat characterized and is clearly capable of encoding tail position (Bell, Grant et al. 1992; Sawtell 2010), a relevant variable in sensory predictions. However, it is not clear what relevant variables CD information may be encoding. In the work here, we performed a cursory examination of CD information in response to MLR and tectal microstimulation, but did not systematically explore the nature of motor responses.

In the case of tectal microstimulation, we observed brief bursts and pauses in MF firing rates. A future direction could be to develop a microstimulation protocol in which we can change stimulus parameters to induce movements with different kinematic profiles. For example, we could systematically evoke movements of higher velocities that reach the same final tail position and ask whether the bursts or pauses increase in depth of modulation, implying that there may be a velocity coding scheme. We could also develop a microstimulation protocol to keep velocity constant while varying final tail position. We could then ask whether burst or pause duration encodes any aspect of tail position. Alternatively, it is possible that bursts or pauses encode other aspects of movements, such as force or acceleration. Microstimulation protocols could be developed to test this hypothesis as well. During all of these experiments, ventral nerve activity could be monitored to ensure that microstimulation parameters influence motor activity.

It is possible that the information carried by MFs may only make sense in light of how they are transformed in the output of GCs. Thus, one future direction is to record from GCs to better understand motor coding. Perhaps MFs are transformed into the relevant variables once recoded in GCs. For example, the brief bursts could be temporally expanded to span the length of the movement, which is much longer than the burst itself. In the process of this temporal expansion, is it possible that the brief bursts are transformed into a velocity or a position signal? GCs are accessible to in vivo recording, which would allow direct testing of this hypothesis.

*Future directions related to Chapter 3: Proprioceptive feedback as a basis for negative images*

CD is probably only part of the story, however. In real life, the fish has access to proprioceptive information as well as CD. Is proprioceptive information rapid and accurate

enough to provide a basis for generating negative images? The results presented in Chapter 3 (**Figures 3.3 and 3.4**) suggest that proprioceptive information can provide a basis in the context of simple, rapid movements, but the full capacity of the system has not been probed.

To test this capacity more directly we determined whether ELL neurons could generate negative images of the electrosensory consequences of rapid tail movements (moving the tail in a random Gaussian pattern low-pass filtered with cut-off frequency of 6 Hz). As in previous experiments, we simulated natural patterns of activation for the electrosensory system by delivering a brief electrical pulse (between the stomach of the fish and the tank) following each EOD motor command, mimicking the duration and timing of the fish's own EOD. We then paralyzed the fish and made extracellular recordings from ELL principal neurons. We compared spiking responses before and after a pairing period (10-15 min) during which the amplitude of a local electrosensory stimulus (ES) delivered at the time of the EOD motor command was smoothly graded as a function of tail position. As described previously, most neurons exhibited responses to the EOD motor command. Before pairing, such responses were similar across tail positions (**Figure 4.1a**, top row). After pairing, such responses resembled smoothly graded negative images, i.e. responses were clearly larger at positions paired with an inhibitory ES and smaller at positions paired with an excitatory ES (**Figure 4.1a**, middle, bottom). Negative images were observed in both E- and I-type cells and regardless of whether we paired with an ES that decreases as tail moves from ipsi to contra, or the reverse (increasing the ES as the tail moves from ipsi to contra). We therefore grouped cells by sensory response to the ES, independent of cell type (decreasing, n=6; increasing, n=4; **Figure 4.1b**) and plotted the difference (post-pre) in the response to the EOD command as a function of tail position. As shown in **Figure 4.1b**, pairing resulted in robust changes in the neural response that were

smoothly graded negative images of the effects of the electrosensory stimulus during pairing. Furthermore, cross-correlation analysis revealed that such negative images were only minimally delayed compared with tail position (11.8 $\pm$ 9.9 ms (mean$\pm$s.d.), n=8; **Figure 4.1c).**

The conclusion of these preliminary results is that proprioception could provide a suitable basis for negative images under a variety of swimming conditions. If proprioceptive coding is sufficient, what is the role for motor signals? A future set of experiments to address this would be to repeat to repeat the "active" experiments described in Chapter 3, **Figures 3.3 and 3.4**, under conditions of rhythmic movements evoked by MLR microstimulation. In these experiments, we would compare the responses of ELL neurons before and after pairing electrosensory input under conditions in which only CD was engaged, only proprioceptive feedback was engaged or both were engaged. Prior to paralysis, microstimulation of the MLR would evoke rhythmic swimming movements, which we could measure with a laser displacement sensor. After paralysis we would, as before, monitor motor commands with ventral nerve recordings. We could then play back the microstimulation-evoked tail movement using a computer-controlled stage to mimic the pre-paralysis movement. This setup, as before, allows us to engage CD and proprioceptive inputs either separately or together and, as before, to control their relationship to an electrosensory stimulus. After observing ELL neuron responses under all three conditions (fictive, active, and passive), we would then pair an electrosensory stimulus under the active conditions, in which we microstimulated the MLR while playing back the tail movements. In our previous results, we observed that both CD and proprioception contributed equivalently to negative images. Is this true in the context of slower, rhythmic swimming movements? These experiments would address that possibility.

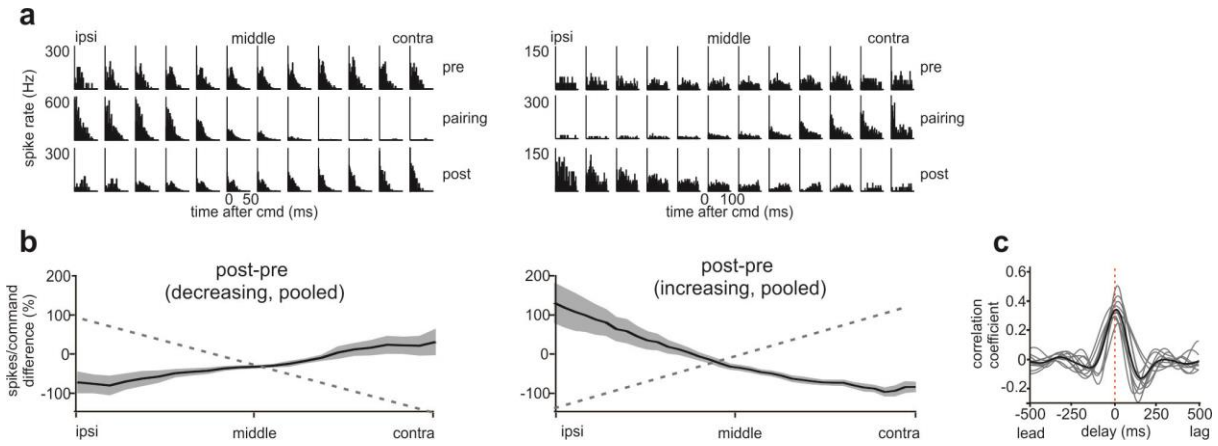


**Figure 4.1. Negative images based on rapid proprioceptive feedback. (a)** Typical responses of two E-type efferent cells before, during, and after pairing with an ES. Histograms are triggered at the time of the EOD motor command and binned by tail position. Note that plastic changes occur regardless of whether the ES is increasing or decreasing as a function of tail position. **(b)** Average of difference traces pooled across cells. The difference traces show the effects of pairing, and were constructed by subtracting the post-pairing response from the pre-pairing response. Cells were pooled independent of type (E- or I-cells) to match polarity of difference trace. Each cell is normalized to its baseline spike count per command prior to pairing. Error bars represent s.e.m. across cells. **(c)** Cross-correlation of measured tail position vs smoothed spike rate. Light gray traces represent cross correlations for individual cells and black trace is the average across cells. Only cells in which the command was microstimulated at a constant rate were included in the analysis. Note the minimal delay.

*Concluding Remarks*

This thesis found that spinal CD and proprioceptive signals can be used as a basis to generate negative images of the sensory consequences of simple tail movements. In Chapter 2, we demonstrated that CD signals can be used to predict the sensory consequences of simple tail movements. In Chapter 3, we demonstrated that both CD and/or proprioceptive signals can be used to predict the sensory consequences of simple tail movements and developed a simple network model to explain interactions between CD and proprioception. The work in these two chapters relates to broader questions in neuroscience in interesting ways, especially in relation to research in the mammalian cerebellum. Predicting the sensory consequences of movements could be useful for a number of reasons. On the one hand, such a prediction could be useful as the output of a forward model to estimate the upcoming motor state, facilitating fast and

coordinated movements. On the other hand, such a prediction could be useful to generate a cancellation signal for removing self-generated sensory input. It is interesting that similar mechanisms could underlie such disparate functions. Another interesting aspect of the work described here is that we have shown that one stream of sensory input can predict another—i.e., proprioceptive input predicts electrosensory input. This is interesting as it supports the notion of cerebellum-like structures acting as adaptive filters. Adaptive filters can use any input signal that is predictive, not just motor commands. In short, the results here support that cerebellar microcircuit can act as a simple forward model, and that adaptive filtering may be the implementation scheme behind it. Further work in electric fish will undoubtedly shed light on some of these issues.

## LITERATURE CITED


Abbott, L. F. and S. B. Nelson (2000). "Synaptic plasticity: taming the beast." Nat Neurosci **3 Suppl**: 1178-1183.

Aitkin, L. M. and J. Boyd (1978). "Acoustic input to the lateral pontine nuclei." Hear Res **1**(1): 67-77.

Albus, J. (1971). "A theory of cerebellar function." Mathematical Biosciences **10**: 25-61.

Anderson, S. R., J. Porrill, et al. (2012). "An internal model architecture for novelty detection: implications for cerebellar and collicular roles in sensory processing." PLoS One **7**(9): e44560.

Angelaki, D. E. and K. E. Cullen (2008). "Vestibular system: the many facets of a multimodal sense." Annu Rev Neurosci **31**: 125-150.

Arenz, A., E. F. Bracey, et al. (2009). "Sensory representations in cerebellar granule cells." Curr Opin Neurobiol **19**(4): 445-451.

Arshavsky, Y. I., I. M. Gelfand, et al. (1978). "Messages conveyed by spinocerebellar pathways during scratching in the cat. II. Activity of neurons of the ventral spinocerebellar tract." Brain Res **151**(3): 493-506.

Barker, D., C. C. Hunt, et al. (1974). Muscle receptors. Berlin, New York,, Springer-Verlag.

Barmack, N. H. and H. Shojaku (1992). "Vestibularly induced slow oscillations in climbing fiber responses of Purkinje cells in the cerebellar nodulus of the rabbit." Neuroscience **50**(1): 1-5.

Barmack, N. H. and V. Yakhnitsa (2008). "Functions of interneurons in mouse cerebellum." J Neurosci **28**(5): 1140-1152.

Bastian, A. J. (2006). "Learning to predict the future: the cerebellum adapts feedforward movement control." Curr Opin Neurobiol **16**(6): 645-649.

Bastian, J. (1995). "Pyramidal-cell plasticity in weakly electric fish: a mechanism for attenuating responses to reafferent electrosensory inputs." J Comp Physiol A **176**(1): 63-73.

Bastian, J. (1996). "Plasticity in an electrosensory system. I. General features of a dynamic sensory filter." J Neurophysiol **76**(4): 2483-2496.

Bell, C., K. Dunn, et al. (1995). "Electric Organ Corollary Discharge Pathways in Mormyrid Fish .1. The Mesencephalic Command Associated Nucleus." Journal of Comparative Physiology a-Sensory Neural and Behavioral Physiology **177**(4): 449-462.

Bell, C. C. (1981). "An efference copy which is modified by reafferent input." Science **214**(4519): 450-453.

Bell, C. C. (1982). "Properties of a modifiable efference copy in an electric fish." J Neurophysiol **47**(6): 1043-1056.

Bell, C. C. (2002). "Evolution of cerebellum-like structures." Brain Behav Evol **59**(5-6): 312-326.

Bell, C. C., A. Caputi, et al. (1997). "Physiology and plasticity of morphologically identified cells in the mormyrid electrosensory lobe." J Neurosci **17**(16): 6409-6423.

Bell, C. C., A. Caputi, et al. (1993). "Storage of a sensory pattern by anti-Hebbian synaptic plasticity in an electric fish." Proc Natl Acad Sci U S A **90**(10): 4650-4654.

Bell, C. C., T. E. Finger, et al. (1981). "Central connections of the posterior lateral line lobe in mormyrid fish." Exp Brain Res **42**(1): 9-22.

Bell, C. C. and K. Grant (1992). "Sensory processing and corollary discharge effects in mormyromast regions of mormyrid electrosensory lobe. II. Cell types and corollary discharge plasticity." J Neurophysiol **68**(3): 859-875.

Bell, C. C., K. Grant, et al. (1992). "Sensory processing and corollary discharge effects in the mormyromast regions of the mormyrid electrosensory lobe. I. Field potentials, cellular activity in associated structures." J Neurophysiol **68**(3): 843-858.

Bell, C. C., V. Han, et al. (2008). "Cerebellum-like structures and their implications for cerebellar function." Annu Rev Neurosci **31**: 1-24.

Bell, C. C., V. Z. Han, et al. (1997). "Synaptic plasticity in a cerebellum-like structure depends on temporal order." Nature **387**(6630): 278-281.

Bell, C. C., S. Libouban, et al. (1983). "Pathways of the electric organ discharge command and its corollary discharges in mormyrid fish." J Comp Neurol **216**(3): 327-338.

Bell, C. C., J. Meek, et al. (2005). "Immunocytochemical identification of cell types in the mormyrid electrosensory lobe." J Comp Neurol **483**(1): 124-142.

Bell, C. C. and C. J. Russell (1978). "Effect of electric organ discharge on ampullary receptors in a mormyrid." Brain Res **145**(1): 85-96.

Bennett, M. V., G. D. Pappas, et al. (1967). "Physiology and ultrastructure of electrotonic junctions. II. Spinal and medullary electromotor nuclei in mormyrid fish." J Neurophysiol **30**(2): 180-208.

Bodznick, D., J. C. Montgomery, et al. (1999). "Adaptive mechanisms in the elasmobranch hindbrain." J Exp Biol **202**(# (Pt 10)): 1357-1364.

Bone, Q. (1979). 6 Locomotor Muscle. Fish Physiology. W. S. Hoar and D. J. Randall, Academic Press. **Volume 7:** 361-424.

Boyd, I. A. (1980). "The Isolated Mammalian Muscle-Spindle." Trends in Neurosciences **3**(11): 258-265.

Boyden, E. S., A. Katoh, et al. (2004). "Cerebellum-dependent learning: the role of multiple plasticity mechanisms." Annu Rev Neurosci **27**: 581-609.

Brooks, J. X. and K. E. Cullen (2013). "The primate cerebellum selectively encodes unexpected self-motion." Curr Biol **23**(11): 947-955.

Bullock, T. H. and W. Heiligenberg (1986). Electroreception. New York, Wiley.

Chadderton, P., T. W. Margrie, et al. (2004). "Integration of quanta in cerebellar granule cells during sensory processing." Nature **428**(6985): 856-860.

Chen, L., J. L. House, et al. (2005). "Modeling signal and background components of electrosensory scenes." J Comp Physiol A Neuroethol Sens Neural Behav Physiol **191**(4): 331-345.

Coltz, J. D., M. T. Johnson, et al. (1999). "Cerebellar Purkinje cell simple spike discharge encodes movement velocity in primates during visuomotor arm tracking." J Neurosci **19**(5): 1782-1803.

Crapse, T. B. and M. A. Sommer (2008). "Corollary discharge across the animal kingdom." Nat Rev Neurosci **9**(8): 587-600.

Crowley, J. J., D. Fioravante, et al. (2009). "Dynamics of fast and slow inhibition from cerebellar golgi cells allow flexible control of synaptic integration." Neuron **63**(6): 843-853.

Cullen, K. E. (2004). "Sensory signals during active versus passive movement." Curr Opin Neurobiol **14**(6): 698-706.

Dean, P. and J. Porrill (2008). "Adaptive-filter models of the cerebellum: computational analysis." Cerebellum **7**(4): 567-571.

Dean, P., J. Porrill, et al. (2010). "The cerebellar microcircuit as an adaptive filter: experimental and computational evidence." Nat Rev Neurosci **11**(1): 30-43.

Deliagina, T. G., P. V. Zelenin, et al. (2002). "Encoding and decoding of reticulospinal commands." Brain Res Brain Res Rev **40**(1-3): 166-177.

Diedrichsen, J., S. E. Criscimagna-Hemminger, et al. (2007). "Dissociating timing and coordination as functions of the cerebellum." J Neurosci **27**(23): 6291-6301.

Ebner, T. J., M. T. Johnson, et al. (2002). "What do complex spikes signal about limb movements?" Ann N Y Acad Sci **978**: 205-218.

Ebner, T. J. and S. Pasalar (2008). "Cerebellum predicts the future motor state." Cerebellum **7**(4): 583-588.

Ekerot, C. F. and H. Jorntell (2001). "Parallel fibre receptive fields of Purkinje cells and interneurons are climbing fibre-specific." Eur J Neurosci **13**(7): 1303-1310.

Engelmann, J., S. Nobel, et al. (2009). "The Schnauzenorgan-response of Gnathonemus petersii." Front Zool **6**: 21.

Fedirchuk, B., K. Stecina, et al. (2013). "Rhythmic activity of feline dorsal and ventral spinocerebellar tract neurons during fictive motor actions." J Neurophysiol **109**(2): 375-388.

Fetcho, J. R. and K. R. Svoboda (1993). "Fictive swimming elicited by electrical stimulation of the midbrain in goldfish." J Neurophysiol **70**(2): 765-780.

Ford, J. M. and D. H. Mathalon (2012). "Anticipating the future: automatic prediction failures in schizophrenia." Int J Psychophysiol **83**(2): 232-239.

Fotowat, H., R. R. Harrison, et al. (2013). "Statistics of the electrosensory input in the freely swimming weakly electric fish Apteronotus leptorhynchus." J Neurosci **33**(34): 13758-13772.

Fujita, M. (1982). "Adaptive filter model of the cerebellum." Biol Cybern **45**(3): 195-206.

Gao, Z., B. J. van Beugen, et al. (2012). "Distributed synergistic plasticity and cerebellar learning." Nat Rev Neurosci **13**(9): 619-635.

Graf, W., J. I. Simpson, et al. (1988). "Spatial organization of visual messages of the rabbit's cerebellar flocculus. II. Complex and simple spike responses of Purkinje cells." J Neurophysiol **60**(6): 2091-2121.

Grant, K., C. C. Bell, et al. (1986). "Morphology and physiology of the brainstem nuclei controlling the electric organ discharge in mormyrid fish." J Comp Neurol **245**(4): 514-530.

Guthrie, B. L., J. D. Porter, et al. (1983). "Corollary discharge provides accurate eye position information to the oculomotor system." Science **221**(4616): 1193-1195.

Han, V. Z., K. Grant, et al. (2000). "Reversible associative depression and nonassociative potentiation at a parallel fiber synapse." Neuron **27**(3): 611-622.

Hantman, A. W. and T. M. Jessell (2010). "Clarke's column neurons as the focus of a corticospinal corollary circuit." Nat Neurosci **13**(10): 1233-1239.

Harvey-Girard, E., J. Lewis, et al. (2010). "Burst-induced anti-Hebbian depression acts through short-term synaptic dynamics to cancel redundant sensory signals." J Neurosci **30**(17): 6152-6169.

Heiney, S. A., J. Kim, et al. (2014). "Precise control of movement kinematics by optogenetic inhibition of Purkinje cell activity." J Neurosci **34**(6): 2321-2330.

Herrero, L., F. Rodriguez, et al. (1998). "Tail and eye movements evoked by electrical microstimulation of the optic tectum in goldfish." Exp Brain Res **120**(3): 291-305.

Hulliger, M. (1984). "The Mammalian Muscle-Spindle and Its Central Control." Reviews of Physiology Biochemistry and Pharmacology **101**: 1-110.

Ito, M. (2001). "Cerebellar long-term depression: characterization, signal transduction, and functional roles." Physiol Rev **81**(3): 1143-1195.

Izawa, J., S. E. Criscimagna-Hemminger, et al. (2012). "Cerebellar contributions to reach adaptation and learning sensory consequences of action." J Neurosci **32**(12): 4230-4239.

Jankowska, E., E. Nilsson, et al. (2011). "Processing information related to centrally initiated locomotor and voluntary movements by feline spinocerebellar neurones." J Physiol **589**(Pt 23): 5709-5725.

Jorntell, H. and C. Hansel (2006). "Synaptic memories upside down: bidirectional plasticity at cerebellar parallel fiber-Purkinje cell synapses." Neuron **52**(2): 227-238.

Kalmijn, A. J. (1971). "The electric sense of sharks and rays." J Exp Biol **55**(2): 371-383.

Ke, M. C., C. C. Guo, et al. (2009). "Elimination of climbing fiber instructive signals during motor learning." Nat Neurosci **12**(9): 1171-1179.

Kennedy, A., G. Wayne, et al. (2014). "A temporal basis for predicting the sensory consequences of motor commands in an electric fish." Nat Neurosci **17**(3): 416-422.

Kim, J. J. and R. F. Thompson (1997). "Cerebellar circuits and synaptic mechanisms involved in classical eyeblink conditioning." Trends Neurosci **20**(4): 177-181.

Kobayashi, Y., K. Kawano, et al. (1998). "Temporal firing patterns of Purkinje cells in the cerebellar ventral paraflocculus during ocular following responses in monkeys II. Complex spikes." J Neurophysiol **80**(2): 832-848.

Kolkman, K. E., L. E. McElvain, et al. (2011). "Diverse precerebellar neurons share similar intrinsic excitability." J Neurosci **31**(46): 16665-16674.

Kyriakatos, A., R. Mahmood, et al. (2011). "Initiation of locomotion in adult zebrafish." J Neurosci **31**(23): 8422-8431.

Lackner, J. R. and P. Dizio (1994). "Rapid adaptation to Coriolis force perturbations of arm trajectory." J Neurophysiol **72**(1): 299-313.

Lacquaniti, F., J. F. Soechting, et al. (1982). "Some Factors Pertinent to the Organization and Control of Arm Movements." Brain Research **252**(2): 394-397.

Le Ray, D., L. Juvin, et al. (2011). "Chapter 4--supraspinal control of locomotion: the mesencephalic locomotor region." Prog Brain Res **188**: 51-70.

Lewis, J. L., J. J. Lo Turco, et al. (1987). "Lesions of the middle cerebellar peduncle disrupt acquisition and retention of the rabbit's classically conditioned nictitating membrane response." Behav Neurosci **101**(2): 151-157.

Lisberger, S. G. and A. F. Fuchs (1974). "Response of flocculus Purkinje cells to adequate vestibular stimulation in the alert monkey: fixation vs. compensatory eye movements." Brain Res **69**(2): 347-353.

Lissmann, H. W. and K. E. Machin (1958). "The Mechanism of Object Location in Gymnarchus-Niloticus and Similar Fish." Journal of Experimental Biology **35**(2): 451-486.

Lundberg, A. (1971). "Function of the ventral spinocerebellar tract. A new hypothesis." Exp Brain Res **12**(3): 317-330.

Maekawa, K. and J. I. Simpson (1972). "Climbing fiber activation of Purkinje cells in the flocculus by impulses transferred through the visual pathway." Brain Res **39**(1): 245-251.

Maler, L., H. J. Karten, et al. (1973). "The central connections of the anterior lateral line nerve of Gnathonemus petersii." J Comp Neurol **151**(1): 67-84.

Maler, L., H. J. Karten, et al. (1973). "The central connections of the posterior lateral line nerve of Gnathonemus petersii." J Comp Neurol **151**(1): 57-66.

Mante, V., D. Sussillo, et al. (2013). "Context-dependent computation by recurrent dynamics in prefrontal cortex." Nature **503**(7474): 78-84.

Marr, D. (1969). "A theory of cerebellar cortex." J Physiol **202**(2): 437-470.

Matsushita, M. and T. Tanami (1987). "Spinocerebellar projections from the central cervical nucleus in the cat, as studied by anterograde transport of wheat germ agglutinin-horseradish peroxidase." J Comp Neurol **266**(3): 376-397.

Mauk, M. D. and B. P. Ruiz (1992). "Learning-dependent timing of Pavlovian eyelid responses: differential conditioning using multiple interstimulus intervals." Behav Neurosci **106**(4): 666-681.

Mauk, M. D., J. E. Steinmetz, et al. (1986). "Classical conditioning using stimulation of the inferior olive as the unconditioned stimulus." Proc Natl Acad Sci U S A **83**(14): 5349-5353.

McClellan, A. D. and S. Grillner (1984). "Activation of 'fictive swimming' by electrical microstimulation of brainstem locomotor regions in an in vitro preparation of the lamprey central nervous system." Brain Res **300**(2): 357-361.

McCormick, D. A., G. A. Clark, et al. (1982). "Initial localization of the memory trace for a basic form of learning." Proc Natl Acad Sci U S A **79**(8): 2731-2735.

McCormick, D. A., J. E. Steinmetz, et al. (1985). "Lesions of the inferior olivary complex cause extinction of the classically conditioned eyeblink response." Brain Res **359**(1-2): 120-130.

McCormick, D. A. and R. F. Thompson (1984). "Cerebellum: essential involvement in the classically conditioned eyelid response." Science **223**(4633): 296-299.

Medina, J. F., K. S. Garcia, et al. (2000). "Timing mechanisms in the cerebellum: testing predictions of a large-scale computer simulation." J Neurosci **20**(14): 5516-5525.

Medina, J. F. and M. D. Mauk (2000). "Computer simulation of cerebellar information processing." Nat Neurosci **3 Suppl**: 1205-1211.

Meek, J., K. Grant, et al. (1996). "Interneurons of the ganglionic layer in the mormyrid electrosensory lateral line lobe: Morphology, immunohistochemistry, and synaptology." Journal of Comparative Neurology **375**(1): 43-65.

Mohr, C., P. D. Roberts, et al. (2003). "The mormyromast region of the mormyrid electrosensory lobe. I. Responses to corollary discharge and electrosensory stimuli." J Neurophysiol **90**(2): 1193-1210.

Montgomery, J. (1984). "Noise cancellation in the electrosensory system of the thornback ray; common mode rejection of input produced by the animal's own ventilatory input." Journal of Comparative Physiology **155**: 8.

Montgomery, J. C. and D. Bodznick (1994). "An adaptive filter that cancels self-induced noise in the electrosensory and lateral line mechanosensory systems of fish." Neurosci Lett **174**(2): 145-148.

Morton, S. M. and A. J. Bastian (2006). "Cerebellar contributions to locomotor adaptations during splitbelt treadmill walking." J Neurosci **26**(36): 9107-9116.

Nixon, P. D. and R. E. Passingham (2001). "Predicting sensory events. The role of the cerebellum in motor learning." Exp Brain Res **138**(2): 251-257.

Noda, H. and T. Warabi (1982). "Eye position signals in the flocculus of the monkey during smooth-pursuit eye movements." J Physiol **324**: 187-202.

Oscarsson, O. (1965). "Functional Organization of the Spino- and Cuneocerebellar Tracts." Physiol Rev **45**: 495-522.

Pasalar, S., A. V. Roitman, et al. (2006). "Force field effects on cerebellar Purkinje cell discharge with implications for internal models." Nat Neurosci **9**(11): 1404-1411.

Paulin, M. G. (2005). "Evolution of the cerebellum as a neuronal machine for Bayesian state estimation." J Neural Eng **2**(3): S219-234.

Pouget, A. and T. J. Sejnowski (1997). "Spatial transformations in the parietal cortex using basis functions." Journal of Cognitive Neuroscience **9**(2): 222-237.

Poulet, J. F. and B. Hedwig (2007). "New insights into corollary discharges mediated by identified neural pathways." Trends Neurosci **30**(1): 14-21.

Requarth, T. and N. Sawtell (2013). Predicting the sensory consequences of movements with spinocerebellar corollary discharge. Society for Neuroscience, San Diego, CA.

Rigotti, M., O. Barak, et al. (2013). "The importance of mixed selectivity in complex cognitive tasks." Nature **497**(7451): 585-590.

Roberts, P. D. and C. C. Bell (2000). "Computational consequences of temporally asymmetric learning rules: II. Sensory image cancellation." J Comput Neurosci **9**(1): 67-83.

Roitman, A. V., S. Pasalar, et al. (2005). "Position, direction of movement, and speed tuning of cerebellar Purkinje cells during circular manual tracking in monkey." J Neurosci **25**(40): 9244-9257.

Rothman, J. S., L. Cathala, et al. (2009). "Synaptic depression enables neuronal gain control." Nature **457**(7232): 1015-1018.

Ruigrok, T. J., R. A. Hensbroek, et al. (2011). "Spontaneous activity signatures of morphologically identified interneurons in the vestibulocerebellum." J Neurosci **31**(2): 712-724.

Saitoh, K., A. Menard, et al. (2007). "Tectal control of locomotion, steering, and eye movements in lamprey." J Neurophysiol **97**(4): 3093-3108.

Sawtell, N. B. (2010). "Multimodal integration in granule cells as a basis for associative plasticity and sensory prediction in a cerebellum-like circuit." Neuron **66**(4): 573-584.

Sawtell, N. B. and A. Williams (2008). "Transformations of electrosensory encoding associated with an adaptive filter." J Neurosci **28**(7): 1598-1612.

Sawtell, N. B., A. Williams, et al. (2007). "Central control of dendritic spikes shapes the responses of Purkinje-like cells through spike timing-dependent synaptic plasticity." J Neurosci **27**(7): 1552-1565.

Schneiderman, N. and I. Gormezano (1964). "Conditioning of the Nictitating Membrane of the Rabbit as a Function of Cs-Us Interval." J Comp Physiol Psychol **57**: 188-195.

Schonewille, M., Z. Gao, et al. (2011). "Reevaluating the role of LTD in cerebellar motor learning." Neuron **70**(1): 43-50.

Sears, L. L. and J. E. Steinmetz (1991). "Dorsal accessory inferior olive activity diminishes during acquisition of the rabbit classically conditioned eyelid response." Brain Res **545**(1-2): 114-122.

Shadmehr, R. and J. W. Krakauer (2008). "A computational neuroanatomy for motor control." Exp Brain Res **185**(3): 359-381.

Shadmehr, R. and F. A. Mussa-Ivaldi (1994). "Adaptive representation of dynamics during learning of a motor task." J Neurosci **14**(5 Pt 2): 3208-3224.

Shadmehr, R., M. A. Smith, et al. (2010). "Error Correction, Sensory Prediction, and Adaptation in Motor Control." Annu Rev Neurosci.

Smith, M. A. and R. Shadmehr (2005). "Intact ability to learn internal models of arm dynamics in Huntington's disease but not cerebellar degeneration." J Neurophysiol **93**(5): 2809-2821.

Smith, M. C., S. R. Coleman, et al. (1969). "Classical conditioning of the rabbit's nictitating membrane response at backward, simultaneous, and forward CS-US intervals." J Comp Physiol Psychol **69**(2): 226-231.

Spanne, A. and H. Jorntell (2013). "Processing of multi-dimensional sensorimotor information in the spinal and cerebellar neuronal circuitry: a new hypothesis." PLoS Comput Biol **9**(3): e1002979.

Sperry, R. W. (1950). "Neural basis of the spontaneous optokinetic response produced by visual inversion." J Comp Physiol Psychol **43**(6): 482-489.

Srivastava, C. B. L. (1979). "Occurrence of Sensory Nerve-Endings (Stretch Receptors) in the Muscles of a Teleost, Gnathonemus-Petersii." National Academy Science Letters-India **2**(5): 199-&.

Stone, L. S. and S. G. Lisberger (1990). "Visual responses of Purkinje cells in the cerebellar flocculus during smooth-pursuit eye movements in monkeys. II. Complex spikes." J Neurophysiol **63**(5): 1262-1275.

Szabo, T., S. Libouban, et al. (1990). "A well defined spinocerebellar system in the weakly electric teleost fish Gnathonemus petersii. A tracing and immuno-histochemical study." Arch Ital Biol **128**(2-4): 229-247.

Szabo, T., S. Libouban, et al. (1979). "Convergence of common and specific sensory afferents to the cerebellar auricle (auricula cerebelli) in the teleost fish Gnathonemus demonstrated by HRP method." Brain Res **168**(3): 619-622.

Toerring, M. J. and P. Moller (1984). "Locomotor and electric displays associated with electrolocation during exploratory behavior in mormyrid fish." Behav Brain Res **12**(3): 291-306.

Tzounopoulos, T., Y. Kim, et al. (2004). "Cell-specific, spike timing-dependent plasticities in the dorsal cochlear nucleus." Nat Neurosci **7**(7): 719-725.

Uematsu, K., Y. Baba, et al. (2007). "Central mechanisms underlying fish swimming." Brain Behav Evol **69**(2): 142-150.

Uematsu, K. and T. Todo (1997). "Identification of the midbrain locomotor nuclei and their descending pathways in the teleost carp, Cyprinus carpio." Brain Res **773**(1-2): 1-7.

Van Opstal, A. J., J. A. Van Gisbergen, et al. (1990). "Comparison of saccades evoked by visual stimulation and collicular electrical stimulation in the alert monkey." Exp Brain Res **79**(2): 299-312.

von Holst, E. M., H. (1950). "The reafference principle." Naturwissenschaften **37**: 464-476.

Wang, X., M. Zhang, et al. (2007). "The proprioceptive representation of eye position in monkey primary somatosensory cortex." Nat Neurosci **10**(5): 640-646.

Williams, A., P. D. Roberts, et al. (2003). "Stability of negative-image equilibria in spike-timing-dependent plasticity." Phys Rev E Stat Nonlin Soft Matter Phys **68**(2 Pt 1): 021923.

Wolpert, D. M., Z. Ghahramani, et al. (1995). "An internal model for sensorimotor integration." Science **269**(5232): 1880-1882.

Wolpert, D. M. and R. C. Miall (1996). "Forward Models for Physiological Motor Control." Neural Netw **9**(8): 1265-1279.

Wolpert, D. M., R. C. Miall, et al. (1998). "Internal models in the cerebellum." Trends in Cognitive Sciences **2**(9): 338-347.

Wurtz, R. H. (2008). "Neuronal mechanisms of visual stability." Vision Res **48**(20): 2070-2089.

Zipser, D. and R. A. Andersen (1988). "A back-propagation programmed network that simulates response properties of a subset of posterior parietal neurons." Nature **331**(6158): 679-684.